



NEUROPATHOGENIC FLAVIVIRUSES: ISOLATION AND CHARACTERIZATION OF ZIKA AND TICK-BORNE ENCEPHALITIS VIRUSES FROM HUMAN BRAINS

SUVI KUIVANEN

Department of Virology
Medicum
The Integrative Life Science Doctoral Program
University of Helsinki
Finland

ACADEMIC DISSERTATION

*To be presented, with the permission of the Faculty of Medicine
at the University of Helsinki, for public examination on Friday, November 3, 2017,
at 12 noon in the Meilahti Hospital Lecture Hall 4, Haartmaninkatu 4, Helsinki*

Helsinki 2017

SUPERVISORS

OLLI VAPALAHTI, MD, PHD
Professor of Zoonotic Virology
Department of Virology
Medicum
University of Helsinki

ANTTI VAHERI, MD, PHD
Professor Emeritus of Virology
Department of Virology
Medicum
University of Helsinki

REVIEWERS

ANNA ÖVERBY WERNSTEDT
Associate Professor
Department of Clinical Microbiology, Virology
Umeå University
Umeå, Sweden

CARITA SAVOLAINEN-KOPRA
Docent of Virology
Expert Microbiology Unit
National Institute for Health and Welfare
Helsinki, Finland

OFFICIAL OPPONENT

DANIEL RŮŽEK, PHD
Associate Professor of Medical Microbiology
Veterinary Research Institute, Brno
Institute of Parasitology, The Czech Academy of Sciences, Ceske Budejovice
Czech Republic

ISBN 978-951-51-3801-9 (paperback)
ISBN 978-951-51-3802-6 (PDF, available at <http://ethesis.helsinki.fi>)
Unigrafia
Helsinki 2017

“The very essence of instinct is that it’s followed independently of reason”

Charles Darwin

TABLE OF CONTENTS

LIST OF ORIGINAL PUBLICATIONS.....	7
ABBREVIATIONS	8
TIIVISTELMÄ	9
ABSTRACT	11
REVIEW OF THE LITERATURE.....	13
<i>Introduction.....</i>	<i>13</i>
<i>Taxonomical classification.....</i>	<i>14</i>
<i>Flavivirus structure and replication.....</i>	<i>16</i>
<i>Genome structure.....</i>	<i>16</i>
<i>Translation and polyprotein processing.....</i>	<i>17</i>
<i>Viral proteins</i>	<i>18</i>
<i>Flavivirus life cycle</i>	<i>21</i>
<i>Immune recognition of flavivirus infection.....</i>	<i>22</i>
<i>Epidemiology.....</i>	<i>24</i>
<i>Tick-borne encephalitis.....</i>	<i>26</i>
<i>Zika virus disease</i>	<i>28</i>
<i>Ecology and transmission.....</i>	<i>30</i>
Tick-borne encephalitis virus	31
Zika virus	32
<i>Clinical picture and pathogenesis.....</i>	<i>34</i>
Tick-borne encephalitis.....	34
Zika virus disease.....	35
<i>Diagnostic tests.....</i>	<i>37</i>
<i>Treatment and prevention.....</i>	<i>37</i>
AIMS OF THE STUDY	39
MATERIALS AND METHODS	40
<i>Materials.....</i>	<i>40</i>
Cells.....	40
Viruses	40
Antiviral agents.....	41
<i>Methods.....</i>	<i>43</i>
RNA extraction and quantitative RT-PCR (I-IV)	43

Virus titrations (II, III)	43
Immunofluorescence assay (IFA) (I-IV).....	44
Next generation sequencing (NGS) (I, IV)	44
Phylogenetic analysis	45
Cell viability assay (II).....	46
Compound-addition assays (II)	46
Gene expression profiling (II).....	47
Metabolomics (II).....	47
Caspase 1, 3/7, 8 and 9 activity assays (II)	48
Phosphoprotein and cytokine profiling (II).....	48
Statistical analysis (I-IV)	48
RESULTS AND DISCUSSION	49
<i>Isolation of ZIKV and TBEV from human brains (I, IV)</i>	<i>49</i>
ZIKV	49
TBEV	52
<i>Anti-ZIKV potential of obatoclax, saliphenylhalamide and gemcitabine (II).....</i>	<i>57</i>
<i>Obatoclax, saliphenylhalamide and gemcitabine differentially affect cellular signaling, transcription and metabolism (II).....</i>	<i>61</i>
<i>ZIKV cell tropism (III).....</i>	<i>63</i>
CONCLUDING REMARKS	68
ACKNOWLEDGEMENTS.....	70
REFERENCES.....	72
ORIGINAL PUBLICATIONS.....	88

LIST OF ORIGINAL PUBLICATIONS

This thesis is based on the following publications, referred to in the text by the Roman numerals. The original publications have been reproduced with permission from the copyright holders.

I Driggers RW*, Ho CY*, Korhonen EM*, **Kuivanen S***, Jääskeläinen AJ, Smura T, Rosenberg A, Hill DA, DeBiasi RL, Vezina G, Timofeev J, Rodriguez FJ, Levanov L, Razak J, Iyengar P, Hennenfent A, Kennedy R, Lanciotti R, du Plessis A, Vapalahti O. Zika virus Infection with prolonged maternal viremia and fetal brain abnormalities. *N Engl J Med*. 2016 Jun 2; 374(22):2142-51. doi: 10.1056/NEJMoa1601824.

II Kuivanen S, Beshpalov MM, Nandania J, Ianevski A, Velagapudi V, De Brabander JK, Kainov DE, Vapalahti O. Obatoclax, saliphenylhalamide and gemcitabine inhibit Zika virus infection *in vitro* and differentially affect cellular signaling, transcription and metabolism. *Antiviral Res*. 2016 Dec 31. pii: S0166-3542(16)30604-0. doi: 10.1016/j.antiviral.2016.12.022.

III Kuivanen S, Korhonen EM, Helisten AA, Huhtamo E, Smura T, Vapalahti O. Differences in the growth properties of Zika virus foetal brain isolate and related epidemic strains *in vitro*. *J Gen Virol*. 2017 Jul 12. doi: 10.1099/jgv.0.000857.

IV Kuivanen S, Smura T, Rantanen K, Kämppe K, Kantonen J, Kero M, Anu Jääskeläinen AE, Jääskeläinen AJ, Sane J, Myllykangas L, Paetau A, Vapalahti O. Fatal tick-borne encephalitis virus infections caused by Siberian and European subtypes emerging in the same focus. *Submitted*.

*These authors contributed equally.

ABBREVIATIONS

ADE	antibody-dependent enhancement
anch-C	anchored capsid protein
C	capsid protein
CPE	cytopathic effect
DENV	dengue virus
dpi	days post-infection
E	envelope protein
ER	endoplasmic reticulum
GBS	Guillain-Barré syndrome
hpi	hours post infection
ICTV	International Committee on the Taxonomy of Viruses
IFN- β	interferon beta
JEV	Japanese encephalitis virus
kDa	kilodalton
NGS	next-generation sequencing
NS	nonstructural protein
prM	precursor of membrane protein
PCR	polymerase chain reaction
RC	replication complex
RdRp	RNA-dependent RNA polymerase
RT-PCR	reverse transcriptase polymerase chain reaction
TBE	tick-borne encephalitis
TBEV	tick-borne encephalitis virus
TLR	Toll-like receptor
TGN	trans-Golgi network
UTR	untranslated region
VLP	virus-like particle
WNV	West Nile virus
ZIKV	Zika virus

TIIVISTELMÄ

Flavivirukset (suku *Flavivirus*, heimo *Flaviviridae*) ovat zoonoottisia viruksia, joista suurin osa tarttuu niveljalkaisten, hyttysten ja puutiaisten, välityksellä. Maailmanlaajuisesti flavivirusten aiheuttamia lievempiä ihottuma- ja kuumetauteja, sekä vakavampia keskushermostoinfektioita todetaan vuosittain satoja miljoonia. Denguekuume, Japanin aivotulehdus eli enkefaliitti, Länsi-Niilin kuume ja keltakuume ovat esimerkkejä flavivirusinfektioista. Hyttysvälitteiset flavivirukset säilyvät luonnossa kädellisten ja hyttysten välillä. Ne voivat myös vaihtaa urbaaniin kiertokulkuun ihmisten ja hyttysten välille, luoden näin mahdollisuuden epidemioille. Viime vuosina Zikavirus (ZIKV) on aiheuttanut laajan epidemian Etelä- ja Väli-Amerikassa. Tätä epidemiaa karakterisoivat erityisesti sikiöillä ja vastasyntyneillä esiintyneet infektiot aiheuttaen eriasteisia keskushermoston kehityshäiriöitä, kuten mikrokefaliaa. Puutiaisten välittämistä flaviviruksista puutiaisaivokuumevirus (TBEV) on kotoperäinen useassa Euroopan maassa. Suomessa sitä esiintyy rannikolla ja itäisessä Suomessa, pohjoisessa aina Simoon asti. Viime vuosina tautitapausten määrä on ollut kasvussa, ja myös kuolemaan johtaneita tapauksia on raportoitu. Tässä väitöskirjatutkimuksessa keskitytään näiden kahden keskushermostoinfektioita aiheuttavien flavivirusten, ZIKV ja TBEV, karakterisointiin.

Väitöskirjatyössä kuvailemme raskaana olevan naisen zikavirusinfektion ja sen aiheuttaman vakavan seurauksen sikiölle. Zikavirusinfektion todettiin aiheuttavan potilaalla poikkeuksellisen pitkittyneen viruserityksen. Eristimme zikaviruksen sikiön aivokudoksesta, ja osoitimme näin osaltaan zikaviruksen ja sikiön aivovaurion yhteyden. Uuden sukupolven sekvensointitekniikkaa hyödyntäen selvitimme viruksen perimän. Zikavirusinfektion hoitoon ei ole vielä tehokasta viruslääkettä. Testasimme valikoitujen, jo tunnettujen antiviraalisina yhdisteinä vaikuttavien lääkkeiden tehoa zikavirusinfektioon soluviljelymallissa eristetyn viruksen avulla. Löysimme kolme solun omiin toimintoihin vaikuttavaa lääkeainetta, obatoclax, SaliPhe ja gempitabiini, jotka estivät tehokkaasti zikaviruksen aiheuttaman solukuoleman. Nämä yhdisteet vaikuttivat viruksen ja isäntäsolun vuorovaikutuksiin viruksen elinkierron eri vaiheissa. Tutkimuksen kohteena olevaa vakavan tautimuodon aiheuttamaa zikaviruskantaa verrattiin soluviljelymallissa muihin lievempiä epidemioita aiheuttaneisiin zikaviruskantoihin. Tutkimuksessa osoitettiin aivokudoksesta eristetyn viruksen

lisääntyvän tehokkaasti kohdusta, napasuonista, munuaisista ja aivoista peräisin olevissa solulinjoissa.

Kotkan saaristossa on viimeisen vuosikymmenen aikana todettu uusi puutiaisaivokuumefokus. Erityisen merkittävän siitä tekee siellä esiintyneet vakavat TBEV-infektiot. Vuonna 2015 Kuutsalon saarella esiintyi useita puutiaisaivokuume tapauksia, joista kaksi johtivat kuolemaan. Eristimme viruksen toisen tapauksen aivokudoksesta soluviljelmässä, ja virus osoittautui TBE-viruksen siperialaiseksi alatyypiksi. Aiemmassa tutkimuksessa Kotkan saaristosta on löydetty saman alatyypin TBE-virusta puutiaisita. Toinen tapauksista osoittautui täten hieman yllättäen viruksen eurooppalaisen alatyypin aiheuttamaksi. Löysimme saaristosta myös tätä alatyyppeä puutiaisesta, mikä osoittaa, että kaksi viruksen alatyyppeä esiintyvät poikkeuksellisesti samassa fokuksessa.

ABSTRACT

Flavivirus is a genus that consists of small RNA viruses transmitted by arthropod vectors, mosquitos and ticks. Flaviviruses cause human diseases of global concern, such as dengue fever, Yellow fever, West Nile disease and Japanese encephalitis, with hundreds of millions of infections every year. Zika virus (ZIKV), a mosquito-borne flavivirus, recently caused a major epidemic with severe and unexpected consequences. Circulating in sylvatic cycles for decades and traditionally causing only mild self-limiting disease, ZIKV quickly spread through the Americas between 2015 and 2016, leading to an unforeseen epidemic that affected hundreds of thousands of people. Following this outbreak of acute ZIKV infections, the number of microcephaly cases reported in neonates accumulated; a causal relationship was suspected and the World Health Organization declared a Public Health Emergency of International Concern in February 2016.

We were able to provide a key piece of evidence in proving the causal relationship between ZIKV infection and microcephaly. We described a case of prolonged maternal viremia from an expectant mother infected with ZIKV at the 11th week of gestation, which led to brain damage in the fetus. Subsequently, we isolated the virus FB-FWUH-2016 from the brain tissue of the fetus in human neuroblastoma cells.

There is no specific anti-viral treatment for ZIKV infections nor is there a fully effective vaccine. Thus, we screened several anti-cancer compounds known to possess anti-viral activities to determine their anti-Zika virus effectivity. We found that gemcitabine, saliphenylhalamide and obatoclax, the latter of which is a novel compound, inhibited ZIKV replication and virus production in retinal pigment epithelial cells. Furthermore, we found that the compounds differentially affect the metabolism of infected cells. These data provide novel information for anti-virus drug development, as these compounds affect the functions of infected cells instead of the virus itself. We further characterized the new epidemic virus isolate and conducted a study on cell tropism. In this study, we compared four ZIKV isolates, three of which were from the epidemic Asian lineage and the other was a prototypic virus of the African lineage. We found differences in cell susceptibility that favored the new strain and a closely related French Polynesian strain, particularly in cell lines originating from the placenta, umbilical veins, kidney and brain.

Tick-borne encephalitis virus (TBEV), another flavivirus that affects the central nervous system, is endemic in many parts of Europe and in the Northern parts of Asia. Three subtypes of the virus, namely, the European, Siberian and Far Eastern subtypes, can cause encephalitis with different degrees of severity. The European subtype is most prominent in most of Europe, but the Siberian subtype is also found in the Baltic countries and Finland. Fatalities are rare, which made the Kotka Archipelago in Finland a new focus after the report of two fatal TBE cases in 2015 from the same island in the archipelago along with two other infected individuals. We isolated the virus from the brain of one of the deceased patients in human neuroblastoma cells and obtained sequence data on both fatal cases. Surprisingly, the viruses were the Siberian and European subtypes. During this and previous studies, we also found both viruses in ticks from the archipelago, which shows that the subtypes coexist in the same focus.

REVIEW OF THE LITERATURE

Introduction

Viruses in the genus *Flavivirus* comprise a group of emerging viruses of global, regional and endemic concern that vary greatly in their pathogenic potential. The mechanisms by which these viruses cause human disease differ, and flaviviruses are associated with a wide spectrum of human disease, from dengue and yellow fever mild febrile disease to hemorrhagic manifestations and from tick-borne encephalitis to severe congenital infections and Guillain-Barré syndrome caused by Zika virus.

Flaviviruses are small positive-sense RNA-viruses in the family *Flaviviridae*. The prototype yellow fever virus (*lat.* flavus = yellow) gives the family its name and is the causative agent of a severe febrile disease in the tropics. The *Flavivirus* genus consists of over 50 viruses, most of which cause emerging and re-emerging human diseases through arthropod vectors (1,2).

Many members of the genus *Flavivirus* are neuropathogenic, i.e., they cause disease in the central nervous system (CNS). Recently, two such emerging viruses with severe and fatal consequences were brought to our attention. In this thesis work, we focus on these neuropathogenic flaviviruses with different epidemiological and ecological characteristics as well as disease associations: mosquito-borne Zika virus (ZIKV) and tick-borne encephalitis virus (TBEV).

Tick-borne encephalitis was first described as “meningitis serosa epidemica” in Austria in 1931 by H. Schneider (3). The causative agent, TBEV, was later isolated in Russia in 1937 after a similarly described illness in the Far East in 1934 (4). In the 1940s, TBE was called Kumlinge disease in Finland, and later in 1948, the first TBE virus was isolated during an epidemic in Czechoslovakia (5,6). During the past few years, ZIKV has caused an alarming epidemic in the Pacific and the Americas that is associated with microcephaly and Guillain-Barré syndrome. ZIKV was first discovered in the Zika forest in Uganda in 1947 during a study on yellow fever virus (7). It was isolated from a rhesus monkey caged in the Zika Forest, and a year later, ZIKV was isolated also from *Aedes africanus* mosquitos trapped in the same forest. While TBEV has caused regional infections in endemic areas since the days of its discovery, ZIKV remained silent for decades. Until 2007, Zika virus caused only sporadic human cases, with altogether fewer than 20 cases reported (8).

Taxonomical classification

The family *Flaviviridae* is divided into four genera: *Flavivirus*, *Hepacivirus*, *Pegivirus* and *Pestivirus*. The viruses are antigenically distinct between the genera, but cross-reactivity within each genus is common. Members in all four genera have enveloped spherical virions 40-60 nm in diameter with a non-segmented single-stranded 9-13 kb RNA genome packed inside a capsid. The four genera share similar genome organization in regions coding for serine protease, helicase and RNA-dependent RNA polymerase (9). Viruses in the genus *Flavivirus* differ in their antigenic, ecological and epidemiological characteristics. Most flaviviruses infect vertebrates and invertebrates, a feature not shared by members in the *Pestivirus*, *Hepacivirus* and *Pegivirus* genera (10). In addition, only flaviviruses have a type 1 cap structure at the 5'-end of their genomes and produce a subgenomic non-coding RNA from the 3'-untranslated region (UTR) (11).

The genus *Flavivirus* (hereafter referred to as flaviviruses; Figure 1) forms a monophyletic lineage that can be divided into three main clades based on their vector association: a mosquito-borne clade (e.g., Yellow fever virus, dengue viruses and Japanese encephalitis viruses), a tick-borne clade (e.g., Tick-borne encephalitis virus, Louping ill virus and Langat virus), and a no-known-vector or mosquito only clade of insect-specific flaviviruses (ISFVs) (e.g., Entebbe bat virus, Dakar bat virus and San Perlita virus) (10). Approximately 50% of known flaviviruses are mosquito-borne, 28% are tick-borne and the remaining 22% are agents with no known arthropod vector or ISFVs (10).

Currently, the tick-borne clade includes twelve recognized species that are divided into two groups, the mammalian tick-borne virus group and the seabird tick-borne virus group. The evolutionary characteristics of these groups are largely determined by their mode of transmission, which affects their antigenic relationships, genetic diversity and geographical distribution (12,13). The mammalian tick-borne virus group consists of six human and animal pathogens: tick-borne encephalitis virus (TBEV), Louping ill virus (LIV), Omsk hemorrhagic fever virus (OHFV), Langat virus (LGTV), Kyasanur Forest disease virus (KFDV) and Powassan virus (POWV). Three other viruses (Royal Farm virus (RFV), Karshi virus (KSIV) and Gadgets Gully virus (GGYV)) that are not known to be human pathogens are currently included in this group (10,12). The TBEV species has three main subtypes: European (Eur; previously Central European Encephalitis

CEE), Siberian (Sib; previously West Siberian encephalitis) and Far Eastern (FE; previously Russian spring-summer encephalitis) (14).

ZIKV belongs to the Spondweni serocomplex together with Spondweni Virus. ZIKV has evolved into three genotypes: West African (Nigerian cluster), East African (prototype MR766 cluster), and Asian. It has been suggested that the virus originated in East Africa and then spread approximately 100 years ago to West Africa and Asia (15). ZIKV is antigenically closely related to dengue viruses (DENV). DENV and ZIKV circulate in the same geographical areas and are transmitted by *Aedes* mosquitoes. There are four serotypes of dengue (DENV 1-4), and they differ from each other by 30-35% in the amino acid sequence of envelope protein E. In turn, the DENV serocomplex differs by 41-46% from ZIKV (16).

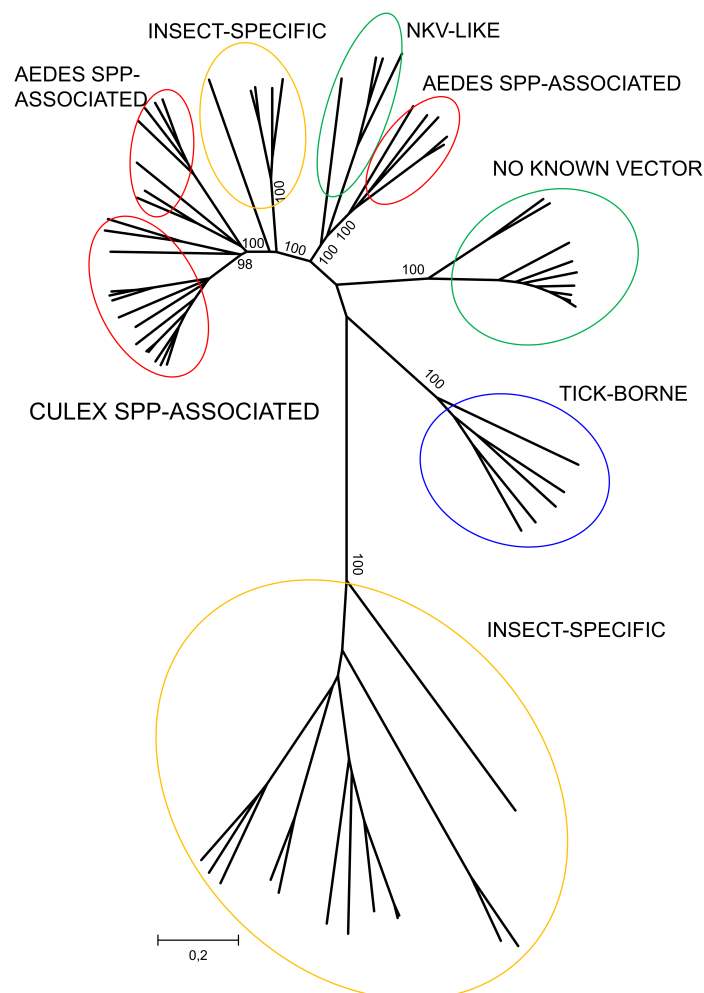


Figure 1. Taxonomical classification of the *Flavivirus* genus. Phylogenetic tree based on representatives of all flavivirus species for which a complete coding sequence is available. For clarity, bootstrap values are shown only for the major clusters. Courtesy of Dr. Teemu Smura.

Flavivirus structure and replication

Flavivirus particles are approximately 50 nm in diameter. The virion consists of three structural proteins (capsid (C), precursor of membrane (prM) and envelope (E)), the positive-sense RNA genome and a lipid membrane. Seven nonstructural proteins (NS1, NS2A, NS2B, NS3, NS4A, NS4B and NS5) are expressed in infected cells (17). Unlike many other enveloped viruses, the envelope protein E lies parallel on the virion surface and is organized in a head-to-tail orientation, forming an icosahedral structure with the other envelope protein M (Figure 4). E protein is the major antigenic determinant of the virus, and it mediates membrane fusion during virus entry. The membrane protein M is a small fragment of the precursor protein prM, and it is formed after virion maturation by furin protease cleavage under low pH conditions prior to exocytosis. The RNA genome is enclosed by the third structural protein capsid (C) (17).

Genome structure

The flavivirus genome is a single positive-stranded RNA of approximately 11 kilobases (Figure 2). It is capped at the 5'-end by a type 1 5' cap ($m^7GpppAmpN_2$). The flavivirus genome is not usually polyadenylated at the 3' end, unlike cellular mRNA, although some TBEV genomes have been shown to contain a poly-A tail (18). The genome has one open reading frame flanked by 5' and 3' untranslated regions (UTRs) that are approximately 100 nucleotides and 400-700 nucleotides long, respectively (Figure 2).

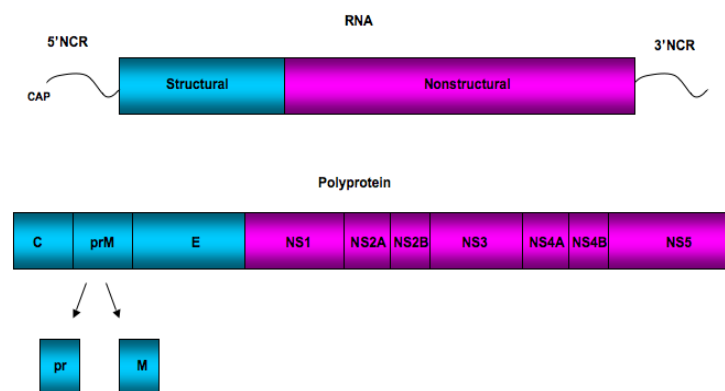


Figure 2. Flavivirus genome structure and organization.

The 5' and 3'UTRs are not well conserved among flaviviruses, but they contain common secondary structures that play a role in translation and replication of the viral genome (19). Several host transcription factors and regulatory and RNA-binding

proteins, such as La, p100, FBP1 and Mov34, have been reported to bind to flaviviral 3' UTR (20-25). Some TBEV strains that are cell-line adapted or were isolated from humans have deletions or polyA insertions in the 3'UTR. These mutations have been reported to increase the virulence of the viruses (26-28).

Translation and polyprotein processing

As for all positive-strand RNA viruses, the flavivirus genome serves as a messenger RNA for translation. The single open reading frame is translated into one long polyprotein of approximately 3500 amino acids, which is cleaved co- and post-translationally into at least 10 proteins (Figure 3). The structural proteins are encoded by the amino-terminal part of the genome, followed by the nonstructural proteins. The one long polyprotein translocates into the endoplasmic reticulum (ER), and individual proteins are released either on the luminal side (prM, E, NS1 and NS4B) or the cytoplasmic side (NS2A, NS2B, NS3, NS4A and NS5) with transmembrane anchors (Figure 3). The protein cleavages are performed by several proteases, most importantly by the host signal peptidase and viral serine protease (NS2B/NS3). The host signal peptidase is known to cleave between the structural glycoproteins, while the cleavages between the nonstructural proteins are made mainly by the viral protease (17). The processing of the NS4A/NS4B junction requires both cellular and viral proteases (29) (Figure 3).

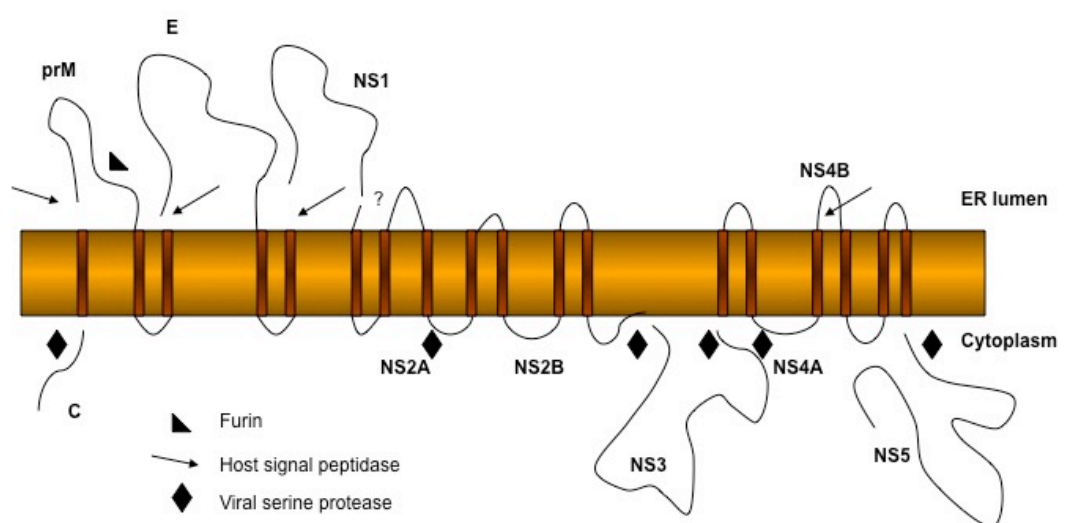


Figure 3. Flavivirus polyprotein processing and ER membrane topology. Modified from ref. (30)

Viral proteins

Capsid protein

Capsid protein (C) is a highly basic protein of relatively small size (11 kDa) (31). The nucleocapsid consists of C homodimers that interact with the positively charged basic residues in both the N- and C-termini with the negatively charged viral genome, enclosing an electron dense core of ca. 30 nm (32,33). Capsid protein plays a role in infectious virus assembly via interactions with viral genome (34). As virion maturation occurs, the viral serine protease releases the C protein from its anchor at the C-terminus (anchored C; anchC), which serves as a signal peptide for prM to translocate into the ER (35,36).

Membrane protein

The glycoprotein precursor of the membrane protein M (prM) is an approximately 26 kDa type I integral membrane protein that contains 1-3 glycosylation sites (37,38). The N-terminal 'pr' segment of the protein is hydrophilic, and it is released into the extracellular milieu along with mature virus particles. prM and E form a 1:1 complex, preventing premature activation of the virion in conditions of low pH in the trans-Golgi network (TGN) (37,39). Prior to virion budding, mature virions are produced by furin cleavage of prM directly after the consensus sequence Arg-X-Arg/Lys-Arg into 'pr' and M (40). The prM protein acts as a chaperone-like protein for E, enabling it to fold correctly into its native conformation (37).

Envelope protein

The envelope protein (E) is the viral hemagglutinin and major antigenic determinant, and it is involved in receptor binding and membrane fusion. E is also a type I membrane protein approximately 53 kDa in size that typically contains 1 to 2 glycosylation sites (37,41). The number of glycosylation sites is not conserved among flaviviruses, and it has been suggested that glycosylation patterns modulate receptor binding (42). The E monomer consists of three structural domains (I, II and III), the structures of which have been determined to a resolution of 2.0 Å (43,44) (Figure 4). The fusion peptide is highly conserved among flaviviruses and is located at the tip of domain II (Figure 4). The putative receptor-binding sites reside in domain III (37,45). The flavivirus E protein forms a distinct class of fusion proteins (class II) with alphavirus E1 that is defined by the presence of the distinct three-domain structure with an internal fusion peptide. After

furin cleavage, the E protein acquires its flat conformation on the mature virion surface (Figure 4).

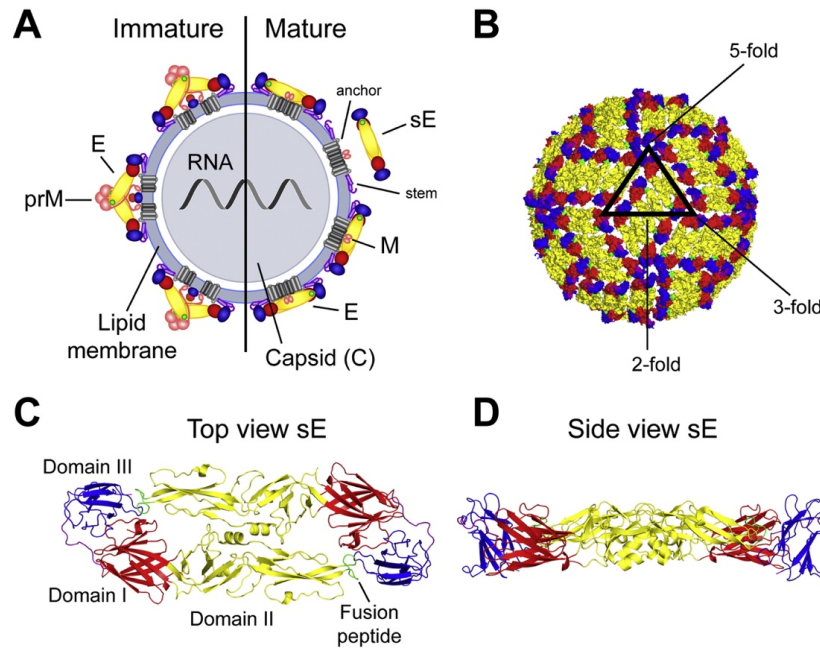


Figure 4. Flavivirus virion structure. (A) Immature and mature particles differ in their orientation of the E protein. (B) Cryo-EM visualization of the virion. E protein dimers form a herringbone-like structure. The 2-, 3- and 5-fold symmetry axes are shown. (C, D) Ribbon diagrams of the crystal structure of the TBEV E protein dimer. Domains I, II and III are in red, yellow and blue, respectively, and the fusion loop is in green. Reproduced with permission from Heinz FX and Stiasny K, *J Clin Virol* 2012 (46).

NS1

NS1 is a multifunctional glycoprotein approximately 46 kDa in size. NS1 translocates into the lumen of the ER through a signal sequence at the C-terminus of E, and it is cleaved from the envelope protein by a host signal peptidase. Downstream cleavage from the NS2A protein is catalyzed by an unknown ER-resident host protease shortly after synthesis (47), at which time NS1 forms homodimers that associate with membranes (32). NS1 exists as a monomer, dimer and a hexamer. NS1 functions in genome replication and is involved in replication complex (RC) formation together with NS4A and NS4B. Dimeric NS1 forms soluble hexamers in the Golgi network, which are released outside of the infected cell (47). NS1 also antagonizes innate immune responses of the host (48,49).

NS1 is highly conserved among flaviviruses: it shares 90% amino acid homology with different TBEV strains and as high as 44% homology with different flaviviruses (50). In natural flavivirus infections, the extracellular form of NS1 elicits a strong immune response in the host. Immunization of mice with the DENV and TBEV NS1 proteins, and of monkeys with the YFV NS1 protein, has been demonstrated to protect them from lethal challenge (51,52).

A ribosomal frameshift in the translation of the polyprotein has been shown to occur in NS1, producing another form of the protein, NS1'. This frameshift has been shown to play a role in virus neuroinvasiveness (53).

NS2A and NS2B

NS2A is a small (22 kDa) hydrophobic protein. It functions in virus replication and assembly and has been shown to antagonize type I interferon (IFN) responses (54). The C-terminal cleavage of NS2A from NS2B occurs via the viral serine protease NS3/NS2B. NS2B is a membrane-associated protein approximately 14 kDa in size. Its conserved hydrophilic core region functions as a key cofactor for the viral serine protease complex it forms with NS3 (55,56). NS2B antagonizes innate immune responses, and, together with NS3, it has been shown to play a role in TBEV neuroinvasiveness (57,58).

NS3

NS3 is a large 70-kDa multifunctional cytoplasmic protein associated with membranes via its interaction with NS2B. The catalytic triad (His-Asp-Ser) in the active site of mammalian serine proteases is critical for their protease function, and it has been found to be conserved in the NS3 proteins of all flaviviruses (59). NS3/2B catalyzes the autocleavage (*cis*) of NS2A/NS2B and NS2B/NS3 and the *trans* cleavage of NS3/NS4A and NS4B/NS5 (60). The C-terminal part of NS3 is involved in viral RNA replication as an RNA helicase, nucleotide 5'-triphosphatase (NTPase) and RNA 5'-triphosphatase (RTPase), and it associates with NS5 to form the RC (61).

NS4A and NS4B

NS4A and NS4B are small integral membrane proteins 16 and 27 kDa in size, respectively. NS4A and NS4B are connected via a conserved signal peptide called 2K. 2K is cleaved by the viral serine protease to form mature NS4A, which is subsequently cleaved from NS4B by a host signal peptidase. NS4A and NS4B function primarily in

replication as they are essential components of the RC (29). NS4B has been shown to interfere in the RNA binding of helicase by binding to NS3, thus removing the single-stranded RNA from NS3 (62,63).

NS5

NS5 is a large 104-kDa protein that contains two distinct domains: the N-terminal S-adenosyl-methionine (SAM) transferase domain and the C-terminal RNA-dependent RNA polymerase domain (RdRp) (64). The methyltransferase activity is associated with the 5'-cap formation of newly synthesized viral RNA. The interdomain region of NS5 is involved in RC formation and also contains a functional nuclear localization signal (NLS), which binds to the nuclear import receptors importin- β 1 and importin- α/β (65). The NTPase activity of NS3 is stimulated by binding of the RdRp domain of NS5, exposing the active site of NS3 to the substrate (66)

Flavivirus life cycle

Flaviviruses enter cells through receptor-mediated endocytosis. Several cell surface proteins have been identified as putative receptors for flaviviruses. Among others, heparan sulfate proteoglycans, dendritic cell-specific ICAM-3 grabbing non-integrin (DC-SIGN) and AXL have been identified as candidate flavivirus receptors, but their precise roles are not clear (42,67,68). Upon attachment, virions are internalized into clathrin-coated pits and vesicles (Figure 5). Virions are stable in slightly basic conditions (~pH 8), and upon attachment, the acidification (pH ~6.6) of the endosome causes the E homodimers to monomerize and rearrange into homotrimers, releasing the nucleocapsid into the cytoplasm (40,43,46). After nucleocapsid uncoating, the genome is translated into one long polyprotein at the ER membrane. Genome replication occurs at membrane-associated RCs localized to the perinuclear region (65).

Flavivirus assembly occurs in the ER, where the proteins and viral RNA are combined into immature virus particles (Figure 5). Virions gain their lipid envelope by budding into the ER. pH and protease-dependent maturation occurs in the TGN, prM is cleaved by the host protease furin, and the E protein undergoes major reorganization (40). prM and mature virions are released from the host cell by exocytosis at the plasma membrane (17). In addition to mature virus particles, immature or partially immature

particles that are infectious through antibody-dependent enhancement (ADE), are released (69).

Virus-like particles

Flavivirus-infected cells have been shown to release particles containing only the envelope proteins E and M and the lipid envelope. These virus-like particles (VLPs) are noninfectious and smaller in size (approximately 30 nm in diameter) than the infectious virions, and they possess hemagglutination activity (77). The maturation and assembly of VLPs seem to be very similar to those of the virus: VLPs undergo low-pH induced rearrangement of envelope proteins and are able to undergo membrane fusion.

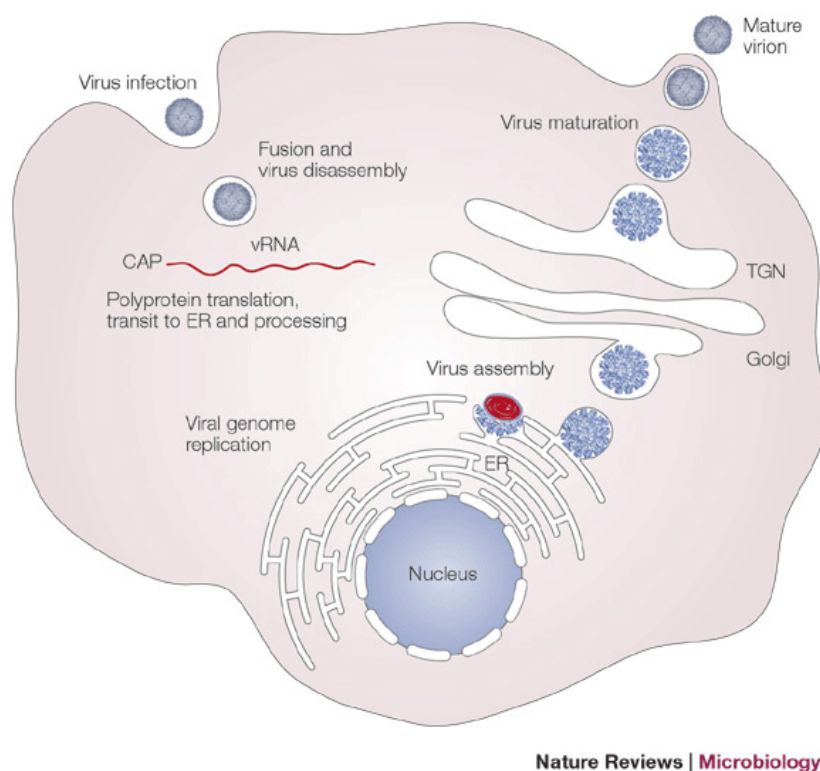


Figure 5. Flavivirus life cycle. Reproduced with permission from Mukhopadhyay *et al. Nat. Rev. Microbiol*, 2005 (17).

Immune recognition of flavivirus infection

While immune reactions are important for restricting (neuropathogenic) virus growth and spread to the brain, these reactions may also cause neurological damage. Immune defense against different pathogens is mediated by early innate immune reactions as

well as the later responses of adaptive immunity. Innate immunity serves as the first-line of response against microbes and includes their possible elimination, effector mechanisms of adaptive immunity, and the stimulation of adaptive immune responses. In host cells, interferons (IFNs) and other cytokines are produced in response to viral infection. A variety of cells, such as macrophages, lymphocytes and monocytes, as well as fibroblasts, endothelial and stromal cells, are able to produce cytokines upon infection.

Cells recognize the products of infection, e.g., viral double-stranded RNA, through pathogen recognition receptor proteins (PRRs). Several families of PRRs exist, but Toll-like receptor (TLR) family proteins in the endosomes and the cytoplasmic RNA helicases (RLR), RIG-I and MDA5, are the most important in flavivirus infection (70). These PRRs recognize pathogen-associated molecular patterns (PAMPs) and induce signal pathways that result in the production of type I interferons (IFN α and - β) and inflammatory cytokines. In particular, IFN α and - β are the key cytokines that mediate the induction of both the innate immune response and the following development of adaptive immunity to viruses (71).

The exact role of TLR-3 in flavivirus infection is not completely understood, but it has been shown to restrict DENV and WNV replication (72,73). Both RLRs, RIG-I and MDA5, are DExD/H box RNA helicases that function independently of TLRs in RNA-virus infection. RIG-I and MDA5 contain tandem caspase activation and recruitment domains (CARDs) that activate downstream signaling (74). RIG-I interacts with the 5'-phosphorylated ends as MDA5 binds internally (75). RIG-I interacts downstream with mitochondrial bound MAVS (also known as Cardif, IPS-1 or VISA) (76), which is important for RIG-I-dependent signaling (77). The interaction of RIG-I and MAVS activates the downstream kinases IKK ϵ and TBK-1, which in turn phosphorylate the IRF-3 and IRF-7 transcription factors. Interferons affect neighboring cells by inducing the JAK/STAT pathway and the subsequent production of several interferon-stimulated genes (ISGs) that further function in limiting the infection. MxA is an interferon-inducible GTPase that is known to have broad antiviral activity against numerous viruses.

Flaviviruses have developed strategies to interfere with innate immune responses. It has been shown that ZIKV fails to induce an ISG response in many cell types. Several proteins have been identified to inhibit IFN induction and signaling. DENV NS2B/NS3 inhibits IFN induction by cleaving the MITA/STING signaling protein (58,78). The

NS5 protein of ZIKV, DENV and TBEV has been shown to interfere with IFN signaling by interacting with STAT proteins (79-81). ZIKV NS5 function in STAT2 cleavage seems to be restricted by host species, as it is functional in humans and non-human primates but not in mice. Interferon antagonism has also been described for NS2A and NS4B of DENV and WNV (82,83). In addition to specific protein functions, TBEV has been shown to delay IFN production by hiding dsRNA in ER-derived membrane structures (84).

The complement system is also considered to be part of innate immunity. The complement system comprises several proteins circulating in blood, and it is activated upon recognition of an invading pathogen. Classical, lectin or alternative pathways are activated, depending on the stimuli. Studies on DENV and WNV have revealed interactions with the NS1 protein and components of the complement system (factor H and C4) to evade the proteolytic activation of the complement system (48,85).

Cellular macroautophagy is a process that results in the lysosomal degradation of cellular organelles and proteins. Autophagy regulates cellular homeostasis and functions as a part of the innate immune response to infections. Autophagy has also been shown to exhibit pro-viral functions, and several viruses have evolved strategies to evade or subvert these lysosomal processes to their advantage during different stages of the replication cycle (86). Flaviviruses have been, although somewhat controversially, reported to usurp autophagy at some stage of the life cycle (87-89). In particular, ZIKV NS4A and NS4B proteins have been shown to induce autophagy by suppressing the Akt-mTOR signaling pathway (86).

Epidemiology

Flaviviruses are distributed worldwide, but individual species are restricted to endemic or epidemic areas. Yellow fever virus is found in tropical and subtropical regions in Africa and South America, Japanese encephalitis virus in Southeast Asia and dengue throughout the tropics and subtropics globally. More than half of flaviviruses are associated with human disease. These diseases may be associated with the central nervous system (e.g., WNV, JEV, TBEV and ZIKV), hemorrhagic fever (e.g., DENV and YFV) or more generalized infections with fever, arthralgia and rash (DENV and ZIKV). Many are also economically important diseases in domestic and wild animals.

Mosquito-borne neuropathogenic flaviviruses have caused epidemics around the world. A major epidemic of West Nile virus occurred in North America in the late 20th century, when the virus was first detected in New York in 1999. WNV caused nearly 6000 cases of meningitis or encephalitis during 2002-2003, causing over 300 deaths (90). WNV has also emerged in several countries in Europe (91). In Asia, Japanese encephalitis virus causes 10 000 deaths annually (92). Other members in the JE-serogroup that cause encephalitis include St Louis encephalitis virus in the USA and Murray Valley encephalitis virus in Australia (90). In many cases, humans are a dead-end-host for the virus, but some mosquito-borne flaviviruses are able to shift the transmission cycle to a human-mosquito-human cycle, enabling their effective spread and increasing their epidemic potential. Tick-borne encephalitis virus is endemic in Europe and Asia, and it is considered an important pathogen that affects the CNS. The impact of Zika virus and its newly identified CNS disease associations are on the verge of being characterized (Table 1).

Table 1. Neuropathogenic flaviviruses. Table of globally important neuropathogenic flaviviruses (90,93-96). *CNS*, central nervous system; *Eur*, European subtype; *Sib*, Siberian subtype; *FE*, Far Eastern subtype; *GBS*, Guillain-Barré syndrome.

VIRUS	GEOGRAPHIC DISTRIBUTION	PRINCIPAL VECTOR SPECIES	CLINICAL TO SUBCLINICAL RATIO	TYPE OF HUMAN CNS DISEASE (PATIENTS PRESENTING SYMPTOMS)	CASE FATALITY RATE
JAPANESE ENCEPHALITIS	Asia	<i>Culex tritaeniorhynchus</i>	1/25 (adults), 1/250-1000 (children)	Encephalitis (60-75%) Meningitis (5-10%)	20-30%
MURRAY VALLEY ENCEPHALITIS	Australia New Guinea	<i>Culex annulirostris</i>	1/700 - 1/1200	Encephalitis (50%) Meningitis (50%)	15-30%
ST LOUIS ENCEPHALITIS	South and Central America	<i>Culex spp</i>	1/250	Encephalitis (58-85%) Meningitis (5-40%) Meningitis (50%)	3-30%
TICK-BORNE ENCEPHALITIS	Europe Asia	<i>Ixodes spp</i>	1/3-5 (10-30% develop CNS disease)	Meningoencephalitis (40%) Meningoencephalomyelitis (10%)	<2% Eur 2-4% Sib 20-40% FE
WEST NILE	Worldwide	<i>Culex spp</i>	1/5 (fever), 1/140-320 (CNS disease)	Encephalitis (60%) Meningitis (15-40%)	4-16%
ZIKA	Africa Asia Americas Oceania	<i>Aedes spp</i>	2/10	Microcephaly (0.88-13.2/1000), GBS (0.24/1000), Meningoencephalitis	Data not established

Tick-borne encephalitis

TBEV is considered the most important arthropod-borne virus in Europe. It is endemic in most European countries, Russia, China and Japan. Close to 3000 cases occur in Europe annually, and up to 10 000 cases have been reported in Russia. In endemic regions, the majority of TBEV infections are subclinical, and fewer than half of the patients report a tick bite (14). TBEV infections usually occur under altitudes of 750 m, but in recent years, the virus has expanded to new areas up to and above 1500 m in altitude (97,98). Human infections follow the seasonal peaks of *I. ricinus* and *I. persulcatus* feeding activity in Europe and of *I. persulcatus* in Asia. In Central Europe, ticks are active in two peaks: from May to June and from September to October, and the peaks in human disease follow 3-4 weeks later. In Fennoscandia, only one peak is recorded in the late summer/autumn, except in areas with *I. persulcatus*, where a peak is observed mainly in the early summer (O. Vapalahti, personal communication).

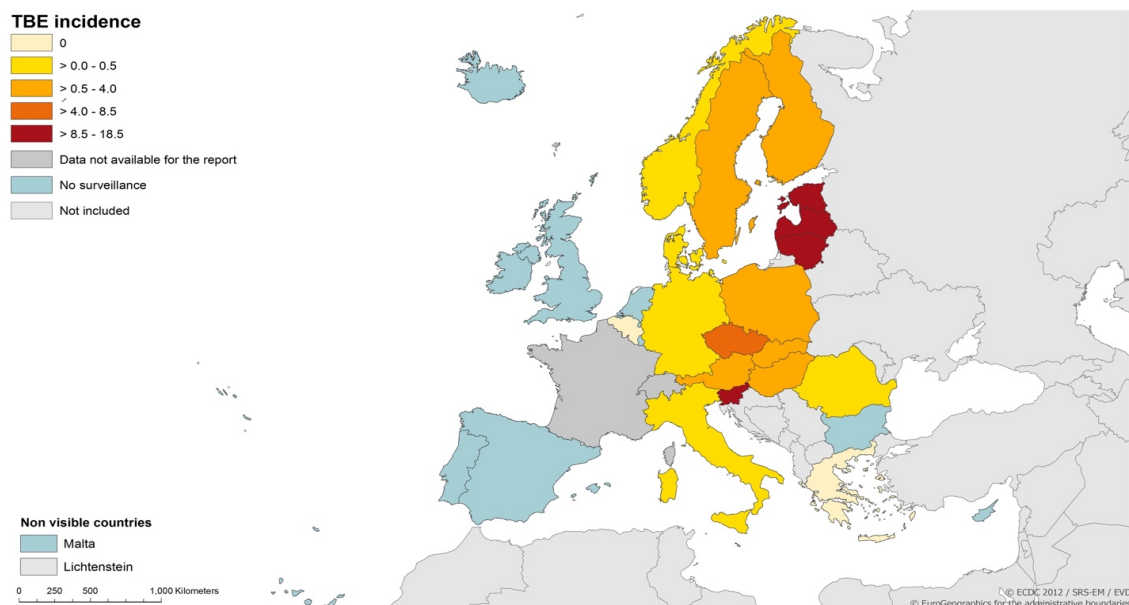


Figure 1. TBE incidence in Europe in 2016 (99).

The highest incidence of tick-borne encephalitis (TBE) is in Baltic countries (Latvia 14.6/100 000, Lithuania 18.5/100 000), Slovenia (18.6/100 000), Czech Republic (10/100 000) and western Siberia (40-80/100 000) (100-102). Before the 1980s and the mass vaccination campaign, the highest morbidity rates of TBE in Europe were recorded in Austria. To date, vaccination coverage includes approximately 85% of

Austrian citizens, and the cases of TBE have decreased from 300-700/year to 70. The incidence among unvaccinated individuals is approximately 5/100 000 (103,104). There is an increasing trend of TBE cases in Europe, and during recent years, the prevalence has expanded to higher latitudes in Finland, Sweden and Russia (105-107). The number of TBE cases has risen in Czech Republic from approximately 350 per year in the beginning of the 1980s to approximately 500-600 per year in 2010 (99).

In Finland, 20-40 cases of TBE were reported up to 2009, but during the last decade, the number has increased to a record of 67 in 2015, followed by 61 reported cases in 2016 (Figure 6). The endemic foci are situated mainly on the Åland Islands, along the coastlines, and in the Lake District, but new foci appear continuously. The endemic areas have spread to Kokkola, Lappeenranta, Simo, Isosaari Island in Helsinki and Kotka; furthermore, the Siberian subtype has been detected in Kokkola and Kotka. A vaccination campaign was started in 2006 in Åland, where the TBE incidence has been the highest in Finland. Vaccination coverage has reached 70%, which has led to a decrease in cases from 70 to 30/100 000 in the archipelago, and mainland cases predominate at present (108). In 2017, TBEV was included in the National vaccination program in Simo and Parainen, municipalities that are high-risk TBE areas, i.e., areas in which the TBE incidence exceeds 5 cases/100 000 per year (109).

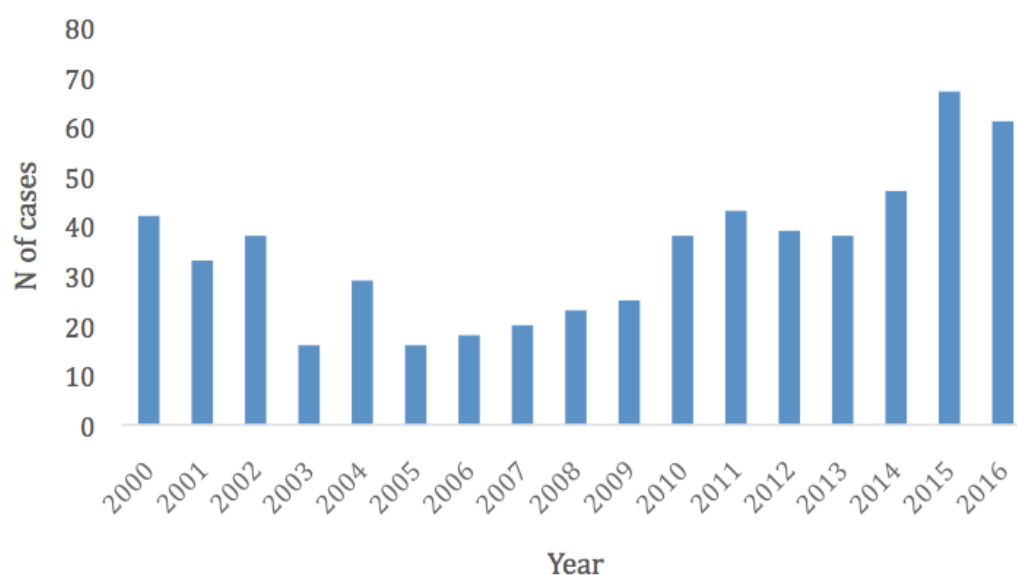


Figure 6. The number of reported TBE cases in Finland 1995-2016 (110).

Zika virus disease

Approximately 3.6 billion people live in tropical or subtropical areas where *Aedes* mosquitos can carry Zika, dengue, Chikungunya and yellow fever viruses and a risk for epidemic transmission exists. However, the epidemiological data for ZIKV has only recently started to accumulate. For many years, ZIKV circulated in sylvatic cycles between non-human primates and mosquitoes in Asia and Africa, causing only sporadic human cases. The transition to human-mosquito-human cycles is a prerequisite for virus transmission in urban environments. Decades after its discovery, the first ZIKV outbreak was detected in 2007 on Yap Island in Oceania, where the overall infection rate (IgM positivity) was as high as 74%, and 37% of those infected were symptomatic (111). A new outbreak was reported in French Polynesia in 2013, where a serosurvey conducted after the outbreak revealed an infection rate of 50-60% with 30 000 symptomatic infections (112). This outbreak was thought to be a new introduction from Asia unlike the virus on Yap Island (113). The outbreaks occurred in previously unaffected areas, and from French Polynesia, ZIKV continued to spread to neighboring islands, affecting New Caledonia, Cook Island and the Easter Islands in early 2014 (114-116). A notifiable outbreak occurred in Martinique in 2015-2016, where autochthonous circulation of ZIKV was confirmed, and the cumulative number of cases was over 32 000 on an island of 400 000 inhabitants (117).

Phylogenetic analyses show that ZIKV was first introduced to South America in Brazil most likely between May 2013 and December 2013 through a single introduction (118). The first cases of undefined febrile illness were reported in the beginning of 2015, and the first confirmed ZIKV cases of the epidemic were reported in May 2015 in Brazil. Retrospectively, clusters of disease characterized by rash were reported in northern Brazil in 2014. By the end of January 2016, 30 000 cases had been reported in Brazil. The epidemic seemed to have peaked in mid-July 2015, with over 90% of the cases reported from Bahia state (118). A striking turn in the epidemic occurred between November 2015 and January 2016, when almost 5,000 suspected cases of microcephaly were reported in Northeast Brazil. An unusual increase in the number of neurological complications (Guillain-Barré syndrome) was also noticed retrospectively after the outbreaks in French Polynesia and Martinique, but it was not until the epidemic in Brazil that the causal relationship of ZIKV and microcephaly in fetuses and newborns was suspected. Data of the causal relationship accumulated and the WHO declared the

ZIKV epidemic to be a Public Health Emergency of International Concern (PHEIC). The cumulative number of confirmed autochthonous ZIKV cases in Brazil was 134 000 by July 2017. The incidence rate for suspected and confirmed cases was 171.19/100 000 (119). Almost 3000 confirmed congenital Zika syndrome cases in newborns have been reported (120).

In September 2015, ZIKV continued to spread from South America northwards to Central America, reaching Mexico in November 2015 and Florida in North America late 2016. In 2015, 61 cases were confirmed in North America in travelers returning from affected areas. During 2016-2017, 225 autochthonous cases were confirmed (incidence rate 0.06), and 5 500 cases were imported. Zika virus congenital syndrome was confirmed in 91 newborns in North America (120). These numbers exclude pregnant women, which account for 2 000 cases of possible ZIKV infection (121).

Zika virus has been circulating in Asia for the past 6-60 years, but no severe epidemics have emerged. In Europe, only imported cases have been reported in travelers. The first case was a German traveler returning from Thailand in November 2013. Large outbreaks are not expected, but since *Aedes albopictus* circulates in southern Europe, autochthonous transmission is possible after introduction during a hot season. Imported cases have been reported from all over Europe, including Finland (traveler returning from the Maldives in June 2015 (122)), Sweden and Denmark. In 2015, the epidemic strain returned back to its place of origin, Africa, where only sporadic cases had been reported. In Cape Verde, 5 000 suspected cases were reported from September to December 2015.

To date, 48 countries and territories in the Americas have confirmed vector-borne transmission of ZIKV (Figure 7). Of over 570 000 suspected autochthonous cases, 214 000 have been confirmed in total in North and South America. A total of 6 000 ZIKV infections have been confirmed in travelers, the total number of deaths related to ZIKV has reached 20 (excluding Guillain-Barré and congenital syndrome), and a total of 3 400 cases of microcephaly in newborns have been reported. The epidemic in the Americas has ended, and in November 2016, the WHO declared that the ZIKV epidemic was no longer a PHEIC.

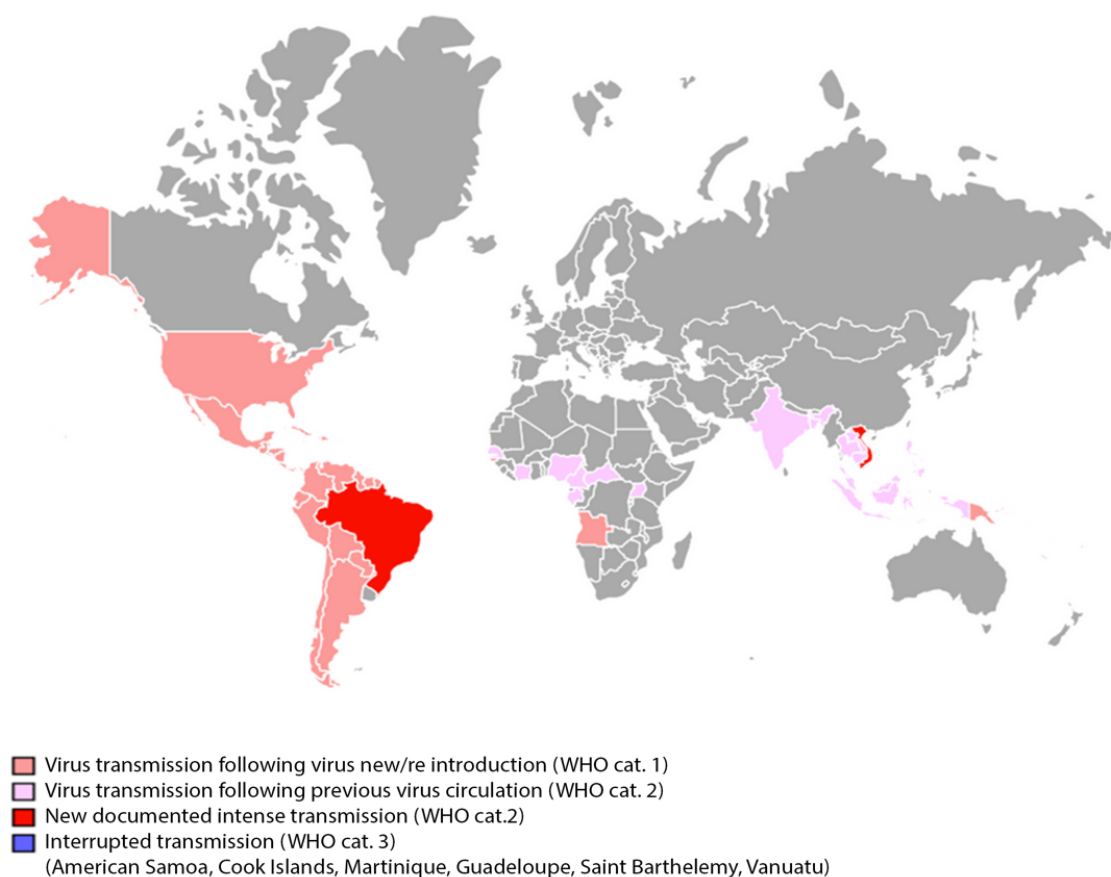


Figure 7. Countries with current Zika virus transmission. ECDC's adaptation of the WHO's Zika virus country classification scheme (123).

Ecology and transmission

Flaviviruses are transmitted through arthropod vectors, mainly by mosquitos and ticks. *Aedes* spp. mosquitos are the most common vectors for DENV and YFV, and *Culex* spp. mosquitos for WNV and JEV. *Aedes aegypti* and *Aedes albopictus* have been shown to be the major vector species for ZIKV transmission, but the virus has also been isolated from several other *Aedes* species (124).

Ectoparasitic ticks are obligate blood-feeding arthropods in the class *Arachnida*. The class is divided into three families, two of which transfer diseases to humans: *Argasidae* and *Ixodidae*. Ticks in the family *Ixodidae* are hard-bodied and more voracious than ticks in the family *Argasidae*, which gives the pathogen a greater chance to infect the host. Most of the vectors for tick-borne flaviviruses are *Ixodes* ticks, but *Haemaphysalis inermis* and *Dermacentor reticulatus* may also carry these pathogens (125).

Tick-borne encephalitis virus

Ixodes ricinus and *Ixodes persulcatus* are the main vector species for TBEV in Europe and Asia; the European subtype is typically transmitted by *I. ricinus* and the Siberian and Far Eastern by *I. persulcatus*. Ticks go through three developmental stages in their life cycle: an adult female tick lays thousands of eggs, which develop into larvae, nymphs and mature females or males; each of these transitions requires a blood meal (126). The life cycle from larvae to adult varies from one to three years, depending on the climate. The transmission cycle of TBEV in ticks is dependent on many aspects in the existing microclimate. Nymphs require a minimum of +7°C and larvae +10°C for activity. Ticks also require a certain humidity for active questing. TBEV is preserved in nature through a cycle involving ticks and wild vertebrate hosts (Figure 8).

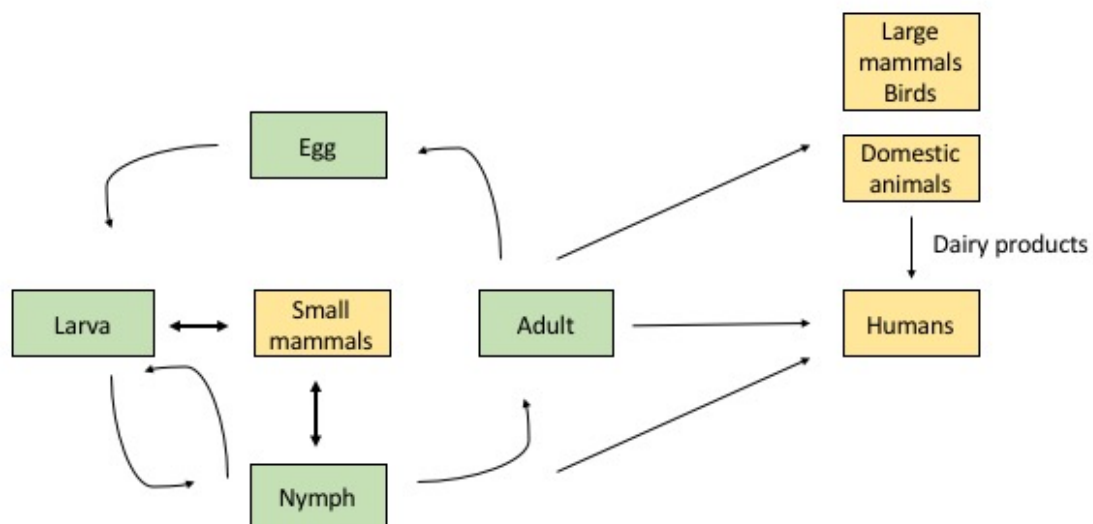


Figure 8. TBEV transmission in nature.

The virus resides in areas where ticks and their hosts co-exist in stable populations. Small rodents such as voles serve as amplifying hosts for TBEV. In addition to their role as vector, ticks are also considered to be important reservoirs of the virus (127). TBEV is maintained in tick populations by ticks feeding on infected animals as well as through transovarial (adult to eggs), transstadial (from one developmental stage to another), or non-viremic transmission between co-feeding ticks (128-130). TBEV can be transmitted from one tick to another when feeding on the same animal in close proximity. Co-feeding is considered an important form of TBEV transmission between

nymphs and larvae (131). This transmission cycle is dependent on delicate climate conditions at the ground level being favorable for nymphs and larvae to be active at the same time. Large mammals are usually accidental hosts and are not considered important sources of TBEV infection, because they experience low and short viremia, yet they play a role in the amplification of the tick population. Humans are dead-end hosts that play no role in natural TBEV circulation (132).

The tick gut lacks digestive enzymes, which favors the survival of ingested microorganisms. The saliva of blood-feeding ticks contains many pharmacologically active molecules that help bypass the host immune defense, including anti-coagulants, inhibitors of platelet aggregation, local anesthetics and anti-inflammatory compounds (133). TBEV can also be transmitted via the consumption of unpasteurized goat, cow or sheep milk. TBEV remains infectious in unpasteurized milk and milk products, such as cheese and yogurt for several days (134). Food-related epidemics occur sporadically (135-137).

Zika virus

The transmission profile of ZIKV differs greatly from TBEV. Mosquitoes are more numerous than ticks, and they have a shorter life span with populations that can be established in suitable conditions fairly easily. Unlike in TBEV transmission, humans can act as reservoir for the virus and transmit the virus further. In the place of its origin, ZIKV is maintained in sylvatic cycles between non-human primates and mosquitoes (Figure 9). Other species, such as bats, goats and rodents, have been found to be positive for ZIKV antibodies in serosurveys, but they likely play minor roles as reservoirs for the virus. In Yap Island and French Polynesian outbreaks, ZIKV was shown to circulate between humans and mosquitoes, which suggests that the virus has adapted to humans as a reservoir host and that the transmission cycle shifted from sylvatic to human-mosquito-human.

Zika virus has been isolated from several mosquito species: *Ae. africanus*, *Ae. luteocephalus*, *Ae. aegypti*, *Ae. vitattus* and *Ae. furcifer* (138-140). During the Yap Island outbreak in 2007, *Ae. hensilli* was the predominant species on the island, but ZIKV could not be detected from any mosquitos (141). ZIKV was first isolated in *Ae. aegypti* in Malaysia in 1966 (139). Virus isolation from a male *Ae. furcifer* suggests vertical transmission, which could be important for maintaining the virus in nature

Clinical picture and pathogenesis

Tick-borne encephalitis

Characteristics of symptomatic infections vary depending on the virus subtype. The typical course for European subtype TBEV infection is biphasic, where the first phase is characterized by mild influenza-like symptoms that often pass without TBE diagnosis. Approximately one week after a tick bite (or the consumption of raw milk products), the first phase begins with abrupt uncharacteristic symptoms, such as fever, headache, nausea, vomiting and myalgia, and the patient is viremic. This phase usually lasts for 5 days (2-10 days) and is followed by a symptomless interval of approximately one week (1-33 days) (146,147). In the first phase, thrombocytopenia, leukopenia and slightly elevated serum transaminase levels can be seen. In one third of the patients, the disease progresses to the second phase with neurological symptoms of differing severity, as the virus enters the central nervous system (CNS) (148). Encephalitic symptoms such as ataxia, dysphasia, altered consciousness and paralysis of the cranial nerve and respiratory muscles are typical (148). During the second phase, leukocytosis and pleocytosis in CSF are observed (147). In up to 18% of patients, MRI shows abnormalities in the thalamus, cerebellum, brainstem and nucleus caudatus (149). The disease severity increases with age, and severe forms are rare in young children. In addition to age, the severity of the disease in the acute phase, low neutralizing antibody titers and IgM response in CSF are associated with more severe forms of TBE (146,150). Approximately 20-40% of patients have been reported to suffer from long-term sequelae up to one year after onset. These include different CNS dysfunctions, such as impairment of memory and decreased ability to concentrate, and occasionally even persisting spinal nerve paralysis (146). The case fatality rate in TBEV-Eur infections is <2%. Infections with the Siberian subtype of TBEV causes often a chronic form of the disease that is usually monophasic. Case fatality rates are reported to be 2-8% for TBEV-Sib infections; death usually occurs 3-7 days after onset of the disease (14,147,148). The onset of the disease in the Far Eastern type of TBEV infection is more often gradual than acute. Typical first-phase symptoms are followed by a stiff neck, sensorial changes, visual disturbances and variable neurological dysfunctions. In fatal cases, death occurs within the first week after illness onset. The fatality rate is reported to be up to 20% for Far Eastern TBE (151). However, these rates may be

biased by the different standards of reporting and medical treatments available in the European and Far Eastern regions.

Langerhans dendritic cells are the primary targets of vector-mediated flavivirus infection. Tick and mosquito saliva contain compounds that modulate the innate immune responses of the first infected cells, thus facilitating the virus infection (152,153). Infected dendritic cells migrate to draining lymph nodes from which the infection spreads to other organs, the spleen, liver and kidney, causing viremia. The major event in TBEV pathogenesis is the entry of the virus into the CNS and brain, which is characterized by neuroinflammation and breakdown of the blood-brain-barrier (BBB). The BBB is a selective semi-permeable physical barrier between the blood circulation and the brain that protects the brain from many pathogens. The BBB consists of epithelial cells that are connected through tight junctions formed by transmembrane proteins (such as occludin and claudins) as well as glial cells, neurons and pericytes (154). Upon infection, the inflammatory responses to viruses may lead to increased permeability of the BBB. Viruses have been suggested to cross the BBB via direct infection, trans- and paracellular transport or the Trojan-horse mechanism (155). Another means for entry to the CNS is retrograde axonal transport. TBEV has been shown to increase the permeability of the BBB, and breakdown of the BBB does not seem to be a prerequisite for TBEV entry into the brain. Rather, the breakdown seems to occur when the virus is already in the brain (156). It was recently suggested that TBEV utilizes the neuronal mRNA transport system and subsequently affects the outcome of the disease (157).

Zika virus disease

As for many flaviviruses, Zika virus infection often appears asymptomatic. Clinical illness is usually mild and lasts for one week. Characteristic symptoms include fever with maculopapular rash, conjunctivitis, myalgia and headache (8). After the outbreaks in French Polynesia and Brazil, neurological complications have been described for ZIKV infections. In adults, ZIKV disease can result in Guillain-Barré syndrome (GBS), meningoencephalitis or myelitis (158,159). GBS is a neuromuscular disease in which the immune system damages peripheral nerve cells, affects motor functions and can cause paralysis. GBS has been reported worldwide and typically arises after viral or bacterial infections (160). The incidence of GBS is reported to be approximately 1.1/100 000 annually (161). The risk of acquiring GBS after ZIKV infection is

estimated to be 0.24/1000 infections, with both symptomatic and asymptomatic ZIKV infections combined. The risk increases with age, and men are more often affected than women (95). In a study conducted with Colombian patients, a prolonged period of ZIKV shedding in urine was found to be connected with the onset of GBS. Additionally, a potential relationship with previous DENV infection was reported in Colombian ZIKV patients with GBS (162).

Virological and epidemiological data have shown the causal relationship of ZIKV infection and microcephaly (163,164). Zika virus RNA can be detected in the placenta and amniotic fluid, as well as in the brain and other organs of fetuses. Microcephaly is a fairly uncommon condition, defined by a developmental defect of the brain with significant reduction in the brain circumference. Congenital microcephaly may be caused by accelerated apoptosis or reduced neuronal proliferation (165). Reports suggest that the risk is increased if the mother is infected during the first trimester, but adverse pregnancy outcomes have also been reported from infections during the second or third trimester (166).

Thus far, little is known about the mechanisms by which ZIKV establishes a persistent infection in certain cells. Zika virus crosses the placenta from mother to fetus and the BBB to infect neurons, and ZIKV has been shown to have tropism for cells of the brain, particularly neural progenitor cells and cortical neurons, as well as many cell types in the reproductive system (167-169). Primary placental macrophages, called Hofbauer cells, together with cytotrophoblasts, have been shown to be permissive for ZIKV infection (170). Hofbauer cells have access to fetal blood vessels and may facilitate transfer or dissemination of the virus to the fetal brain. Mladinich and others showed recently that ZIKV persistently infects and replicates in primary human brain microvascular endothelial cells without cytopathology. Furthermore, ZIKV was released basolaterally from these cells, suggesting a direct means to cross the BBB (171).

A phenomenon called antibody-dependent enhancement (ADE) facilitates the antibodies from previous DENV infection with different serotypes to the binding and internalization of virus particles via the Fc receptors attached to leukocytes. Additionally, immature virus particles are infectious through ADE. DENV antibodies at sub-neutralizing titers have also been shown to enhance ZIKV infection (172-174). In addition, monoclonal antibodies to DENV were shown to bind, but not to neutralize ZIKV, thus promoting infection through ADE. Since DENV and ZIKV are circulating

in the same geographical areas, ADE seems possible, but the impact on disease severity needs to be elucidated.

Diagnostic tests

Flaviviruses are highly cross-reactive, which makes serological assays challenging. Other flavivirus infections or vaccinations (JEV, TBEV, YFV, and WNV) can result in false-positive results or homologous IgM responses, and with both TBE and ZIKV diseases, their clinical pictures resemble that of many others. ZIKV circulates in the same areas as DENV and mosquito-borne alphavirus chikungunya (CHIKV), and patients can even be infected with two of the pathogens from the same mosquito. The patient is viremic from day 4 to 10, and IgM antibodies can be detected in blood for several weeks. In flavivirus diagnostics, IgM antibody positivity is verified by IgG antibody conversion. Previous DENV infection can suppress ZIKV IgM antibodies. Serological tests used in diagnostics include enzyme immunoassays (EIAs), immunofluorescence assays (IFAs), hemagglutination inhibition tests (HIs) and virus neutralization tests (NTs), which are used as a reference test. Viral nucleic acids can be detected by RT-PCR; however, for TBE diagnostics, this is not usually the case, since the patient is viremic only in the first phase, which often goes undiagnosed as a mild flu-like disease, and the virus is cleared from blood before the second phase. ZIKV RNA or antigens can be detected from several body fluids (serum, urine, saliva, or whole blood) and tissues from early disease onset. It has also been shown that ZIKV persists in body fluids and can be detected in saliva or semen weeks and even months after disease onset (175).

Treatment and prevention

There is no effective antiviral treatment for TBE, and patients are treated according to their symptoms. TBE can be prevented by vaccination. TBE vaccines contain formalin-inactivated virus and are widely used across Europe. Wearing protective clothes and repellents and avoiding the consumption of unpasteurized milk products from endemic areas are effective preventative measures (176). The virus is transmitted directly after a tick bite, which makes tick removal an uncertain measure of prevention for TBE. Increasing people's knowledge of TBEV in endemic areas and vaccination are important for the prevention of TBE.

Similar to TBE, there is no effective antiviral treatment for Zika virus disease. Currently, there are several candidate ZIKV vaccines. A DNA-based vaccine is in phase 2 clinical trials in the Americas, and a purified inactivated virus vaccine is in phase 1 (177). A live-attenuated and several investigational DNA, RNA and recombinant vaccines are under development (178). Effective non-specific prevention measures include protective clothing, repellents and removing or emptying water-containing items from surroundings. As ZIKV is a risk for pregnant women or women planning to get pregnant, travel should be planned according to the latest travel recommendations (179).

AIMS OF THE STUDY

We isolated two neuropathogenic flaviviruses, Zika virus and tick-borne encephalitis virus, from human brains. Our aims were:

- to characterize the ZIKV and TBEV cases and analyze the subsequent viral isolates;
- to provide potential proof that congenital ZIKV infections are a causative agent of fetal brain abnormalities;
- to screen and study the antiviral potential of several compounds against the isolated ZIKV; and
- to characterize the new ZIKV isolate by studying its cell tropism in comparison with related epidemic strains.

MATERIALS AND METHODS

Materials

Cells

Cells were maintained in Eagle's Minimal Essential Medium (MEM); Dulbecco's Modified Eagle Medium (DMEM or D-MEM); Roswell Park Memorial Institute (RPMI) 1640 supplemented with glutamine, 100 units/ml penicillin, 100 µg/ml streptomycin and 10% fetal bovine serum (FBS); DMEM-F12 medium supplemented with 50 U/ml PenStrep, 2 mM l-glutamine, 10% FBS, and 0.25% sodium bicarbonate (Sigma-Aldrich); or in a specific culture medium (Table 2) at 37 °C with 5% CO₂ (human cell lines) or at room temperature (mosquito cell lines). During infections, media contained 2% FBS.

For infections (III), the cells were grown in T25 flasks to 80% confluency or in multiwall plates (6, 24 and 96) (II). Cells were infected with a multiplicity of infection (MOI) of 0.1 or 0.2 (III) for 1 h at +37°C (human cell lines) or room temperature (mosquito cell lines), after which the cells were washed once with phosphate buffered saline (PBS), and then cell culture media was added. Thereafter, the cells were incubated for three days either at +37°C (human cell lines) or room temperature (mosquito cell lines). Cells were infected with an MOI of 8.5 (II) without removing the virus stock.

Viruses

The ZIKV FB-GWUH-2016 strain was isolated from a fetal brain in VE6 and SK-N-SH cells (I) and was passaged once in VE6 cells prior to its use in other studies (II), or it was used directly after isolation in SK-N-SH cells (III). Fetal brain tissue was homogenized in 0.2 Dulbecco's bovine serum albumin (BSA) and was then used to inoculate SK-N-SH cells. Viral RNA and the cytopathic effect (CPE) were monitored using an in-house ZIKV RT-PCR (reverse transcription polymerase chain reaction) assay, and the presence of viral antigens was determined on day 6 post-inoculation by immunofluorescence assays (IFAs). The prototypic ZIKV MR766 strain was obtained from Dr. Jonas Schmidt-Chanasit (Berhard-Nocht-Institut für Tropenmedizin, Hamburg, Germany), and it was propagated twice in VeroE6 cells. Freeze-dried Zika virus strains H/PF/2013 (clinical isolate from French Polynesia 2013; H/PF) and

MRS_OPY_Martinique_PaRi_2015 (clinical isolate from Martinique 2015; MRS OPY) were obtained from EVA (European Virus Archive, Marseille, France), and they were propagated once in VeroE6 cells, obtaining passages 2 and 6, respectively (III).

Siberian subtype TBEV was isolated from a human brain in SK-N-SH cells (IV). Virus isolations were attempted from a diseased case's cerebellum tissues. Cerebellum tissue was homogenized in 0.2 Dulbecco's BSA and was then used to inoculate SK-N-SH cells. CPE and viral RNA were monitored using RT-PCR, and the presence of viral antigens was determined on day 6 post-inoculation via immunofluorescence assays (IFAs).

Antiviral agents

Obatoclax, MK2206, SNS-032, dinaciclib and gemcitabine were purchased from Selleck Chemicals, USA. SaliPhe was synthesized by Jef De Brabander's group as described previously (180). Each compound was dissolved in 100% dimethyl sulfoxide (Sigma-Aldrich, MO, USA) to obtain a 10 mM stock solution.

Table 2. Cell lines used in these studies

Organism, Cell line	Anatomic origin	Source	Culture media	Study
Human				
HaCaT	keratinocyte cell line from adult human skin	Kindly provided by Prof. Dr. Petra Boukamp and Prof. Dr. Norbert E. Fusenig, DKFZ, Heidelberg, Germany	D-MEM	III
HFSF	human foreskin dermal fibroblast	Kindly provided by Dr. Magdalena Eisinger, Memorial Sloan-Kettering Cancer Center, New York, NY, USA	D-MEM	III
MRC-5	fetal lung fibroblast	ATCC® CCL-171™	MEM	III
SK-UT-1	uterus epithelial grade III, mesodermal tumor (mixed); consistent with leiomyosarcoma	ATCC® HTB-114™	MEM	III
JAR	placenta epithelial choriocarcinoma	ATCC® HTB-144™	RPMI 1640	III
HUVEC	umbilical vein/vascular endothelium	ATCC® CRL1730™	EBM MV	III
HMEC-1	dermal microvascular endothelium, newborn	ATCC® CRL-3243™	EBM MV	III
A498	kidney epithelial carcinoma	ATCC® HTB-44™	MEM	III
H-2	glioblastoma cell line from a rapidly expanding local brain tumor	(181)	MEM	III
H-4	brain epithelial neuroglioma	ATCC® HTB-148™	D-MEM	III
SK-N-SH	neuroblastoma	ATCC® HTB-11™)	MEM	I, IV
RPE	retinal pigment epithelium	ATCC® CRL-4000™	D-MEM/F12 supplemented with sodium bicarbonate	II
Nonhuman				
Vero E6	Green monkey kidney	ATCC® CRL-1586™	MEM	I, II, III
AE	<i>Aedes aegypti</i>	Kindly provided by X. de Lamballerie, Université de la Méditerranée & Institut de Recherche pour le Développement	L-15 supplemented with tryptose phosphate broth	III
C6/36	<i>Aedes albopictus</i>	ATCC® CRL-1660	L-15	III
AP-61	<i>Aedes pseudoscutellaris</i>	Kindly provided by X. de Lamballerie	L-15 supplemented with tryptose-phosphate broth	III

Methods

RNA extraction and quantitative RT-PCR (I-IV)

RNA was extracted using a Viral RNA Mini Kit according to the manufacturers' instructions (Qiagen, Hilden, Germany). ZIKV RNA was monitored using a ZIKV-RT-qPCR targeting the NS5 protein (163). TBEV RT-PCR was performed as described previously (182). Viral RNA loads were quantitated using a synthetic ZIKV or TBEV RNA transcript as a standard curve. Briefly, RNA was generated from the last 3500 nucleotides of the TBEV (strain Kumlinge A52) and ZIKV NS5 genes (strain MR766) and was then cloned into pGEM®-T vector (Promega, Madison, USA) using the RiboMAX™ Large Scale RNA production system with SP6 polymerase (Promega, Madison, USA) according to the manufacturer's instructions. The viral loads were calculated from pre-quantitated synthetic RNA transcripts.

Cellular RNA was extracted using a RNeasy Mini Kit (Qiagen) according to the manufacturers' instructions. The expression of cellular MxA (183) (forward primer: 5'-AGTATGGTGTGCGACATACCGGA-3' and reverse primer: 5'-AGTATGGTGTGCGACATACCGGA-3'), and RNA polymerase II (184), which was used as a housekeeping gene, (forward primer: 5'-GCACCACGTCCAATGACAT-3' and reverse primer: 5'-GTGCGGCTGCTTCCATAA-3') were analyzed from 50 ng of total cellular RNA using a qScript One-Step SYBR Green RT-qPCR kit (Quantabio, Beverly, MA, USA). The expression of cellular *IFIT1* (forward primer: 5'-TCTCAGAGGAGCCTGGCTAA-3' and reverse primer 5'-TGACATCTCAATTGCTCCAG-3', Sigma Aldrich), *IFIT2* (forward primer: 5'-AAGAGTGCAGCTGCCTGAA-3' and reverse primer: 5'-GGCATTTTAGTTGCCGTAGG-3', Sigma-Aldrich), and *IFIT3* (forward: 5'-GAACATGCTGACCAAGCAGA-3' and reverse: 5'-CAGTTGTGTCCACCCTTCCT-3') were analyzed using a qScript One-Step SYBR Green RT-qPCR kit (Quantabio, Beverly, MA, USA). Samples were analyzed in duplicate. The relative RNA levels were calculated, and the results were represented as fold induction compared to the control.

Virus titrations (II, III)

Supernatants were collected 48 hours post-infection (hpi) from ZIKV-infected RPE cells (II) or 3 days post-infection (dpi) ZIKV-infected cells (III). Infectious virus

particle amounts were determined by plaque assays (II) or end-point titration assays (III). In the plaque assays, virus-containing supernatants were diluted in PBS and added to VeroE6 cells in 6-well plates for 1 h. Virus was removed and cells were overlaid with 1% melted agarose in MEM with 2% FBS, 2 mM l-glutamine, and 50 units/ml PenStrep for 4-6 days. Cells were fixed with 10% formaldehyde for 30 min and stained with 0.1% crystal violet in 2% ethanol. In the end-point titration assays, logTCID₅₀ values were determined using the method of Reed and Muench (185). Briefly, VeroE6 cells were plated in 96-well plates for 24 h prior to infection, and they were then infected in quadruples of each virus dilution from three independent experiments. CPE was observed, and logTCID₅₀ values were calculated.

Immunofluorescence assay (IFA) (I-IV)

IFA slides from ZIKV and TBEV-infected cells were prepared 6 dpi (I, IV) or 3 dpi (III), and cells were fixed with 100% ice-cold acetone. RPE cells were grown on coverslips, treated with the antiviral compounds being studied, infected and fixed with 80% ice-cold acetone (II). ZIKV antigens were stained with ZIKV IgG-positive patient serum (1:40 dilution I; 1:80 dilution II-III) or mouse monoclonal antibody against the TBEV E protein (kindly provided by Dr. Matthias Niedrig, Robert Koch Institute, Berlin, Germany) and were then visualized with Fluorescein (FITC)-conjugated goat anti-human IgG (H+L) or rabbit anti-mouse immunoglobulin (Jackson ImmunoResearch, West Grove, PA, USA) secondary antibody. The nuclei were stained with Hoechst33342.

Next generation sequencing (NGS) (I, IV)

RNA was extracted from SK-N-SH cell supernatant 5 (I; IV, case 1) days after inoculation with a brain tissue sample using a QIAamp viral RNA kit (Qiagen) without carrier RNA. The cerebellum sample from case 2 (IV) was homogenized using a MagnaPure homogenizer for 1 min at 3000 rpm and was then centrifuged through a 0.8- μ m PES filter (Sartorius Vivaclear Mini). The homogenized sample was treated with an ApoH-CaptoVIR kit (ApoH Technologies, La Grande-Motte, France), followed by nuclease treatment for 2 h at +37°C using a micrococcal nuclease (New England Biolabs, MA, USA) and benzonase (Millipore, MA, USA). RNA was extracted with

TriSure reagent (Bioline, London, UK). Ribosomal RNA was removed using a Ribo-Zero Gold rRNA Removal Kit for Epidemiology (Illumina, CA, USA) according to the manufacturer's instructions. The homogenization and RNA extraction of a TBEV-positive tick pool was described in ref. (186). All RNA samples were treated with DNase I (Thermo Scientific, MA, USA).

TBEV RNA (IV) was reverse transcribed and amplified using a WTA2 Complete whole transcriptome amplification kit (Sigma-Aldrich). The sequencing libraries for NGS were prepared using an Illumina NexteraXT sample preparation kit (Illumina) according to the manufacturer's instructions. A ZIKV NGS library was prepared using an Illumina TruSeq Stranded Total RNA LT with Ribo-Zero Gold sample preparation kit (Illumina) according to the manufacturer's instructions.

A NEBNext Library Quant Kit for Illumina (New England Biolabs) was used for library quantitation. Sequencing was conducted using an Illumina MiSeq system with a MiSeq Reagent Kit v2 (I) or v3 (IV), generating 150 or 300-base pair (bp) paired-end reads. Reads were demultiplexed, adapter sequences were removed, and FASTQ files were produced using the MiSeq reporter. De novo sequence assembly was conducted using the MIRA sequence assembler (version 4.9.5) (187,188), followed by the re-mapping of sequence reads to the de novo assembled consensus sequences using the Bowtie2 algorithm (189) implemented in UGENE software (190).

Phylogenetic analysis

All available ZIKV complete genomes or complete coding regions were downloaded from GenBank (27/Feb/2016) (I). Three alignments were constructed for TBEV phylogenetic analysis (IV): one that contained all available TBEV-Eu complete coding sequences, one that contained all available TBEV-Sib complete coding sequences, and one that contained representatives of all major clades of TBEV Eu, Sib and FE (GenBank search May 2017). The sequences were aligned using the ClustalW algorithm implemented in MEGA6 software (191), and the best-fit substitution model was sought. The analyses were conducted using a GTR+G (I) or GTR+G+I (IV) substitution model, an uncorrelated log-normal distributed relaxed molecular clock and a Bayesian skyline demographic model (192). The Bayesian analysis was run for 100 million states and sampled every 1000 states. Posterior probabilities were calculated with a burn-in of 10 million states and checked for convergence using Tracer version 1.6 (193). The

phylogenetic trees were constructed using the Bayesian Markov chain Monte Carlo method implemented in BEAST version 1.8.0 (194).

Cell viability assay (II)

Typically, 40,000 RPE cells were seeded per well and grown for 24 h. The antiviral compounds being studied were added to the cells in 3-fold dilutions at seven different concentrations starting at 10 μ M. No compounds were added to the control wells. The cells were infected with the viruses at an MOI of 0.5-8.5, depending on the strain. When virus-induced CPE was observed (48 hpi), cell viability was measured using Cell Titer Glo assays (CTG; Promega, Madison, WI, USA). The luminescence was measured with a Hidex sense microplate reader (Hidex Oy, Turku, Finland). The half maximal cytotoxic concentration (CC_{50}), the half maximal effective concentration (EC_{50}) and selectivity index (SI) were determined for each compound as described previously in ref. (195).

In the drug combination experiment, RPE cells were treated with increasing concentrations of one drug and a constant concentration of another. The cells were infected with ZIKV at an MOI of 8.5. Cell viability was measured 48 hpi using the CTG assay. To test the synergy of the drug combinations, a zero interaction potency (ZIP) model was used to analyze the observed responses in comparison to the expected combination responses. Drug combinations were classified as synergistic or antagonistic based on the deviations of the observed and expected responses.

Compound-addition assays (II)

In time-of addition assays, 1 μ M obatoclax, SaliPhe, or gemcitabine was added to ZIKV-infected (MOI 8.5) or mock infected RPE cells at 0, 2, 4, 6, 8 and 10 hpi. Cell viability was measured at 48 hpi using the CTG assay (Promega). In the second experiment, ZIKV-infected (MOI 8.5) RPE cells were treated with 1 μ M obatoclax, SaliPhe, or gemcitabine at 0, 2, 4, and 8 hpi. After 2 h of treatment the media was exchanged with plain media. Cell viability was measured at 48 hpi using the CTG assay.

Gene expression profiling (II)

RNA was extracted from ZIKV- or mock-infected RPE cells 10 hpi using an RNeasy Mini kit (Qiagen, Hilden, Germany). Gene expression profiles were generated with an Illumina Human HT-12 v4 Expression BeadChip Kit as described previously. Differentially expressed genes between the samples and controls were determined using the Limma package in the Bioconductor suite for R (196). The Benjamini-Hochberg multiple correction testing method was used to filter out differentially expressed genes based on a q-value threshold ($q < 0.05$). Filtered data were sorted by logarithmic fold change ($\log_2 Fc$). A heatmap was generated using Breeze, an in-house developed interface. Gene set enrichment analysis was performed using open-source software (197).

Metabolomics (II)

Metabolomics analysis was performed as described previously. Briefly, 10 μ L of a labeled internal standard mixture and 0.4 mL of solvent (99% acetonitrile (ACN) and 1% formic acid (FA)) were added to 100 μ L of sample (cell culture media). The extracts were dispensed in Ostro™ 96-well plates (Waters Corporation, Milford, USA) and filtered by applying vacuum at a delta pressure of 300-400 mbar for 2.5 min on a Hamilton StarLine robot's vacuum station. Sample analysis was performed on an Acquity UPLC-MS/MS system (Waters Corporation, Milford, MA, USA). The detection system, a Xevo TQ-S tandem triple quadrupole mass spectrometer (Waters, Milford, MA, USA), was operated in both positive and negative polarities with a polarity switching time of 20 msec with electrospray ionization (ESI) at a capillary voltage of 0.6 kV for both polarities. The source temperature and desolvation temperature of 120°C and 650°C, respectively, were maintained constantly throughout the experiment. The Multiple Reaction Monitoring (MRM) acquisition mode was used to quantify the metabolites with an individual span time of 0.1 sec given in their individual MRM channels. Data acquisition, data handling and instrument control was accomplished using MassLynx 4.1 software. Data processing was performed with TargetLynx software, and metabolites were quantified by calculating curve area ratios using labeled internal standards (IS) (area of metabolites/area of IS) and external calibration curves. Metabolomics data were \log_2 transformed for linear modeling and empirical-Bayes-moderated t-tests using the Limma package. To analyze the differences

in metabolite levels, a linear model was fit to each metabolite. The significant metabolites were determined at a controlled Benjamini-Hochberg false discovery rate (FDR) of 10%. A heatmap was generated using the Pheatmap package (198) based on log transformed profiling data. MataboAnalyst 3.0 was used to identify pathways related to ZIKV infection.

Caspase 1, 3/7, 8 and 9 activity assays (II)

Caspase-Glo-1, 3/7, 8 and 9 assays (Promega) were used to measure the respective caspase activities in the antiviral compound experiments at 40 hpi according to the manufacturer's instructions. The luminescence was measured with a Hidex sense microplate reader (Hidex Oy, Turku, Finland).

Phosphoprotein and cytokine profiling (II)

Cells were lysed 10 hpi, and phosphorylation profiles of 43 kinases and 2 kinase substrates were analyzed using the human phosphokinase array (R&D Systems) according to the manufacturer's instructions. Cytokines were analyzed from the media of ZIKV- or mock-infected un- or compound-treated RPE-cells at 48 hpi using a Proteome Profiler Human Cytokine Array Kit (R&D Systems) according to the manufacturer's instructions. The results were analyzed using ImageJ software. An at least 2-fold difference in the expression levels between mock and ZIKV-infected, compound-treated or ZIKV-infected/compound-treated samples was considered differentially expressed.

Statistical analysis (I-IV)

Student's *t*-test was used for all statistical analyses. A *P*-value of <0.05 was considered statistically significant.

RESULTS AND DISCUSSION

Isolation of ZIKV and TBEV from human brains (I, IV)

ZIKV

We monitored a case of a 33-year-old pregnant female who was suspected to have contracted Zika infection during the 11th week of gestation while travelling in Central America, most likely in Guatemala, in late November 2015. Prolonged maternal viremia was detected in the patients' sera, showing positive RT-PCR results with approximately 1 copy per ml of serum in samples taken at 16 and 21 weeks of gestation. Serologic evidence for ZIKV infection was obtained during week 17, showing a titer of more than 1:2560 in a plaque reduction neutralization test (PRNT) performed in the US. Amniotic fluid was positive for ZIKV RNA at week 19. No evidence of microcephaly or other abnormalities was seen via ultrasonography performed 1, 4 and 5 weeks after resolution of the symptoms. However, there was a decrease in fetal head circumference from 16 to 20 weeks of gestation. MRI performed at 20 weeks showed abnormal features in the developing brain: diffuse atrophy of the cerebral mantle, enlarged ventricles and a shortened corpus callosum. The pregnancy was terminated at week 21. Serum, blood, peripheral blood mononuclear cells, saliva, urine and plasma of the mother obtained 11 and 13 days after termination were negative for ZIKV RNA (Figure 10).

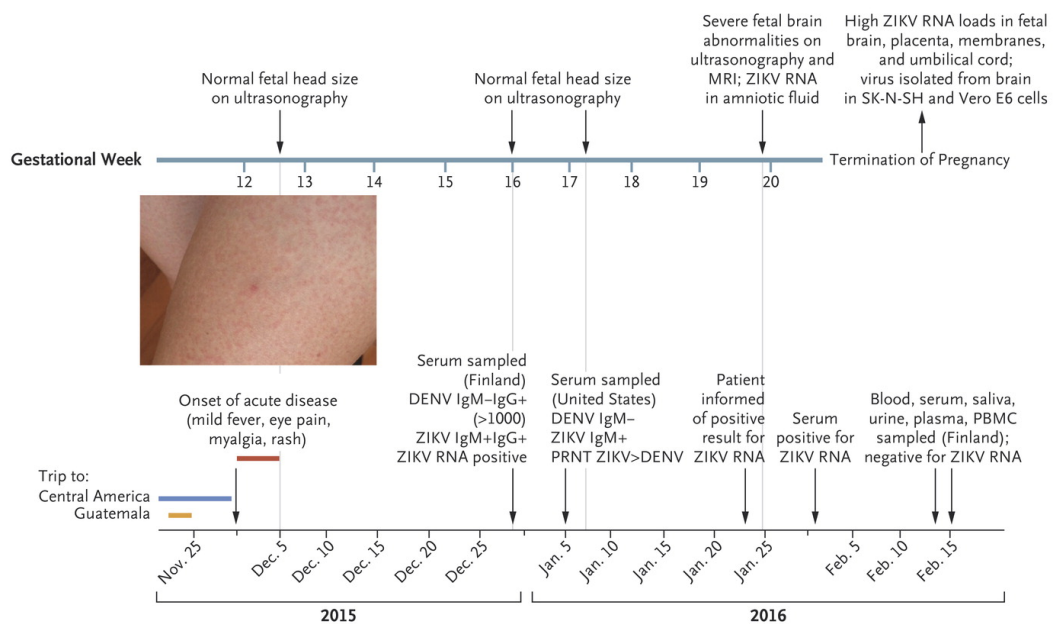
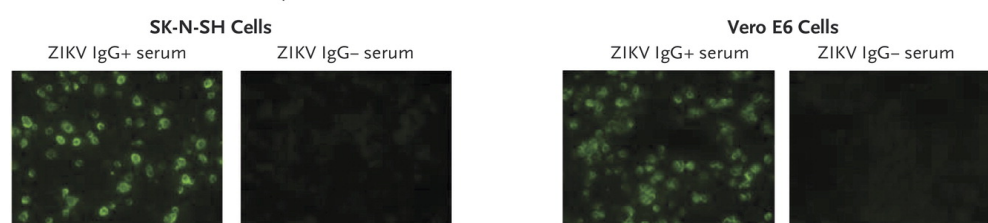


Figure 10. Timeline of symptoms and clinical and laboratory findings. Reproduced with permission from Driggers *et al. NEJM* 2016.

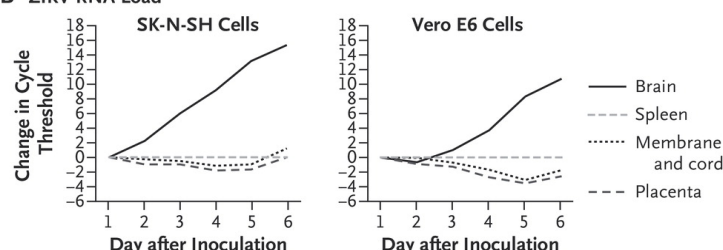
Post-mortem analysis showed abundant apoptosis primarily affecting the intermediately differentiated post-migratory neurons in the neocortex. In contrast, well-differentiated neurons in the basal ganglia and limbic regions appeared unaffected. In addition, white matter and the subventricular zone showed severe volume loss with axonal rarefaction and macrophage infiltrates.

Zika virus isolations were attempted from the tissues of the affected mother and the fetus, in whom the presence of viral nucleic acids was detected by RT-PCR; the serum of the patient, fetal brain, placenta, fetal membranes/umbilical cord and spleen were used to inoculate SK-N-SH human neuroblastoma, Vero E6 green monkey kidney and C6/36 *Aedes albopictus* mosquito cells. A ZIKV strain designated FB-GWUH-2016 (FB-GWUH, for short) was isolated from fetal brain tissue in human SK-N-SH cells and VE6 cells. The virus growth was more pronounced in the neuroblastoma cells from the day of inoculation compared to VE6 cells, which presented an initial lag phase of three days before substantial virus replication occurred. CPE was monitored and viral RNA load was determined daily from cell culture supernatants using an in-house ZIKV real-time RT-PCR (ZIKV-RT-qPCR) assay, and the presence of viral antigens was determined on day 6 post-inoculation via immunofluorescence assays (IFA) (Figure 11).

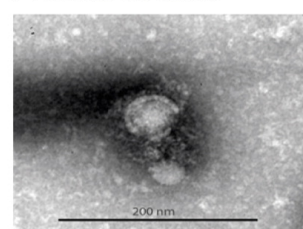
A ZIKV on Immunofluorescence Assay



B ZIKV RNA Load



C Flavivirus-like Particle



D Amino Acid Difference in Newly Isolated ZIKV Strain

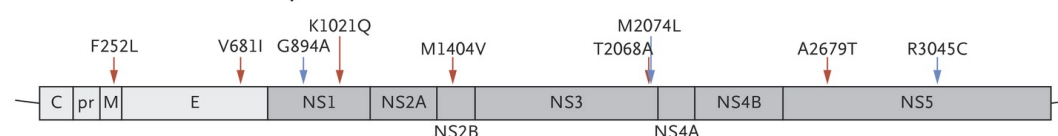


Figure 11. Isolation of the FB-GWUH-2016 strain from a fetal brain. Reproduced with permission from Driggers *et al. NEJM* 2016.

The complete genome sequence of the isolated virus was obtained by next generation sequencing (NGS) of the cell culture supernatant on day 5 post-inoculation. Phylogenetic analysis of the FB-GWUH (GenBank accession number KU870645) viral strain showed that the virus was a member of the Asian genotype and was closely related to ZIKV sequences previously obtained from Guatemala. FB-GWUH has 8-14 amino acid mutations compared to previous virus strains from the Americas. Five of the mutations were specific to FB-GWUH compared to the other Guatemalan viruses sequenced at the time. Three of the amino acid mutations were specific for the three Guatemalan strains discussed here, and one amino acid substitution was a reversion to the African genotype (Figure 11).

The magnitude of the ZIKV epidemic in the Americas was striking. Previous outbreaks had shown the capability of the virus to cause neurological manifestations, but the epidemic of microcephaly was unforeseen. The isolation of ZIKV FB-GWUH from affected fetus' brain was considered a key piece of evidence in the search for causal relationship of ZIKV and microcephaly. The spread of ZIKV to a previously naïve population with favorable socio-economical structures has most likely considerably affected the course of the epidemic. The epidemiological and virological studies on ZIKV have multiplied by the hundreds during 2016 compared to the preceding time. Reports suggest that the ZIKV virus strains now circulating in the Americas could be more neuropathogenic and virulent than other strains. The ZIKV strains show cell tropism especially to undifferentiated neural progenitor and neural stem cells. The characteristic prolonged viremia and virus shedding from certain tissues is specific to ZIKV infection.

The FB-GWUH strain showed unique amino acid differences when compared to ZIKV isolates from the same geographical area. Amino acid differences are also found from the virus sequence obtained directly from the brain tissue of the fetus compared to the sequence obtained from the blood of the expectant mother taken the day of the disease onset (Teemu Smura, unpublished results). These mutations in the nonstructural region seem to be indicative of selection when infecting the fetus. The impact of these mutations is to be investigated.

The mechanism by which ZIKV crosses the placenta from infected mother to fetus is not yet fully known. It has been suggested that the virus particularly infects placental macrophages, Hofbauer cells, and traverses through the developing placenta to gain access to placental veins and subsequently the fetus. Disease severity in dengue

infections is related to secondary DENV infections through ADE. Intriguing question is, whether ADE would play a role in virus dissemination in the placenta. Primary infection with one DENV serotype provides lifelong immunity to the same but not different serotypes. In sub-neutralizing conditions, it enhances the secondary infection, potentially causing severe dengue with hemorrhagic fever or shock (199). DENV antibodies have also been shown to enhance ZIKV infections (172), which could have in part affected the course of the ZIKV epidemic. Whether it is the genetic differences of these viruses or the hosts, or both, that have had an impact on the epidemic, remains to be elucidated.

TBEV

In 2015, two fatal cases were reported from a recently emerged TBE focus in the Kotka Archipelago, Finland. Both of the fatal cases, as well as two other (nonfatal) cases, were reported from the same small island of Kuutsalo. The first fatal case was a previously healthy 36-year-old female. She experienced a febrile illness that lasted for one week before the sudden onset of disturbed vision, severe headache and numbness of the right arm. Her MRI was normal. Two days later, she was admitted to a tertiary care unit due to disorientation and right hemiparesis. MRI showed indications of viral meningeal process in cortical sulcus regions, and CSF demonstrated pleocytosis. Her condition deteriorated rapidly, and a head CT scan revealed cerebellar herniation. The patient died after three days in the hospital. CSF and blood were positive for TBEV-IgM, and TBEV specific antibodies were detected by hemagglutination inhibition (HI) at a titer of 20.

Post-mortem, massive brain edema and tonsillar herniation were detected. Severe signs of widespread viral encephalitis, such as meningeal and perivascular inflammation, neuronophagy and endothelial damage, were observed. A marked inflammation was observed throughout the CNS with lymphocytes, macrophages, plasma cells and microglial reactions (Figure 12).

The medulla, cerebellum, spinal cord and spleen were positive for TBEV RNA by RT-PCR (Figure 12). Virus isolation was successful from the cerebellum in SK-N-SH cells, but not in VE6 cells. Viral RNA copy numbers were monitored using TBEV RT-PCR, and the presence of viral antigens was determined on day 6 post-inoculation by immunofluorescence assays (IFA). A full genome sequence was obtained from the cell culture supernatant on day 6 by NGS. The isolated virus was of the Siberian subtype,

and phylogenetic analysis showed its close relationship to a previous isolate from the serum of an acute TBE patient in Latvia (Figure 13).

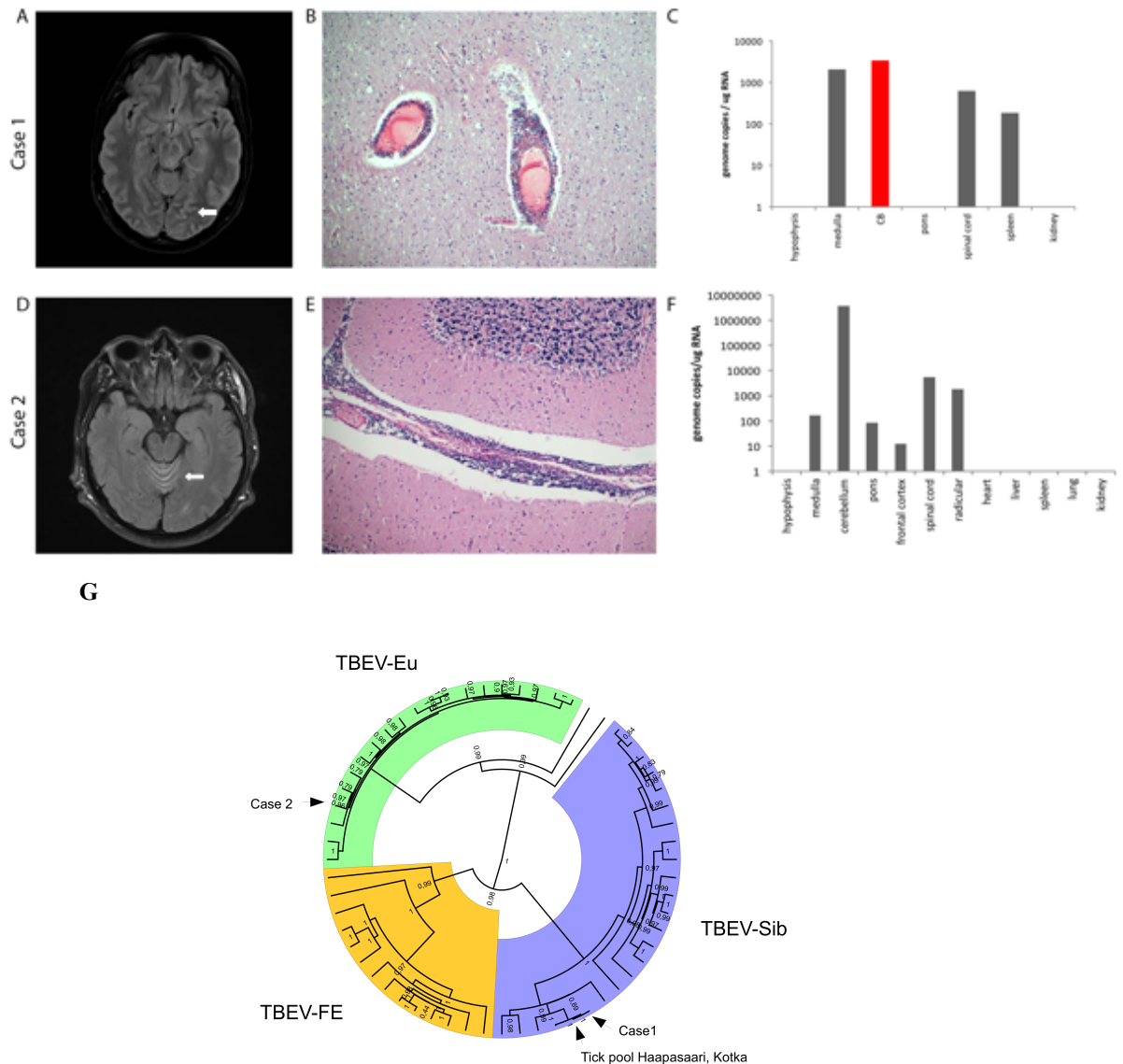


Figure 12. Pathological and virological findings. (A) MRI of case 1 demonstrated pathologically increased signal in cortical sulcus regions indicative of viral meningeal process. Hematoxylin and eosin (HE) staining of the frontal cortex of case 1 showed inflammation throughout the CNS from the spinal cord to the cortex (B) and cerebellum. Increased signal is shown in the MRI of case 2 in the facial nerves, cortical sulci radicular regions and cerebellar vermis (D). Neuropathological examination showed microscopically abundant perivascular lymphocytosis in the cerebellum of case 2 (E). TBEV RNA was detected in several parts of the brain of both cases and in the spleen of case 1 (C, F). The Siberian subtype of TBEV was isolated from the cerebellum of case 1, and the full-length genome was sequenced. The whole genome sequence of a new European subtype was obtained directly from the cerebellum of case 2. (G) A phylogenetic tree of the complete coding regions using the Bayesian MCMC method with a TN93-G-I model of substitution, a lognormal relaxed clock model and a Bayesian skyline demographic model. Posterior probabilities are shown at each node.

Previously, a TBEV-positive *I. ricinus* tick pool was collected from a neighboring island, Haapasaari (186). We subjected all RNA in this tick pool to metagenomic analysis, and a whole TBEV genome was obtained directly from the tick material; this tick TBEV sequence was almost identical to the sequence of the brain isolate. The two genomes have 3 nucleotide differences, which result in two amino acid substitutions: R868K in NS1 and V1452A in NS2B, suggesting virus adaptation either to the human brain or cell culture (Figure 13).

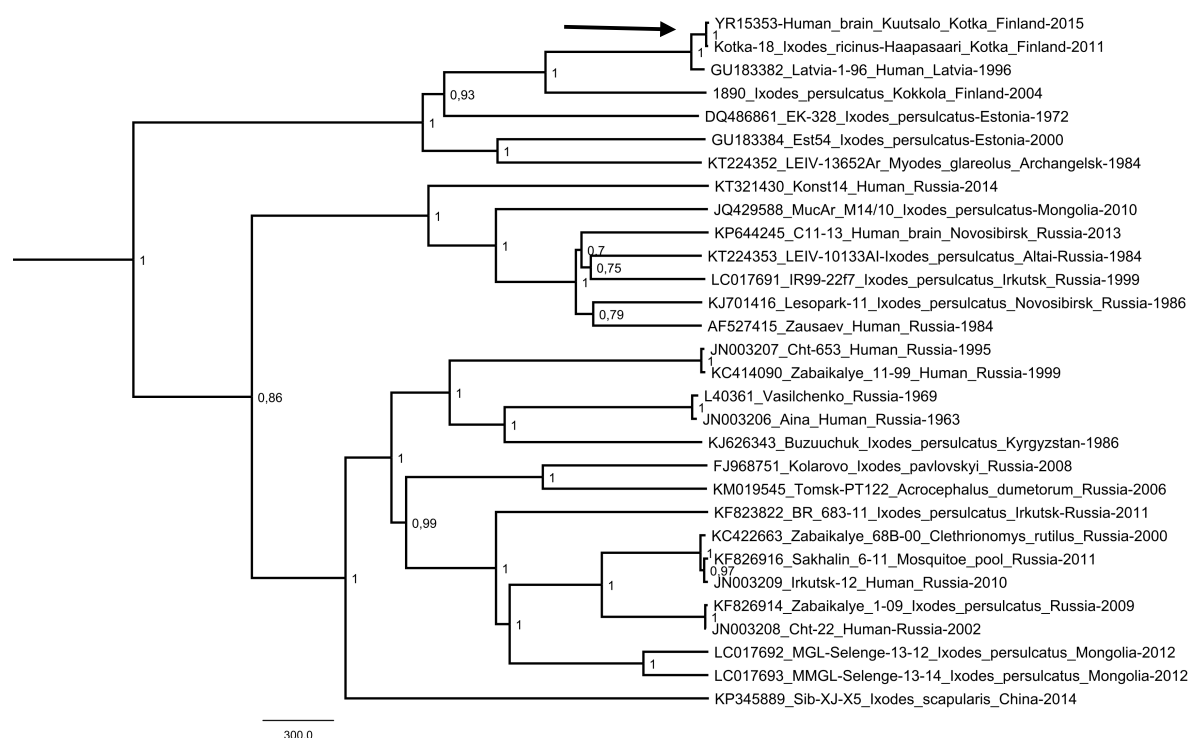


Figure 13. Maximum clade credibility tree of a TBEV-Sib strain isolated in Kuutsalo and a whole genome obtained from an infected tick pool (arrow) in Haapasaari, Finland.

Case 2 was a 66-year-old immunocompromised male with hypertension, diabetes and chronic lymphatic leukemia. The patient had persistent fever two weeks before hospitalization. At admission, he had developed tetraparesis and urinary retention. Increased signal was observed in the cerebellar vermis, facial nerves, cortical sulci and radicular regions in MRI (Figure 12). Pleocytosis was observed in CSF, but both CSF and serum were TBEV-IgM negative. CSF was IgM positive one week later. The patient had hypogammaglobulinemia, which likely aggravated the course of the disease and delayed serological diagnosis. The patient died after four weeks in the hospital.

Severe coronary disease, cardiac hypertrophy and atherosclerosis as well as bronchopneumonia were observed in the post-mortem examination. Disseminated encephalitis of viral origin was observed in the neuropathological examination: perivascular lymphocytosis continuing to the brain parenchyma, causing neuronophagy and glial reactivity. The frontal cortex, pons, medulla, radicular, spinal cord, and cerebellum were RT-PCR positive for TBEV (Figure 12). Virus isolation trials from the RNA-positive tissues were unsuccessful. However, through metagenomics, the whole virus sequence was obtained directly from the cerebellum. The virus was of the European subtype and was phylogenetically closely related to the previously described virus strain Kubinova, with the most common recent ancestor dating back hundreds of years (675, 95% CI 298-1003 years) (Figure 14). A TBEV-positive tick was collected in Kuutsalo in 2017, and the sequence analysis confirmed the virus to be of European subtype, and furthermore, highly similar to the genome sequenced from the cerebellum of case 2 (our unpublished results).

TBE has spread to new areas in Finland during the past decade. The Kotka archipelago represents a newly established TBEV focus, since no cases were reported before 2010. Thereafter, 20 cases have been reported, two of which were fatal. Siberian subtype TBEV was already previously found in an unusual combination with *I. ricinus* ticks in the Kotka archipelago (186), which is why TBEV-Eur was a somewhat surprising finding as the causative agent of the second fatal infection. The coexistence of two TBEV subtypes was further confirmed by TBEV-infected tick collected in Kuutsalo, which makes the focus unique.

There is a considerable infection pressure in this small focus, given that the virus was found in a tick in the same area, where TBE cases were reported. The underlying reasons for the seemingly high virulence of the two cocirculating subtypes remain to be elucidated. Several important risk factors for disease severity and development in flavivirus infections have been identified in epidemiological studies. Age and gender are predisposing factors for severe disease outcome in many flavivirus infections (the young are more susceptible to DENV and JEV, while older people are more susceptible to WNV and TBEV). With ZIKV disease, in addition to the risk for pregnant women, men are more often affected by GBS. In TBEV infections, men in older patient groups tend to be more at risk of contracting severe encephalitis. In addition, genetic variation in several host genes, such as MHC-1 and phospholipase C in DENV infection and DC-

SIGN, CCR5, TLR3, OAS and TNF- α in TBEV, may influence the severity of the disease (200-204).

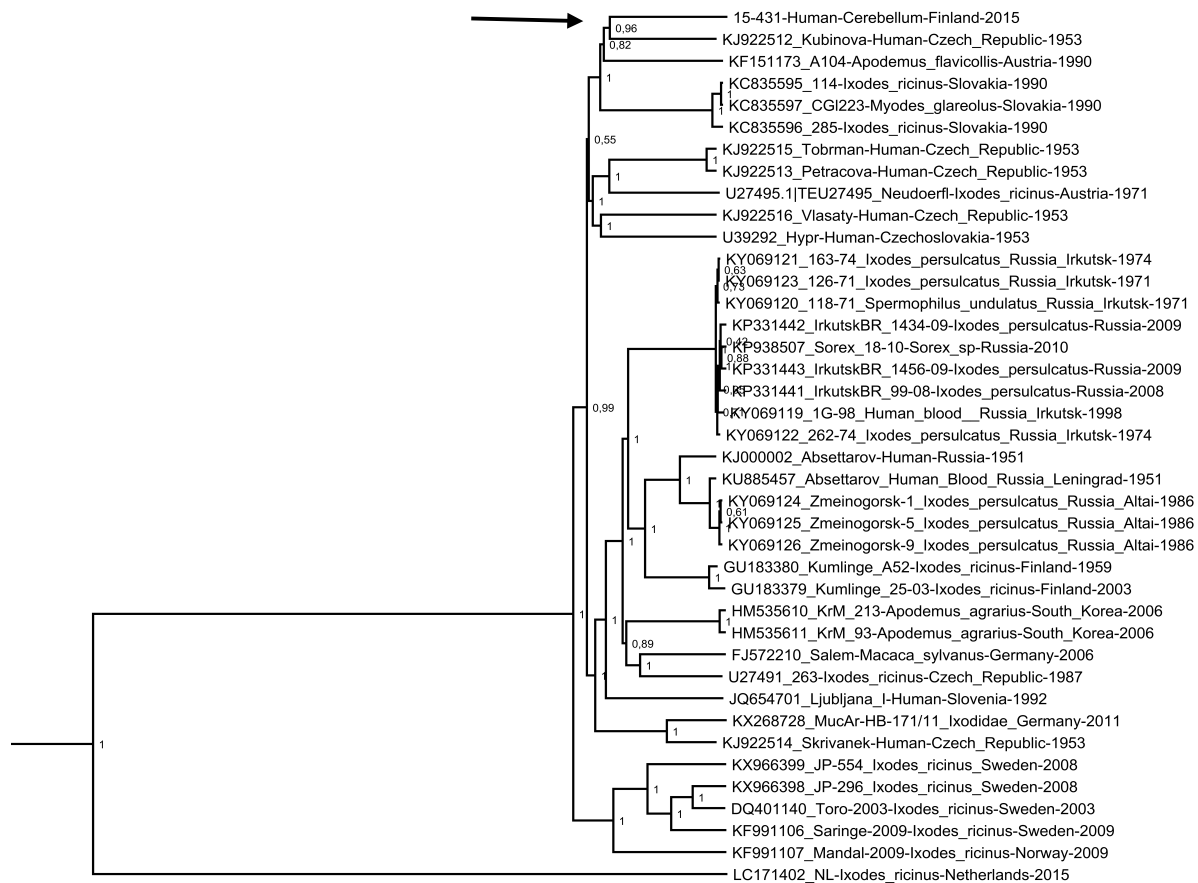


Figure 14. Maximum clade credibility tree of TBEV-Eur isolated in Kuutsalo (arrow), Finland.

The two patients described here had very aggressive and rapid progression of the disease. The first patient was young and previously healthy, and she died after three days of hospitalization due to herniation. The second patient was immunocompromised, and he died after four weeks in the hospital due to tetraplegia and subsequent complications. Notably, in both cases, initial antibody titers to TBEV were low. The impact of the amino acid substitutions of the Siberian strains on virulence requires further investigation, as does potential host susceptibility factors. The coexistence of the two TBEV subtypes in the same focus is surprising. Furthermore, two fatal cases occurring in a small focus a few weeks apart is uncommon. These findings warrant further surveys on the distribution and prevalence of these viruses.

Anti-ZIKV potential of obatoclax, saliphenylhalamide and gemcitabine (II)

As there is no specific antiviral treatment for ZIKV infections, we wanted to screen several potential antiviral compounds using the new clinical isolate, the ZIKV FB-GWUH strain. We investigated six anti-cancer compounds for their efficiency to inhibit ZIKV infection: obatoclax, SaliPhe, gemcitabine, SNS-032, dinaciclib and MK2206. Obatoclax (GX15-070) is a phase two anti-cancer drug that inhibits Bcl-2 family proteins, inducing apoptosis in cancer cells. It has been shown to inhibit the endocytosis of several viruses, such as influenza A and B and Sindbis virus by targeting the cellular Mcl-1 protein (205). Saliphenylhalamide (SaliPhe) is a vacuolar ATPase (vATPase) inhibitor that prevents the acidification of endosomes. SaliPhe is in pre-clinical phase for cancer treatment and it has been shown to be effective against influenza viruses and papilloma virus by arresting viral entry into endosomes (180,206). Gemcitabine (difluorodeoxycytidine) is a pyrimidine analogue that has been used to treat breast, lung and pancreatic cancer, for example. Gemcitabine can incorporate into DNA and RNA (207). It has also been shown to inhibit replication of the abovementioned viruses (205). Compounds that inhibit cyclin-dependent kinases (CDKs) (SNS-032 and dinaciclib) and protein kinase B (PLB, also known as Akt) (MK2206) and have an effect on influenza A virus infection were also included in this study (195,208). We tested these compounds on FB-GWUH-infected retinal pigment epithelial cells, which are also involved in ZIKV pathogenesis.

We found that obatoclax, SaliPhe and gemcitabine were able to inhibit ZIKV replication, protein synthesis and infectious virus particle production at non-cytotoxic concentrations via the measurement of cell viability, viral RNA production, antigen presentation and infectious virus production (Figures 15 and 16). Furthermore, inhibition was observed at nanomolar concentrations when the cells were treated with different combinations of the compounds. A substantially lower concentration (62 nM compared to 1 μ M) of SaliPhe together with 62 nM obatoclax was sufficient to inhibit ZIKV infection. To evaluate the significance of the combined effect of the given compounds, we compared the observed responses to the expected combination responses using a zero interaction potency (ZIP) model (209). Although obatoclax-gemcitabine, obatoclax-SaliPhe and SaliPhe-gemcitabine combinations were classified as antagonistic, synergistic interactions were found at multiple doses for these combinations. Based on the average synergy scores over the whole landscape, we

concluded that a combination of obatoclast-SaliPhe at non-cytotoxic concentrations could enhance the inhibition of ZIKV infection. We also investigated the effect of the time of addition and the time of treatment on cell viability of infected cells. Obatoclast and SaliPhe were able to protect cells from ZIKV-induced cell death when added during the first hours of infection, but the effect of gemcitabine was notable even when added several hours post-infection.

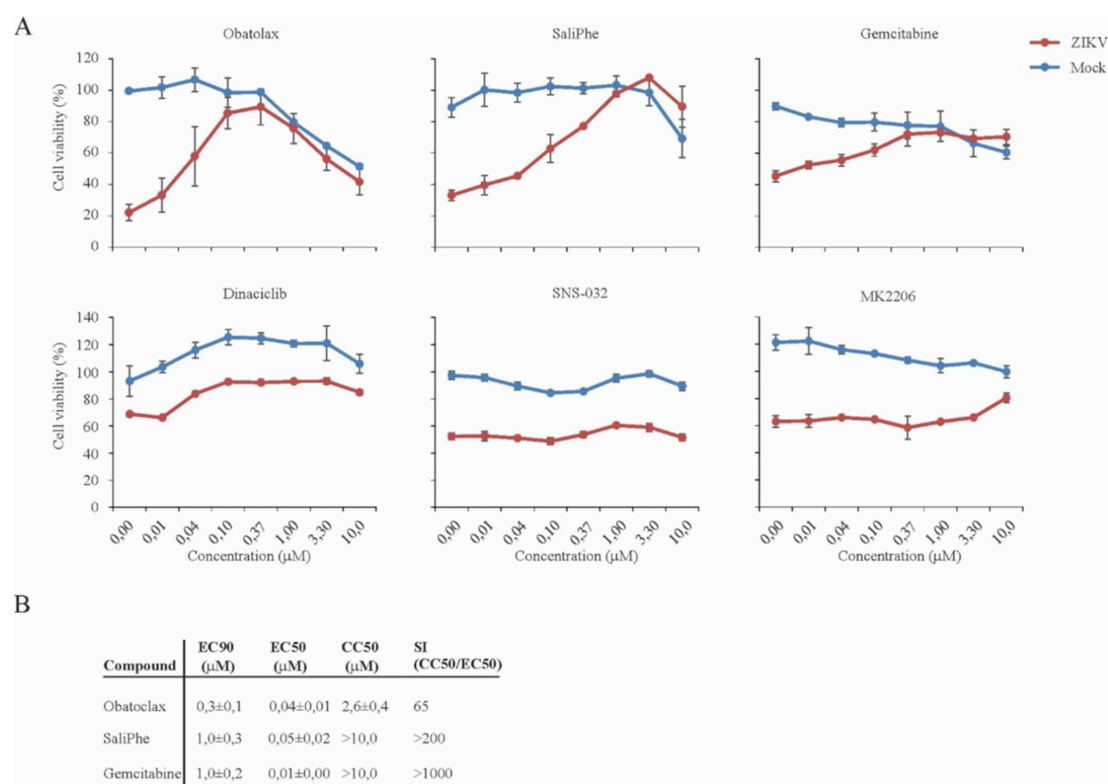


Figure 15. Obatoclast, SaliPhe and gemcitabine, but not dinaciclib, SNS-032 or MK2206, inhibit ZIKV-induced cell death at μM concentrations. (A) Cells were treated with compounds at increasing concentrations in mock and ZIKV-infected cells. The cell viability was measured via CTG assays. (B) The effective concentration (EC) 90, EC₅₀, and cytotoxic concentration (CC₅₀) values and the SI indexes were calculated. Reproduced with permission from Kuivanen *et al. Antiviral Res.* 2017.

Traditionally, the antiviral agents target the virus components. Flaviviral enzymatic proteins, such as NS3, are well conserved among different species and thus provide a solid base for broad-spectrum antiviral agents. In comparison, treating HIV and HCV with protease inhibitors have proven effective (210). Polymerase inhibitors are also attractive targets for antiviral development as NS5 lacks a eukaryotic homologue. Another approach for antiviral screening and development are the cellular targets.

Several cellular target candidates for anti-ZIKV and anti-flavivirus agents have been reported. α -Glucosidase modifies the N-linked glycans and participates in the folding and maturation of flaviviral glycoproteins. α -Glucosidase inhibitors have been shown to possess broad-spectrum antiviral activity against flaviviruses and many other enveloped viruses, but they need to be administered at high dosages and are relatively toxic (30). Chloroquine, which is an anti-malarial drug, is shown to inhibit ZIKV infection by raising the endosomal pH in cells of neural origin (211). Similar to chloroquine, SaliPhe also functions in the early steps of ZIKV infection by inhibiting the endocytosis. Host targets have high potential for broad-spectrum antiviral development, which is also a prerequisite, since even closely related flaviviruses can use cellular targets differently. ZIKV is neurotropic, which directly affects the approach of drug design and discovery. Flaviviruses can be in high loads in the brains, which makes the crossing of the BBB a crucial pharmacokinetic aspect. In addition, ZIKV infection affects the fetus most severely, which makes the antiviral challenge even greater. Many (antiviral) compounds are not recommended for use during pregnancy. Recently, a large library of US Food and Drug Administration (FDA) -approved drugs was screened for anti-ZIKV activity (212). All together 20 compounds showed anti-ZIKV effect, and the nucleoside analogue gemcitabine was discovered effective in HUH7 cells, simultaneously to our study. Together with previous studies, anti-flaviviral activity was shown for bortezomib, ivermectin and mycophenolic acid (MPA) by inhibiting virus replication (213-215). However, many of these drugs warrant caution of use during pregnancy, gemcitabine among them. Obatoclax inhibits a wide range of Bcl-2 proteins that possess pro and anti-apoptotic properties. Mcl-1 is an anti-apoptotic protein that has been identified as a target for obatoclax. Obatoclax is also reported to reduce the acidity in endosomal vesicles, and is thus able to inhibit the entry of ZIKV. Identification of Mcl-1 provides a foundation for further anti-ZIKV drug development. Furthermore, there is an indication that obatoclax mesylate is able to cross the BBB (216).

The search for anti-ZIKV drugs has accelerated after the epidemic in the Americas. However, the discovery of new antiviral agents is its initial steps towards approved treatments for acute ZIKV or flavivirus infections in general. Drugs targeting the cellular functions is a promising approach as RNA viruses are prone to mutations. In the present study, we found anti-ZIKV compounds that inhibit the endosomal acidification and *de novo* pyrimidine synthesis, and which function in non-cytotoxic concentrations. Our data provides a foundation for the further identification of anti-ZIKV compounds

and widens the application spectrum of obatoclax, SaliPhe and gemcitabine. These three compounds inhibit ZIKV infection *in vitro* in retinal cells, and the results need to be further verified in cells of neural origin as well as *in vivo*.

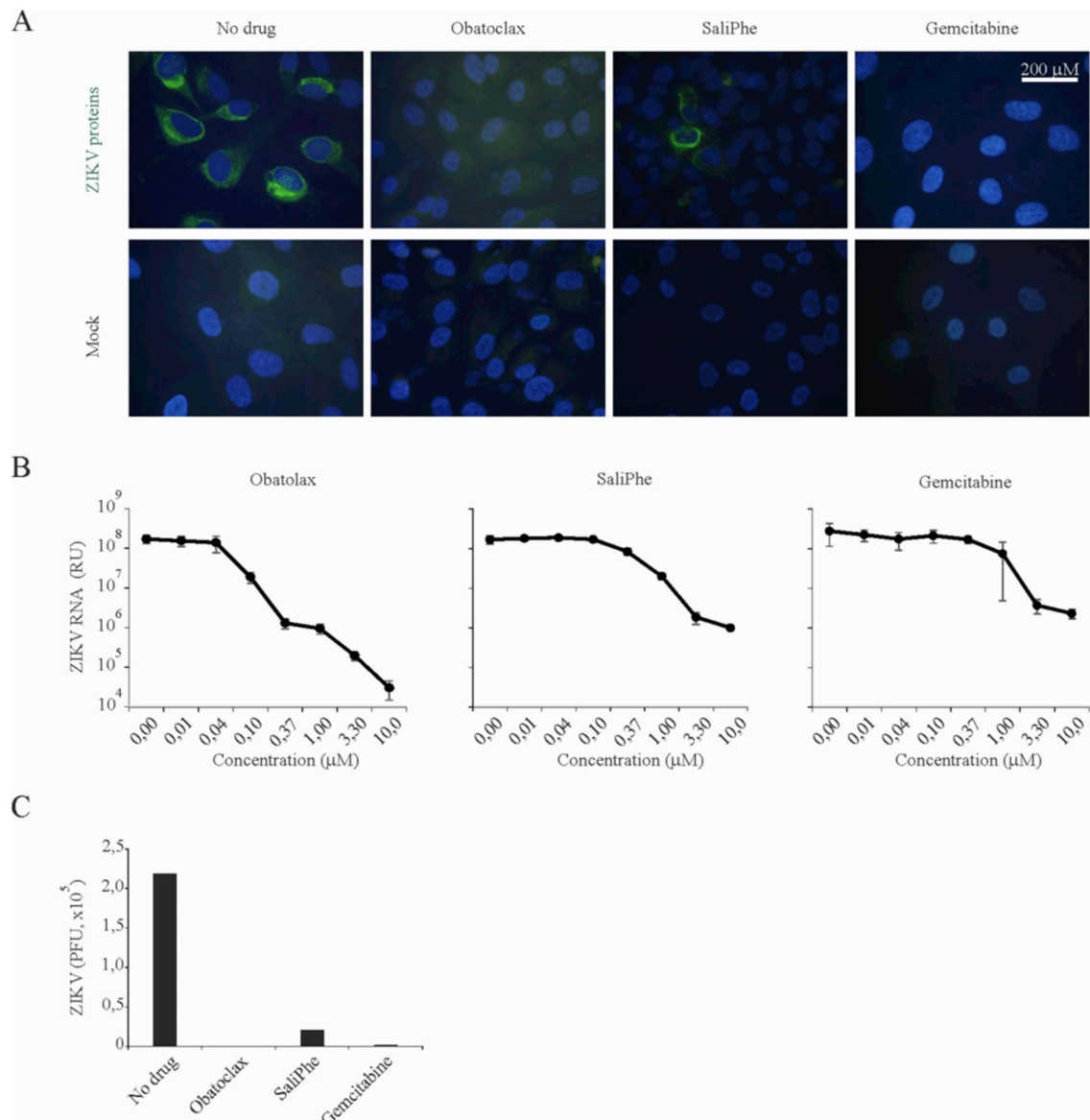


Figure 16. Obatoclax, SaliPhe and gemcitabine inhibit ZIKV virus replication in RPE cells. (A) Mock, ZIKV-infected and compound-treated cells were stained for ZIKV antigens using ZIKV-positive patient serum and a FITC-conjugated secondary antibody. (B) RT-qPCR of ZIKV RNA from mock, ZIKV-infected and compound-treated cell culture supernatants. (C) ZIKV virus titers were determined from ZIKV-infected and compound-treated (2 μ M) cell culture supernatants. Reproduced with permission from Kuivanen *et al. Antiviral Res.* 2017.

Obatoclax, saliphenylhalamide and gemcitabine differentially affect cellular signaling, transcription and metabolism (II)

We further investigated the effect of the three compounds on cellular transcription, signaling, metabolism and apoptosis in ZIKV-infected and uninfected cells. Recently, Frumence and others showed that ZIKV infection activates caspases 3 and 9 to induce apoptosis in lung epithelial A549 cells (217). ZIKV-induced apoptosis has also been reported in neural progenitor cells where caspase 3/7 was activated at 24 hpi (218). We tested the effect of the compounds on caspase activation. RPE cells were treated with 1 μ M concentrations of the compounds and were then infected with ZIKV. At 40 hpi, caspase 1, caspase 3/7, caspase 8 and caspase 9 activities were measured. Obatoclax, SaliPhe and gemcitabine were able to block ZIKV-induced apoptosis by inhibiting caspase 3/7. Inhibitors of caspases could further broaden the targets for ZIKV antivirals. We next tested the effect of these compounds on the transcription and phosphorylation statuses of cellular proteins. Using a targeted phosphoprotein-profiling assay, we found that at 10 hpi, ZIKV infection and gemcitabine treatment affected the phosphorylation status of CREB1, a cyclic AMP-responsive element binding protein. CREB1 is involved in cell survival, growth, differentiation and transcriptional regulation of antiviral responses (219). All compounds affected the phosphorylation status of CREB1 in uninfected cells, but only gemcitabine did in ZIKV-infected cells. The phosphorylation status of cyclin-dependent kinase (CDK) inhibitor 1B (p27) was affected by obatoclax and gemcitabine treatment in ZIKV-infected and uninfected cells. In addition to CDK inhibition, p27 regulates the progression of the cell cycle (220). It has been suggested that ZIKV reduces cell proliferation and increases apoptosis (218). Using an RNA microarray, we were able to profile cellular target gene expression. Obatoclax and SaliPhe inhibited several cellular genes, whereas gemcitabine-treated cells also expressed antiviral genes. We further verified these results through mRNA detection of *IFIT1*, *IFIT2* and *IFIT3* (Figure 17). The three compounds differentially affected uninfected cells, and SaliPhe had no effect on cellular gene expression (Figure 17).

We analyzed 110 metabolites in cell culture supernatants from ZIKV infected and compound-treated cells at 48 hpi. Reliable quantification was achieved for 92 metabolites. Surprisingly, the purine metabolite levels were affected by obatoclax and

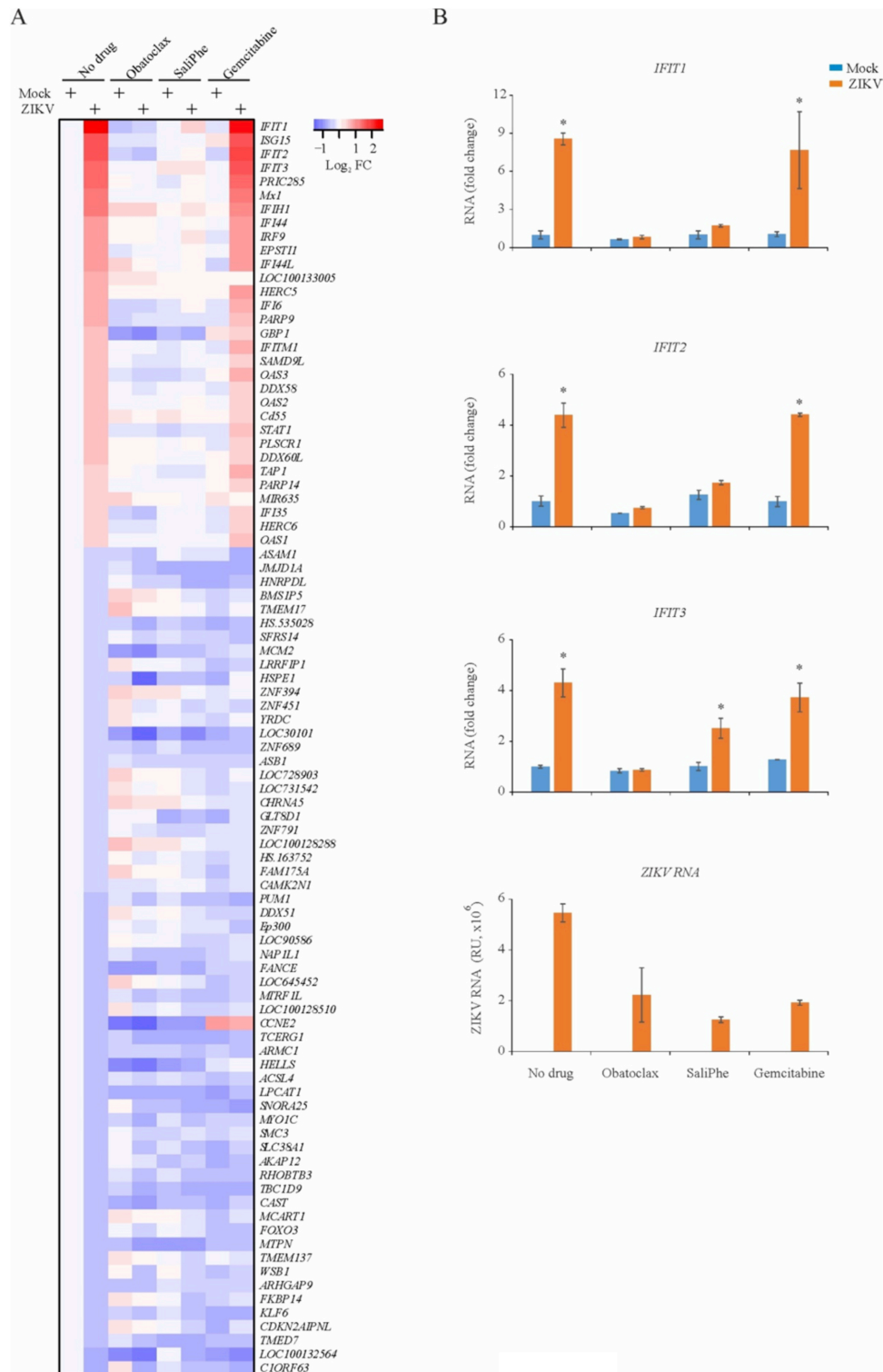


Figure 17. Obatoclox and SaliPhe, but not gemcitabine, deregulated the transcription of antiviral genes. (A) Heatmap showing the 96 most variable genes affected by ZIKV infection and the tested compounds. (B) RT-PCR analysis of the *IFIT1*, -2 and -3 genes and ZIKV RNA from infected and compound-treated cells. Reproduced with permission from Kuivanen *et al. Antiviral Res.* 2017.

SaliPhe and, to a lesser extent, by gemcitabine. For example, adenosine, guanosine, inosine monophosphate (IMP) and adenosine levels were deregulated by the three compounds and by ZIKV infection.

We conclude that gemcitabine inhibits ZIKV replication by interfering with the transcription of viral (but not cellular) RNA, whereas obatoclax and SaliPhe target the endocytosis of ZIKV. Furthermore, this data provides information on ZIKV-host interactions. ZIKV infection did not induce antiviral responses in RPE cells, as seen in the transcription profiles: the expression levels of IFNs or IFN-stimulated genes were not increased in response to ZIKV infection. In addition, none of the proteins involved in antiviral gene expression, such as interferon regulatory factor 3 (IRF3), heat shock protein 27 (HSP27), p38 mitogen-activated protein kinase (MAPK), c-Jun N-terminal kinases (Jnk), protein kinase B (Akt) and extracellular signal regulated kinases (ERK), were shown to be activated in the phosphoprotein-profiling assay, indicating that the IFN pathway was not activated in ZIKV-infected RPE cells. To assess the regulation of IFN responses upon ZIKV warrant for further functional studies both *in vitro* and *in vivo*.

ZIKV cell tropism (III)

ZIKV has been shown to possess vast tissue tropism and persistence in tissues and body fluids, such as urine, saliva and semen (135,136). In addition to three mosquito cell lines derived from tissues and organisms important in ZIKV infection, we investigated the *in vitro* cell susceptibility of ten human cell lines originating from the brain, skin, kidney, fetal lung, uterus, placenta, and umbilical vein to four ZIKV strains. We compared the infectivity of the fetal brain isolate FB-GWUH to two closely related strains isolated from serum samples of acute ZIKV cases in French Polynesia in 2013 (H/PF) and Martinique in 2015 (MRS OPY) as well as to the prototypic strain MR766 from Uganda in 1947. The three clinical isolates were of low passage: FB-GWUH-2016 was of passage 0, H/PF was of passage 2 and MRS OPY was of passage 6. The prototypic strain MR766 has been passaged numerous times in VeroE6 cells and mouse brains, hampering interpretations of the results using this strain as a representative of African ZIKV viruses.

We chose day three post infection as the analysis time point, since we wanted to observe the initial replication competence and virus production in these cells. The

apparent tropism of ZIKV to neuronal cells has initiated several studies on different cell types of the brain. ZIKV preferentially infects neural stem cells, oligodendrocyte precursor cells, astrocytes and microglia, whereas neurons are not reported to be as readily infected (221). FB-GWUH has also been shown to infect neural progenitor cells, causing premature differentiation in human brain organoids (222). In our study, we used two cell lines originating from adult human brains, glial cell lines H2 and H4. Both cell lines were infected by FB-GWUH and MR766 (>1 log growth), but replication was lower for H/PF and MRS OPY (Figure 18). However, infectious virus production was more efficient in H/PF-infected H-2 cells compared to those infected with MR766, showing similar competence as FB-GWUH (Figure 19). In H4 glioma cells, only FB-GWUH was able to replicate and produce a notable amount of infectious virus particles. H-2 cells were ZIKV-antigen positive for all four strains via IFAs, whereas no antigen could be detected by day 3 in H-4 cells. The infection did not induce any antiviral MxA measured by mRNA production in either H-2 or H-4 cells (Figure 20). All of the ZIKV strains induced a cytopathic effect (CPE) in H2 cells, whereas the replication of only FB-GWUH was high enough to induce CPE in H4 cells.

The uterus (SK-UT-1), newborn microvascular endothelial (HMEC-1) and human keratinocyte (HaCaT) cells were more readily infected by FB-GWUH and MR766 than by H/PF and MRS OPY, as shown by increases in viral RNA and detectable amounts of antigen in the IFAs. However, the infectious virus particle production of FB-GWUH was most efficient in SK-UT-1 and HMEC-1 cells. The infection did not induce MxA expression in any of these cell lines, despite the efficient production of virus.

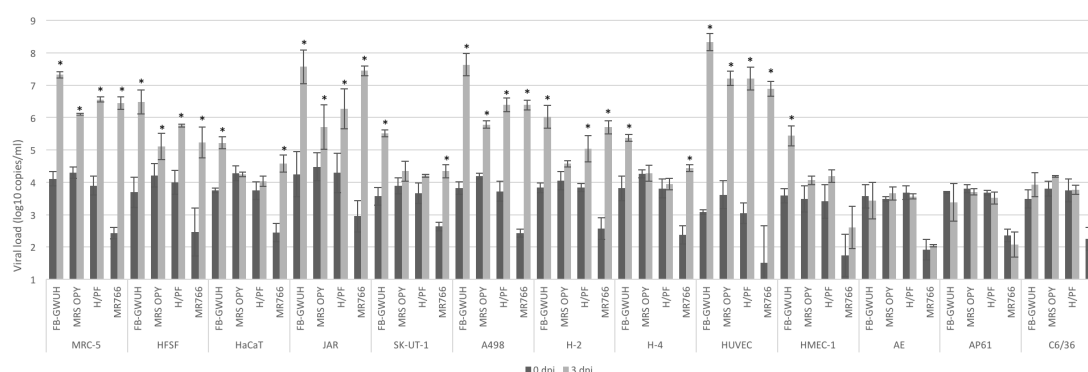


Figure 18. ZIKV viral RNA load in 10 human and 3 mosquito cell culture supernatants at 0 and 3 days post-infection. Values presented are log-transformed viral loads from three independent experiments. **P*-value <0.05 compared to day 0. Reproduced with permission from Kuivanen *et al. J Gen Virol.* 2017.

Cell lines from the placenta (JAR), umbilical vein (HUVEC) and adult kidney (A498) were susceptible to infection and showed high rates of replication of all four strains (>1 log, except for MRS OPY in JAR) (Figure 18). CPE was pronounced in these cells as virus production was highly effective. Interestingly, the infection induced high MxA expression levels only in A498 cells, whereas in JAR or HUVEC cells, MxA mRNA was not detected (Figure 20). The cell lines and tissue sections from the female reproductive system have previously been shown to be highly permissive for ZIKV. El Costa and others have shown in an *ex vivo* transplant model that the maternal decidua, placenta and umbilical cord are permissive to ZIKV infection (169). Placenta origin cells and endometrial stromal cells have been shown to be important for virus persistence and dissemination (168). Placental macrophages, or Hofbauer cells, are highly susceptible to ZIKV, but trophoblasts are to a lesser extent, which further addresses the higher risk of infection during the first trimester of pregnancy (170).

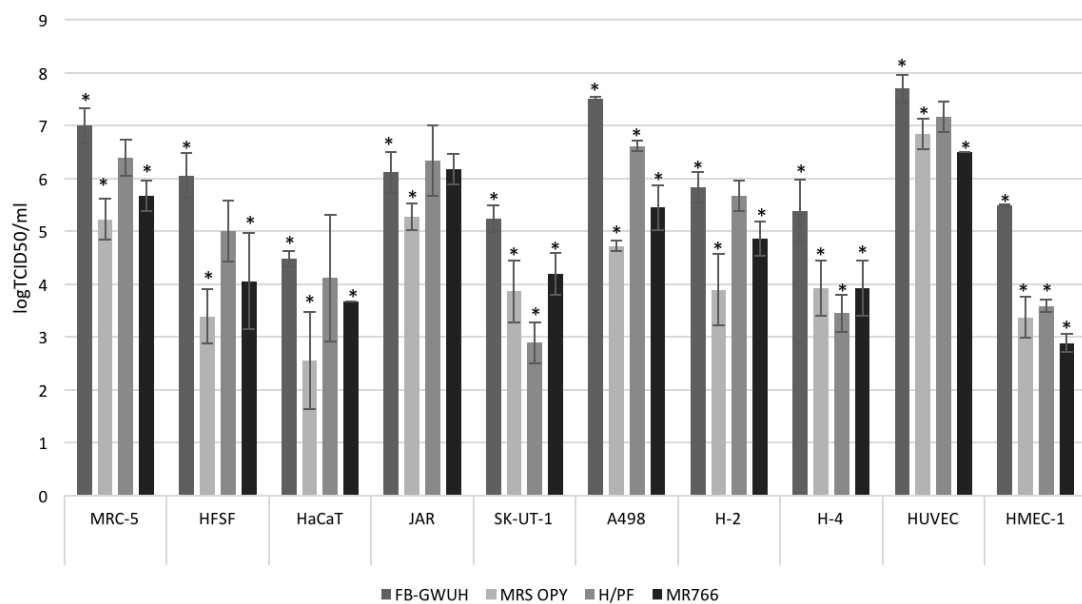


Figure 19. Infectivity of ZIKV in 10 human cell lines at 3 dpi. **P*-value <0.05 compared to FB-GWUH. Reproduced with permission from Kuivanen *et al. J Gen Virol.* 2017

Newborn foreskin epithelial (HFSF) and fetal lung (MRC-5) fibroblasts were infected (>1 log replication) by all viruses (except for the slightly lower replication of MRS OPY in HFSF) (Figure 18). Fibroblasts are one of the foundational cell types shown to be infected by ZIKV (169). Fetal MRC-5 fibroblasts showed a higher rate of ZIKV antigen positivity via IFAs than newborn HFSF fibroblasts. ZIKV infection did not

induce a cytopathic effect in either of the HFSF or MRC-5 cell lines, but a productive infection was still established. Unlike most of cell lines studied here, infection induced MxA expression in both HFSF and MRC-5 cells. The MxA expression levels were higher in FB-GWUH and H/PF infected cells, in accordance to infectious virus production (Figure 20).

In this study, we also tested three mosquito cell lines for their susceptibility to ZIKV infection. We used cell lines representative of the main vector for ZIKV, *Aedes aegypti* (AE), as well as cell lines from *Aedes pseudocutellaris* (AP61) and *Aedes albopictus* (C6/36), the latter of which is commonly used for the isolation of mosquito-borne flaviviruses. Somewhat surprisingly, using the same infection conditions as with the human cell lines, these mosquito cells showed no or little replication of any of the strains at day 3 post-infection (Figure 17). Therefore, the experiment was repeated with a higher MOI (0.2) and longer time scale (0, 5 and 12 days). Efficient replication (>1 log) was observed in the iRNA deficient C6/36 cells, whereas only modest growth was observed in the other two cell lines (our unpublished results). The isolation trial from the fetal and maternal tissues (I) was also unsuccessful when attempted directly in C6/36 cells.

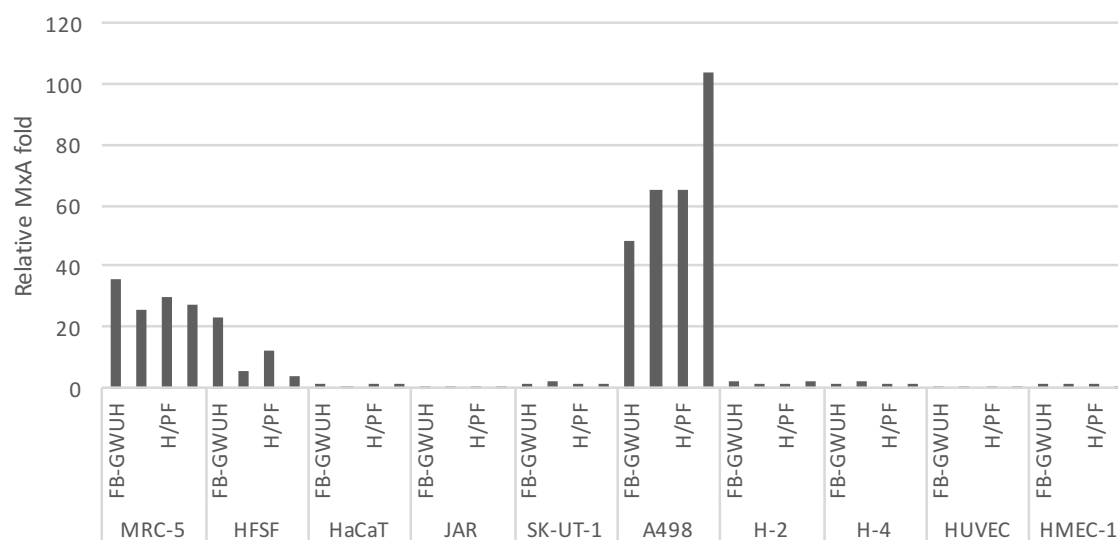


Figure 20. Induction of MxA mRNA production at 3 dpi. The fold change between ZIKV-infected and mock-infected cells is shown. Reproduced with permission from Kuivanen *et al. J Gen Virol.* 2017.

To obtain a general overview of innate immune activation in the human cell lines used in the study, we measured the relative induction of MxA mRNA in the infected cells.

Interestingly, ZIKV infection induced MxA mRNA in only three of the 10 cell lines, fibroblasts, HFSF and MRC-5, and in A498 adult kidney epithelial cells. Flaviviruses have evolved strategies to circumvent or inhibit innate immune responses in the host or to mask antigen presentation to avoid immune responses (62,82). Many of the non-structural proteins, as well as sub-genomic flavivirus RNA (sfRNA), have been shown to function in antagonizing the initial innate immune responses. ZIKV NS5 induces proteasomal degradation of STAT2, and sfRNA of ZIKV inhibits signaling downstream of RIG-I/MDA5 (75). The failed induction of MxA in the studied cell lines remains merely an observation, and the underlying reason can only be speculated.

Our study highlights the differences in biological properties of the three epidemic ZIKV strains. The fetal brain-derived FB-GWUH strain was able to replicate and produce a productive infection in all of the ten human cell lines tested. We found differences in cell susceptibility particularly in cell lines originating from the placenta, umbilical veins, kidney and brain that favored the new strain and a closely related French Polynesian strain. Key aspects in ZIKV pathogenesis is the production of productive infection without cytopathology. In our study, ZIKV induced cytopathic effect in most of the cell lines, except for fibroblasts. ZIKV has been shown to be able to produce persistent infection in primary human brain microvascular endothelial cells as well as in prostatic, testicular and renal cell lines without inducing CPE (171,223).

FB-GWUH has 10 and 13 amino acid differences compared to the epidemic H/PF and MRS OPY strains, respectively. Nine of the amino acid substitutions are specific for FB-GWUH, which suggests that one or more of the amino acid differences between the epidemic strains is responsible for the differences in their replication efficiency. MRS OPY and H/PF are more closely related to each other, having only 5 amino acid differences. The amino acid substitutions between the epidemic strains and the prototypic MR766 strain are too numerous to allow any profound conclusions on their differences. However, one of the mutations between FB-GWUH and MRS OPY and H/PF is a convergent mutation towards the African lineage. Both MR766 and FB-GWUH have a threonine in site 2679 (NS5). The impact of these amino acid substitutions requires further studies.

CONCLUDING REMARKS

In a constantly changing world, viruses evolve and adapt to prevailing circumstances. Members of the *Flavivirus* genus are of arthropod-borne RNA-viruses that have the ability to evolve and spread rapidly along with their vector hosts. The focus of this thesis work was two neuropathogenic flaviviruses, Zika virus and tick-borne encephalitis virus, viruses that have emerged during the last few years.

Zika virus has caused an alarming epidemic in the Americas in 2015-2016. In the beginning of the epidemic, new disease manifestations were connected to ZIKV infections: CNS complications including microcephaly and Guillain-Barré syndrome. These suspected disease associations were new, and a large number of studies were warranted to uncover the epidemiological and virological characteristics of the disease and to prove the causal link between the pathogen and the disease. We were able to provide key evidence of causality by isolating ZIKV from an affected fetal brain. We described for the first time a case of prolonged maternal viremia weeks after ZIKV infection during pregnancy, suggesting infection and active ZIKV replication in the fetoplacental system, and we subsequently isolated the pathogen, ZIKV FB-GWUH-2016.

We studied the effect of known anti-cancer and potent antiviral compounds to ZIKV FB-GWUH infection. We found that novel compounds obatoclax and saliphenylhalamide, as well as the previously known gemcitabine, inhibit ZIKV-mediated cell death in retinal epithelial cells. These results provide a foundation for the future identification of antiviral agents and further broaden the spectrum of activities of these three compounds. We further elaborated cell-virus interactions during ZIKV infection using these compounds.

We characterized the new ZIKV isolate *in vitro* by investigating its potential to infect human cell lines. Furthermore, we compared FB-GWUH to two other related epidemic strains of Asian lineage isolated from the sera of adult febrile patients in French Polynesia and Martinique. We also included the prototypic strain MR766 from the African lineage in our comparison. We found that cell lines from the placenta, umbilical veins, kidney and brain favor FB-GWUH replication.

We also described two fatal cases of tick-borne encephalitis virus in a new focus in Finland, as well as the subsequent isolation of TBEV-Sib from a brain using the same human neuroblastoma cell line that was used for ZIKV isolation. We found that both

the European and Siberian subtypes of the virus circulate in the same focus. Fatal TBEV infections are rare, and two cases reported temporally and geographically close to each other are uncommon. The emergence of more pathogenic variants of TBEV requires further surveys on their spread and studies on their virulence.

ACKNOWLEDGEMENTS

This thesis work was carried out at the Department of Virology, Medicum, University of Helsinki. The head of the department, Professor Kalle Saksela is acknowledged for providing excellent facilities for work and an inspiring scientific atmosphere. I wish to thank Associate Professor Anna Överby-Wernstedt and Docent Carita Savolainen-Kopra for their critical review and valuable comments and discussions on my thesis.

My sincere appreciation goes to my supervisor Professor Olli Vapalahti. Your immense knowledge of science is inspiring. You have always given me support and advice, and freedom to think. Thank you. I wish to express my gratitude to my other supervisor Professor Emeritus Antti Vaheri for giving me the opportunity to work in the field of zoonotic viruses. Your dedication to science is incomparable.

I thank all the collaborators in Finland and around the world. I wish to especially thank Dr. Ashley Hill, who was the driving force in the beginning of the project. Docent Denis Kainov is acknowledged for excellent collaboration.

I have had the privilege to work with the most talented laboratory technicians. Leena, Tytti and Irina, your expertise is indescribable. You have been the cornerstones of our lab and have taught me what I now know about working in a lab. Irina, I wish to thank you for all your help and support, I sincerely appreciate our friendship.

I wish to thank all the people in the extended community of zoonotic virologists with a big and warm Thank You. The best fellow workers one can think of. Satu, Liina, Tarja, Anne, Anu, Anna, Niina, Eili, Satu, Jussi, Tomas, Maria, Agne, Perttu, Erika and Elina: I am ancient, but you are more. Thank you for that. Essi, Alma, Teemu and Anne: this story began with you. I am grateful to have shared it with you. I also wish to thank one special group of extraordinary people. The group that cannot, by any means, be defined as normal. Thank you, you are awesome *per se*.

My dear friends, Satu, Ellu, Katja, Kikka, Unnu, Riina and Eila, thank you for being you. Life needs a balance and you give me that. Satu, no words are enough to express my gratitude.

I owe my deepest gratitude to one big group of people, my family. Mom and dad, my rocks, always believing in me and supporting me. Mom, you always have the right answers, the answers that I want to hear. And dad, you have the rest. Whatever the problem is, you fix it and make it happen. Johanna, thank you for all the discussions, discussions about life aside science, the important things. Ile, you always make me laugh. It's a gift to make people happy. You two have not only given me the greatest sister- and brother-in-laws Kirsimarja and Antti, but have also made a five-time aunt of me, which brings me so much joy I can't even describe. Oiva, Tilda, Enni, Taito and Kaisu, you rock!

This work has been financially supported by Jenny and Antti Wihuri Foundation, Pfizer Ltd. and Finnish Cultural Foundation.

Helsinki, October 2017

Suvi

REFERENCES

- (1) Chu JJ, Ng ML. Interaction of West Nile virus with alpha v beta 3 integrin mediates virus entry into cells. *J Biol Chem* 2004 Dec 24;279(52):54533-54541.
- (2) Gaunt MW, Sall AA, de Lamballerie X, Falconar AK, Dzhivanian TI, Gould EA. Phylogenetic relationships of flaviviruses correlate with their epidemiology, disease association and biogeography. *J Gen Virol* 2001 Aug;82(Pt 8):1867-1876.
- (3) Schneider H. Über epidemische Meningitis serosa. *Wien Klin Wschr* 1931;44:350.
- (4) Smorodintsev AA. Tick-borne spring-summer encephalitis. *Prog Med Virol* 1958;1:210-247.
- (5) Wahlberg P, Saikku P, Brummer-Korvenkontio M. Tick-borne viral encephalitis in Finland. The clinical features of Kumlinge disease during 1959-1987. *J Intern Med* 1989 Mar;225(3):173-177.
- (6) Brummer-Korvenkontio M, Salminen A, Oker-Blom N. Hemagglutination-inhibiting antibodies to tick-borne encephalitis virus in mammals and birds. *Acta Pathol Microbiol Scand Suppl* 1962;Suppl 154:337-338.
- (7) Dick GW, Kitchen SF, Haddow AJ. Zika virus. I. Isolations and serological specificity. *Trans R Soc Trop Med Hyg* 1952 Sep;46(5):509-520.
- (8) Musso D, Gubler DJ. Zika Virus. *Clin Microbiol Rev* 2016 Jul;29(3):487-524.
- (9) Miller RH, Purcell RH. Hepatitis C virus shares amino acid sequence similarity with pestiviruses and flaviviruses as well as members of two plant virus supergroups. *Proc Natl Acad Sci U S A* 1990 Mar;87(6):2057-2061.
- (10) Simmonds P, Becher P, Bukh J, Gould EA, Meyers G, Monath T, et al. ICTV Virus Taxonomy Profile: Flaviviridae. *J Gen Virol* 2017 Jan;98(1):2-3.
- (11) Ng WC, Soto-Acosta R, Bradrick SS, Garcia-Blanco MA, Ooi EE. The 5' and 3' Untranslated Regions of the Flaviviral Genome. *Viruses* 2017 Jun 6;9(6):10.3390/v9060137.
- (12) Grard G, Moureau G, Charrel RN, Lemasson JJ, Gonzalez JP, Gallian P, et al. Genetic characterization of tick-borne flaviviruses: New insights into evolution, pathogenetic determinants and taxonomy. *Virology* 2006 Dec 12.
- (13) Zanotto PM, Gould EA, Gao GF, Harvey PH, Holmes EC. Population dynamics of flaviviruses revealed by molecular phylogenies. *Proc Natl Acad Sci U S A* 1996 Jan 23;93(2):548-553.
- (14) Gritsun TS, Lashkevich VA, Gould EA. Tick-borne encephalitis. *Antiviral Res* 2003 Jan;57(1-2):129-146.
- (15) Faye O, Freire CC, Iamarino A, Faye O, de Oliveira JV, Diallo M, et al. Molecular evolution of Zika virus during its emergence in the 20(th) century. *PLoS Negl Trop Dis* 2014 Jan 9;8(1):e2636.

- (16) Dejnirattisai W, Supasa P, Wongwiwat W, Rouvinski A, Barba-Spaeth G, Duangchinda T, et al. Dengue virus sero-cross-reactivity drives antibody-dependent enhancement of infection with Zika virus. *Nat Immunol* 2016 Sep;17(9):1102-1108.
- (17) Mukhopadhyay S, Kuhn RJ, Rossmann MG. A structural perspective of the flavivirus life cycle. *Nat Rev Microbiol* 2005 Jan;3(1):13-22.
- (18) Wallner G, Mandl CW, Kunz C, Heinz FX. The flavivirus 3'-noncoding region: extensive size heterogeneity independent of evolutionary relationships among strains of tick-borne encephalitis virus. *Virology* 1995 Oct 20;213(1):169-178.
- (19) Hahn CS, Hahn YS, Rice CM, Lee E, Dalgarno L, Strauss EG, et al. Conserved elements in the 3' untranslated region of flavivirus RNAs and potential cyclization sequences. *J Mol Biol* 1987 Nov 5;198(1):33-41.
- (20) Chien HL, Liao CL, Lin YL. FUSE binding protein 1 interacts with untranslated regions of Japanese encephalitis virus RNA and negatively regulates viral replication. *J Virol* 2011 May;85(10):4698-4706.
- (21) De Nova-Ocampo M, Villegas-Sepulveda N, del Angel RM. Translation elongation factor-1alpha, La, and PTB interact with the 3' untranslated region of dengue 4 virus RNA. *Virology* 2002 Apr 10;295(2):337-347.
- (22) Lei Y, Huang Y, Zhang H, Yu L, Zhang M, Dayton A. Functional interaction between cellular p100 and the dengue virus 3' UTR. *J Gen Virol* 2011 Apr;92(Pt 4):796-806.
- (23) Ta M, Vratil S. Mov34 protein from mouse brain interacts with the 3' noncoding region of Japanese encephalitis virus. *J Virol* 2000 Jun;74(11):5108-5115.
- (24) Vashist S, Anantpadma M, Sharma H, Vratil S. La protein binds the predicted loop structures in the 3' non-coding region of Japanese encephalitis virus genome: role in virus replication. *J Gen Virol* 2009 Jun;90(Pt 6):1343-1352.
- (25) Vashist S, Bhullar D, Vratil S. La protein can simultaneously bind to both 3'- and 5'-noncoding regions of Japanese encephalitis virus genome. *DNA Cell Biol* 2011 Jun;30(6):339-346.
- (26) Asghar N, Lee YP, Nilsson E, Lindqvist R, Melik W, Kroger A, et al. The role of the poly(A) tract in the replication and virulence of tick-borne encephalitis virus. *Sci Rep* 2016 Dec 16;6:39265.
- (27) Sakai M, Yoshii K, Sunden Y, Yokozawa K, Hirano M, Kariwa H. Variable region of the 3' UTR is a critical virulence factor in the Far-Eastern subtype of tick-borne encephalitis virus in a mouse model. *J Gen Virol* 2014 Apr;95(Pt 4):823-835.
- (28) Sakai M, Muto M, Hirano M, Kariwa H, Yoshii K. Virulence of tick-borne encephalitis virus is associated with intact conformational viral RNA structures in the variable region of the 3'-UTR. *Virus Res* 2015 May 4;203:36-40.
- (29) Zou J, Xie X, Wang QY, Dong H, Lee MY, Kang C, et al. Characterization of dengue virus NS4A and NS4B protein interaction. *J Virol* 2015 Apr;89(7):3455-3470.

- (30) Boldescu V, Behnam MAM, Vasilakis N, Klein CD. Broad-spectrum agents for flaviviral infections: dengue, Zika and beyond. *Nat Rev Drug Discov* 2017 Aug;16(8):565-586.
- (31) Trent DW. Antigenic characterization of flavivirus structural proteins separated by isoelectric focusing. *J Virol* 1977 Jun;22(3):608-618.
- (32) Khromykh AA, Westaway EG. Completion of Kunjin virus RNA sequence and recovery of an infectious RNA transcribed from stably cloned full-length cDNA. *J Virol* 1994 Jul;68(7):4580-4588.
- (33) Ma L, Jones CT, Groesch TD, Kuhn RJ, Post CB. Solution structure of dengue virus capsid protein reveals another fold. *Proc Natl Acad Sci U S A* 2004 Mar 9;101(10):3414-3419.
- (34) Khromykh AA, Westaway EG. RNA binding properties of core protein of the flavivirus Kunjin. *Arch Virol* 1996;141(3-4):685-699.
- (35) Amberg SM, Nestorowicz A, McCourt DW, Rice CM. NS2B-3 proteinase-mediated processing in the yellow fever virus structural region: in vitro and in vivo studies. *J Virol* 1994 Jun;68(6):3794-3802.
- (36) Yamshchikov VF, Compans RW. Processing of the intracellular form of the west Nile virus capsid protein by the viral NS2B-NS3 protease: an in vitro study. *J Virol* 1994 Sep;68(9):5765-5771.
- (37) Lorenz IC, Allison SL, Heinz FX, Helenius A. Folding and dimerization of tick-borne encephalitis virus envelope proteins prM and E in the endoplasmic reticulum. *J Virol* 2002 Jun;76(11):5480-5491.
- (38) Markoff L, Falgout B, Chang A. A conserved internal hydrophobic domain mediates the stable membrane integration of the dengue virus capsid protein. *Virology* 1997 Jun 23;233(1):105-117.
- (39) Heinz FX, Stiasny K, Puschner-Auer G, Holzmann H, Allison SL, Mandl CW, et al. Structural changes and functional control of the tick-borne encephalitis virus glycoprotein E by the heterodimeric association with protein prM. *Virology* 1994 Jan;198(1):109-117.
- (40) Stadler K, Allison SL, Schalich J, Heinz FX. Proteolytic activation of tick-borne encephalitis virus by furin. *J Virol* 1997 Nov;71(11):8475-8481.
- (41) Barba-Spaeth G, Dejnirattisai W, Rouvinski A, Vaney MC, Medits I, Sharma A, et al. Structural basis of potent Zika-dengue virus antibody cross-neutralization. *Nature* 2016 Aug 4;536(7614):48-53.
- (42) Navarro-Sanchez E, Altmeyer R, Amara A, Schwartz O, Fieschi F, Virelizier JL, et al. Dendritic-cell-specific ICAM3-grabbing non-integrin is essential for the productive infection of human dendritic cells by mosquito-cell-derived dengue viruses. *EMBO Rep* 2003 Jul;4(7):723-728.
- (43) Stiasny K, Allison SL, Schalich J, Heinz FX. Membrane interactions of the tick-borne encephalitis virus fusion protein E at low pH. *J Virol* 2002 Apr;76(8):3784-3790.
- (44) Rey FA, Heinz FX, Mandl C, Kunz C, Harrison SC. The envelope glycoprotein from tick-borne encephalitis virus at 2 Å resolution. *Nature* 1995 May 25;375(6529):291-298.

- (45) Bhardwaj S, Holbrook M, Shope RE, Barrett AD, Watowich SJ. Biophysical characterization and vector-specific antagonist activity of domain III of the tick-borne flavivirus envelope protein. *J Virol* 2001 Apr;75(8):4002-4007.
- (46) Heinz FX, Stiasny K. Flaviviruses and their antigenic structure. *J Clin Virol* 2012 Dec;55(4):289-295.
- (47) Rastogi M, Sharma N, Singh SK. Flavivirus NS1: a multifaceted enigmatic viral protein. *Virol J* 2016 Jul 29;13:131-016-0590-7.
- (48) Avirutnan P, Fuchs A, Hauhart RE, Somnuk P, Youn S, Diamond MS, et al. Antagonism of the complement component C4 by flavivirus nonstructural protein NS1. *J Exp Med* 2010 Apr 12;207(4):793-806.
- (49) Chung KM, Liszewski MK, Nybakken G, Davis AE, Townsend RR, Fremont DH, et al. West Nile virus nonstructural protein NS1 inhibits complement activation by binding the regulatory protein factor H. *Proc Natl Acad Sci U S A* 2006 Dec 12;103(50):19111-19116.
- (50) Bakhvalova VN, Rar VA, Tkachev SE, Matveev VA, Matveev LE, Karavanov AS, et al. Tick-borne encephalitis virus strains of Western Siberia. *Virus Res* 2000 Sep;70(1-2):1-12.
- (51) Schlesinger JJ, Brandriss MW, Cropp CB, Monath TP. Protection against yellow fever in monkeys by immunization with yellow fever virus nonstructural protein NS1. *J Virol* 1986 Dec;60(3):1153-1155.
- (52) Jacobs SC, Stephenson JR, Wilkinson GW. High-level expression of the tick-borne encephalitis virus NS1 protein by using an adenovirus-based vector: protection elicited in a murine model. *J Virol* 1992 Apr;66(4):2086-2095.
- (53) Melian EB, Hinzman E, Nagasaki T, Firth AE, Wills NM, Nouwens AS, et al. NS1' of flaviviruses in the Japanese encephalitis virus serogroup is a product of ribosomal frameshifting and plays a role in viral neuroinvasiveness. *J Virol* 2010 Feb;84(3):1641-1647.
- (54) Morrison J, Aguirre S, Fernandez-Sesma A. Innate immunity evasion by Dengue virus. *Viruses* 2012 Mar;4(3):397-413.
- (55) Chambers TJ, Nestorowicz A, Amberg SM, Rice CM. Mutagenesis of the yellow fever virus NS2B protein: effects on proteolytic processing, NS2B-NS3 complex formation, and viral replication. *J Virol* 1993 Nov;67(11):6797-6807.
- (56) Chambers TJ, Grakoui A, Rice CM. Processing of the yellow fever virus nonstructural polyprotein: a catalytically active NS3 proteinase domain and NS2B are required for cleavages at dibasic sites. *J Virol* 1991 Nov;65(11):6042-6050.
- (57) Ruzek D, Gritsun TS, Forrester NL, Gould EA, Kopecky J, Golovchenko M, et al. Mutations in the NS2B and NS3 genes affect mouse neuroinvasiveness of a Western European field strain of tick-borne encephalitis virus. *Virology* 2008 May 10;374(2):249-255.
- (58) Aguirre S, Maestre AM, Pagni S, Patel JR, Savage T, Gutman D, et al. DENV inhibits type I IFN production in infected cells by cleaving human STING. *PLoS Pathog* 2012;8(10):e1002934.

- (59) Wengler G, Czaya G, Farber PM, Hegemann JH. In vitro synthesis of West Nile virus proteins indicates that the amino-terminal segment of the NS3 protein contains the active centre of the protease which cleaves the viral polyprotein after multiple basic amino acids. *J Gen Virol* 1991 Apr;72 (Pt 4)(Pt 4):851-858.
- (60) Lin C, Amberg SM, Chambers TJ, Rice CM. Cleavage at a novel site in the NS4A region by the yellow fever virus NS2B-3 proteinase is a prerequisite for processing at the downstream 4A/4B signalase site. *J Virol* 1993 Apr;67(4):2327-2335.
- (61) Zeidler JD, Fernandes-Siqueira LO, Barbosa GM, Da Poian AT. Non-Canonical Roles of Dengue Virus Non-Structural Proteins. *Viruses* 2017 Mar 13;9(3):10.3390/v9030042.
- (62) Umareddy I, Chao A, Sampath A, Gu F, Vasudevan SG. Dengue virus NS4B interacts with NS3 and dissociates it from single-stranded RNA. *J Gen Virol* 2006 Sep;87(Pt 9):2605-2614.
- (63) Miller S, Sparacio S, Bartenschlager R. Subcellular localization and membrane topology of the Dengue virus type 2 Non-structural protein 4B. *J Biol Chem* 2006 Mar 31;281(13):8854-8863.
- (64) Johansson M, Brooks AJ, Jans DA, Vasudevan SG. A small region of the dengue virus-encoded RNA-dependent RNA polymerase, NS5, confers interaction with both the nuclear transport receptor importin-beta and the viral helicase, NS3. *J Gen Virol* 2001 Apr;82(Pt 4):735-745.
- (65) Brooks AJ, Johansson M, John AV, Xu Y, Jans DA, Vasudevan SG. The interdomain region of dengue NS5 protein that binds to the viral helicase NS3 contains independently functional importin beta 1 and importin alpha/beta-recognized nuclear localization signals. *J Biol Chem* 2002 Sep 27;277(39):36399-36407.
- (66) Cui T, Sugrue RJ, Xu Q, Lee AK, Chan YC, Fu J. Recombinant dengue virus type 1 NS3 protein exhibits specific viral RNA binding and NTPase activity regulated by the NS5 protein. *Virology* 1998 Jul 5;246(2):409-417.
- (67) Meertens L, Labeau A, Dejarnac O, Cipriani S, Sinigaglia L, Bonnet-Madin L, et al. Axl Mediates ZIKA Virus Entry in Human Glial Cells and Modulates Innate Immune Responses. *Cell Rep* 2017 Jan 10;18(2):324-333.
- (68) Germi R, Crance JM, Garin D, Guimet J, Lortat-Jacob H, Ruigrok RW, et al. Heparan sulfate-mediated binding of infectious dengue virus type 2 and yellow fever virus. *Virology* 2002 Jan 5;292(1):162-168.
- (69) Zhang Y, Corver J, Chipman PR, Zhang W, Pletnev SV, Sedlak D, et al. Structures of immature flavivirus particles. *EMBO J* 2003 Jun 2;22(11):2604-2613.
- (70) Munoz-Jordan JL, Fredericksen BL. How flaviviruses activate and suppress the interferon response. *Viruses* 2010 Feb;2(2):676-691.
- (71) Le Bon A, Tough DF. Links between innate and adaptive immunity via type I interferon. *Curr Opin Immunol* 2002 Aug;14(4):432-436.
- (72) Tsai YT, Chang SY, Lee CN, Kao CL. Human TLR3 recognizes dengue virus and modulates viral replication in vitro. *Cell Microbiol* 2009 Apr;11(4):604-615.

- (73) Suthar MS, Diamond MS, Gale M, Jr. West Nile virus infection and immunity. *Nat Rev Microbiol* 2013 Feb;11(2):115-128.
- (74) Yoneyama M, Kikuchi M, Natsukawa T, Shinobu N, Imaizumi T, Miyagishi M, et al. The RNA helicase RIG-I has an essential function in double-stranded RNA-induced innate antiviral responses. *Nat Immunol* 2004 Jul;5(7):730-737.
- (75) Cumberworth SL, Clark JJ, Kohl A, Donald CL. Inhibition of type I interferon induction and signalling by mosquito-borne flaviviruses. *Cell Microbiol* 2017 May;19(5):10.1111/cmi.12737. Epub 2017 Mar 22.
- (76) Meylan E, Curran J, Hofmann K, Moradpour D, Binder M, Bartenschlager R, et al. Cardif is an adaptor protein in the RIG-I antiviral pathway and is targeted by hepatitis C virus. *Nature* 2005 Oct 20;437(7062):1167-1172.
- (77) Seth RB, Sun L, Ea CK, Chen ZJ. Identification and characterization of MAVS, a mitochondrial antiviral signaling protein that activates NF-kappaB and IRF 3. *Cell* 2005 Sep 9;122(5):669-682.
- (78) Yu CY, Chang TH, Liang JJ, Chiang RL, Lee YL, Liao CL, et al. Dengue virus targets the adaptor protein MITA to subvert host innate immunity. *PLoS Pathog* 2012;8(6):e1002780.
- (79) Werme K, Wigerius M, Johansson M. Tick-borne encephalitis virus NS5 associates with membrane protein scribble and impairs interferon-stimulated JAK-STAT signalling. *Cell Microbiol* 2008 Mar;10(3):696-712.
- (80) Ashour J, Laurent-Rolle M, Shi PY, Garcia-Sastre A. NS5 of dengue virus mediates STAT2 binding and degradation. *J Virol* 2009 Jun;83(11):5408-5418.
- (81) Kumar A, Hou S, Airo AM, Limonta D, Mancinelli V, Branton W, et al. Zika virus inhibits type-I interferon production and downstream signaling. *EMBO Rep* 2016 Dec;17(12):1766-1775.
- (82) Munoz-Jordan JL, Laurent-Rolle M, Ashour J, Martinez-Sobrido L, Ashok M, Lipkin WI, et al. Inhibition of alpha/beta interferon signaling by the NS4B protein of flaviviruses. *J Virol* 2005 Jul;79(13):8004-8013.
- (83) Liu WJ, Wang XJ, Clark DC, Lobigs M, Hall RA, Khromykh AA. A single amino acid substitution in the West Nile virus nonstructural protein NS2A disables its ability to inhibit alpha/beta interferon induction and attenuates virus virulence in mice. *J Virol* 2006 Mar;80(5):2396-2404.
- (84) Overby AK, Popov VL, Niedrig M, Weber F. Tick-borne encephalitis virus delays interferon induction and hides its double-stranded RNA in intracellular membrane vesicles. *J Virol* 2010 Jun 16.
- (85) Chung KM, Liszewski MK, Nybakken G, Davis AE, Townsend RR, Fremont DH, et al. West Nile virus nonstructural protein NS1 inhibits complement activation by binding the regulatory protein factor H. *Proc Natl Acad Sci U S A* 2006 Dec 12;103(50):19111-19116.
- (86) Liang Q, Luo Z, Zeng J, Chen W, Foo SS, Lee SA, et al. Zika Virus NS4A and NS4B Proteins Deregulate Akt-mTOR Signaling in Human Fetal Neural Stem Cells to Inhibit Neurogenesis and Induce Autophagy. *Cell Stem Cell* 2016 Nov 3;19(5):663-671.

- (87) Beatman E, Oyer R, Shives KD, Hedman K, Brault AC, Tyler KL, et al. West Nile virus growth is independent of autophagy activation. *Virology* 2012 Nov 10;433(1):262-272.
- (88) Blazquez AB, Escribano-Romero E, Merino-Ramos T, Saiz JC, Martin-Acebes MA. Infection with Usutu virus induces an autophagic response in mammalian cells. *PLoS Negl Trop Dis* 2013 Oct 24;7(10):e2509.
- (89) Kobayashi S, Orba Y, Yamaguchi H, Takahashi K, Sasaki M, Hasebe R, et al. Autophagy inhibits viral genome replication and gene expression stages in West Nile virus infection. *Virus Res* 2014 Oct 13;191:83-91.
- (90) Solomon T. Flavivirus encephalitis. *N Engl J Med* 2004 Jul 22;351(4):370-378.
- (91) Rizzoli A, Jimenez-Clavero MA, Barzon L, Cordioli P, Figuerola J, Koraka P, et al. The challenge of West Nile virus in Europe: knowledge gaps and research priorities. *Euro Surveill* 2015 May 21;20(20):21135.
- (92) Solomon T, Dung NM, Kneen R, Gainsborough M, Vaughn DW, Khanh VT. Japanese encephalitis. *J Neurol Neurosurg Psychiatry* 2000 Apr;68(4):405-415.
- (93) Gould EA, Solomon T. Pathogenic flaviviruses. *Lancet* 2008 Feb 9;371(9611):500-509.
- (94) Kaiser R. Tick-borne encephalitis (TBE) in Germany and clinical course of the disease. *Int J Med Microbiol* 2002 Jun;291 Suppl 33:58-61.
- (95) Cao-Lormeau VM, Blake A, Mons S, Lastere S, Roche C, Vanhomwegen J, et al. Guillain-Barre Syndrome outbreak associated with Zika virus infection in French Polynesia: a case-control study. *Lancet* 2016 Apr 9;387(10027):1531-1539.
- (96) Johansson MA, Mier-y-Teran-Romero L, Reefhuis J, Gilboa SM, Hills SL. Zika and the Risk of Microcephaly. *N Engl J Med* 2016 Jul 7;375(1):1-4.
- (97) Lukan M, Bullova E, Petko B. Climate warming and tick-borne encephalitis, Slovakia. *Emerg Infect Dis* 2010 Mar;16(3):524-526.
- (98) Kriz B, Maly M, Benes C, Daniel M. Epidemiology of tick-borne encephalitis in the Czech Republic 1970-2008. *Vector Borne Zoonotic Dis* 2012 Nov;12(11):994-999.
- (99) European Centre for Disease Control and Prevention, ECDC, Technical report. 2012; Available at: <https://ecdc.europa.eu/sites/portal/files/media/en/publications/Publications/TBE-in-EU-EFTA.pdf>, 2017.
- (100) Donoso Mantke O, Escadafal C, Niedrig M, Pfeffer M, Working Group For Tick-Borne Encephalitis Virus,C. Tick-borne encephalitis in Europe, 2007 to 2009. *Euro Surveill* 2011 Sep 29;16(39):19976.
- (101) Karelis G, Bormane A, Logina I, Lucenko I, Suna N, Krumina A, et al. Tick-borne encephalitis in Latvia 1973-2009: epidemiology, clinical features and sequelae. *Eur J Neurol* 2012 Jan;19(1):62-68.
- (102) Stefanoff P, Orlikova H, Prikazsky V, Bene C, Rosinska M. Cross-border surveillance differences: tick-borne encephalitis and lyme borreliosis in the Czech Republic and Poland, 1999-2008. *Cent Eur J Public Health* 2014 Mar;22(1):54-59.

- (103) Heinz FX, Holzmann H, Essl A, Kundi M. Field effectiveness of vaccination against tick-borne encephalitis. *Vaccine* 2007 Oct 23;25(43):7559-7567.
- (104) Schwarz B. Health economics of early summer meningoencephalitis in Austria. Effects of a vaccination campaign 1981 to 1990. *Wien Med Wochenschr* 1993;143(21):551-555.
- (105) Jaenson TG, Hjertqvist M, Bergstrom T, Lundkvist A. Why is tick-borne encephalitis increasing? A review of the key factors causing the increasing incidence of human TBE in Sweden. *Parasit Vectors* 2012 Aug 31;5:184-3305-5-184.
- (106) Tonteri E, Kurkela S, Timonen S, Manni T, Vuorinen T, Kuusi M, et al. Surveillance of endemic foci of tick-borne encephalitis in Finland 1995-2013: evidence of emergence of new foci. *Euro Surveill* 2015;20(37):10.2807/1560-7917.ES.2015.20.37.30020.
- (107) Tokarevich NK, Tronin AA, Blinova OV, Buzinov RV, Boltenkov VP, Yurasova ED, et al. The impact of climate change on the expansion of *Ixodes persulcatus* habitat and the incidence of tick-borne encephalitis in the north of European Russia. *Glob Health Action* 2011;4:8448.
- (108) National Institute for Health and Welfare, Pitäisikö TBE-rokotusohjelmaa laajentaa? Puutiaisaivokuume-työryhmän raportti. 2013; Available at: https://www.julkari.fi/bitstream/handle/10024/110860/URN_ISBN_978-952-245-627-4.pdf?sequence=1.
- (109) WHO, Immunization, Vaccines and Biologicals. 2011; Available at: http://www.who.int/immunization/topics/tick_encephalitis/en/. Accessed September/13, 2017.
- (110) National Institute for Health and Welfare, Infectious diseases in Finland, annual reports. Available at: <https://www.thl.fi/en/web/infectious-diseases/surveillance/infectious-disease-register/infectious-diseases-in-finland-annual-reports>.
- (111) Lanciotti RS, Kosoy OL, Laven JJ, Velez JO, Lambert AJ, Johnson AJ, et al. Genetic and serologic properties of Zika virus associated with an epidemic, Yap State, Micronesia, 2007. *Emerg Infect Dis* 2008 Aug;14(8):1232-1239.
- (112) Cao-Lormeau VM, Roche C, Teissier A, Robin E, Berry AL, Mallet HP, et al. Zika virus, French polynesia, South pacific, 2013. *Emerg Infect Dis* 2014 Jun;20(6):1085-1086.
- (113) Gatherer D, Kohl A. Zika virus: a previously slow pandemic spreads rapidly through the Americas. *J Gen Virol* 2016 Feb;97(2):269-273.
- (114) Dupont-Rouzeyrol M, O'Connor O, Calvez E, Daures M, John M, Grangeon JP, et al. Co-infection with Zika and dengue viruses in 2 patients, New Caledonia, 2014. *Emerg Infect Dis* 2015 Feb;21(2):381-382.
- (115) Pyke AT, Daly MT, Cameron JN, Moore PR, Taylor CT, Hewitson GR, et al. Imported zika virus infection from the cook islands into australia, 2014. *PLoS Curr* 2014 Jun 2;6:10.1371/currents.outbreaks.4635a54dbffba2156fb2fd76dc49f65e.
- (116) Tognarelli J, Ulloa S, Villagra E, Lagos J, Aguayo C, Fasce R, et al. A report on the outbreak of Zika virus on Easter Island, South Pacific, 2014. *Arch Virol* 2016 Mar;161(3):665-668.

- (117) Daudens-Vaysse E, Ledrans M, Gay N, Ardillon V, Cassadou S, Najioullah F, et al. Zika emergence in the French Territories of America and description of first confirmed cases of Zika virus infection on Martinique, November 2015 to February 2016. *Euro Surveill* 2016 Jul 14;21(28):10.2807/1560-7917.ES.2016.21.28.30285.
- (118) Faria NR, Azevedo RDS, Kraemer MUG, Souza R, Cunha MS, Hill SC, et al. Zika virus in the Americas: Early epidemiological and genetic findings. *Science* 2016 Apr 15;352(6283):345-349.
- (119) Pan American Health Organization / World Health Organization, PAHO/WHO, Case definitions for suspected and confirmed Zika cases. 2016; Available at: http://www.paho.org/hq/index.php?option=com_content&view=article&id=11117&Itemid=41532&lang=en. Accessed July/20, 2017.
- (120) Pan American Health Organization/World Health Organization, PAHO/WHO, Zika cumulative cases. 2017; Available at: http://www.paho.org/hq/index.php?option=com_content&view=article&id=12390&Itemid=42090&lang=en. Accessed July/20, 2017.
- (121) Centers for Disease Control and Prevention, CDC, Pregnant women with any laboratory evidence of possible Zika virus infection in the United States and territories. 2017; Available at: <https://www.cdc.gov/zika/reporting/pregwomen-uscases.html>. Accessed July/23, 2017.
- (122) Korhonen EM, Huhtamo E, Smura T, Kallio-Kokko H, Raassina M, Vapalahti O. Zika virus infection in a traveller returning from the Maldives, June 2015. *Euro Surveill* 2016;21(2):10.2807/1560-7917.ES.2016.21.2.30107.
- (123) Current Zika virus transmission - list of countries: European Centre for Disease Control and Prevention, ECDC, adaptation of WHO's Zika virus country classification scheme. 2017; Available at: <https://ecdc.europa.eu/en/publications-data/current-zika-virus-transmission-list-countries-ecdc-adaptation-whos-zika-virus>. Accessed July/22, 2017.
- (124) Hayes EB. Zika virus outside Africa. *Emerg Infect Dis* 2009 Sep;15(9):1347-1350.
- (125) Biernat B, Karbowiak G, Werszko J, Stanczak J. Prevalence of tick-borne encephalitis virus (TBEV) RNA in *Dermacentor reticulatus* ticks from natural and urban environment, Poland. *Exp Appl Acarol* 2014 Dec;64(4):543-551.
- (126) Randolph SE. Ticks are not Insects: Consequences of Contrasting Vector Biology for Transmission Potential. *Parasitol Today* 1998 May;14(5):186-192.
- (127) Nuttall PA, Labuda M. Dynamics of infection in tick vectors and at the tick-host interface. *Adv Virus Res* 2003;60:233-272.
- (128) Labuda M, Danielova V, Jones LD, Nuttall PA. Amplification of tick-borne encephalitis virus infection during co-feeding of ticks. *Med Vet Entomol* 1993 Oct;7(4):339-342.
- (129) Labuda M, Nuttall PA, Kozuch O, Eleckova E, Williams T, Zuffova E, et al. Non-viraemic transmission of tick-borne encephalitis virus: a mechanism for arbovirus survival in nature. *Experientia* 1993 Sep 15;49(9):802-805.

- (130) Labuda M, Kozuch O, Zuffova E, Eleckova E, Hails RS, Nuttall PA. Tick-borne encephalitis virus transmission between ticks cofeeding on specific immune natural rodent hosts. *Virology* 1997 Aug 18;235(1):138-143.
- (131) Randolph SE, Green RM, Peacey MF, Rogers DJ. Seasonal synchrony: the key to tick-borne encephalitis foci identified by satellite data. *Parasitology* 2000 Jul;121 (Pt 1)(Pt 1):15-23.
- (132) Mlera L, Melik W, Bloom ME. The role of viral persistence in flavivirus biology. *Pathog Dis* 2014 Jul;71(2):137-163.
- (133) Kotal J, Langhansova H, Lieskovska J, Andersen JF, Francischetti IM, Chavakis T, et al. Modulation of host immunity by tick saliva. *J Proteomics* 2015 Oct 14;128:58-68.
- (134) Offerdahl DK, Clancy NG, Bloom ME. Stability of a Tick-Borne Flavivirus in Milk. *Front Bioeng Biotechnol* 2016 May 11;4:40.
- (135) Kerbo N, Donchenko I, Kutsar K, Vasilenko V. Tickborne encephalitis outbreak in Estonia linked to raw goat milk, May-June 2005. *Euro Surveill* 2005 Jun 23;10(6):E050623.2.
- (136) Markovinovic L, Kosanovic Licina ML, Tesic V, Vojvodic D, Vladusic Lucic I, Kniewald T, et al. An outbreak of tick-borne encephalitis associated with raw goat milk and cheese consumption, Croatia, 2015. *Infection* 2016 Oct;44(5):661-665.
- (137) Hudopisk N, Korva M, Janet E, Simetinger M, Grgic-Vitek M, Gubensek J, et al. Tick-borne encephalitis associated with consumption of raw goat milk, Slovenia, 2012. *Emerg Infect Dis* 2013 May;19(5):806-808.
- (138) Fagbami AH. Zika virus infections in Nigeria: virological and seroepidemiological investigations in Oyo State. *J Hyg (Lond)* 1979 Oct;83(2):213-219.
- (139) Marchette NJ, Garcia R, Rudnick A. Isolation of Zika virus from *Aedes aegypti* mosquitoes in Malaysia. *Am J Trop Med Hyg* 1969 May;18(3):411-415.
- (140) McCrae AW, Kirya BG. Yellow fever and Zika virus epizootics and enzootics in Uganda. *Trans R Soc Trop Med Hyg* 1982;76(4):552-562.
- (141) Duffy MR, Chen TH, Hancock WT, Powers AM, Kool JL, Lanciotti RS, et al. Zika virus outbreak on Yap Island, Federated States of Micronesia. *N Engl J Med* 2009 Jun 11;360(24):2536-2543.
- (142) Diallo D, Sall AA, Diagne CT, Faye O, Faye O, Ba Y, et al. Zika virus emergence in mosquitoes in southeastern Senegal, 2011. *PLoS One* 2014 Oct 13;9(10):e109442.
- (143) Musso D, Roche C, Robin E, Nhan T, Teissier A, Cao-Lormeau VM. Potential sexual transmission of Zika virus. *Emerg Infect Dis* 2015 Feb;21(2):359-361.
- (144) Besnard M, Lastere S, Teissier A, Cao-Lormeau V, Musso D. Evidence of perinatal transmission of Zika virus, French Polynesia, December 2013 and February 2014. *Euro Surveill* 2014 Apr 3;19(13):20751.
- (145) Motta IJ, Spencer BR, Cordeiro da Silva SG, Arruda MB, Dobbin JA, Gonzaga YB, et al. Evidence for Transmission of Zika Virus by Platelet Transfusion. *N Engl J Med* 2016 Sep 15;375(11):1101-1103.

- (146) Gunther G, Haglund M, Lindquist L, Forsgren M, Skoldenberg B. Tick-borne encephalitis in Sweden in relation to aseptic meningo-encephalitis of other etiology: a prospective study of clinical course and outcome. *J Neurol* 1997 Apr;244(4):230-238.
- (147) Lindquist L, Vapalahti O. Tick-borne encephalitis. *Lancet* 2008 May 31;371(9627):1861-1871.
- (148) Charrel RN, Attoui H, Butenko AM, Clegg JC, Deubel V, Frolova TV, et al. Tick-borne virus diseases of human interest in Europe. *Clin Microbiol Infect* 2004 Dec;10(12):1040-1055.
- (149) Lorenzl S, Pfister HW, Padovan C, Yousry T. MRI abnormalities in tick-borne encephalitis. *Lancet* 1996 Mar 9;347(9002):698-699.
- (150) Kaiser R, Holzmann H. Laboratory findings in tick-borne encephalitis--correlation with clinical outcome. *Infection* 2000 Mar-Apr;28(2):78-84.
- (151) Bogovic P, Strle F. Tick-borne encephalitis: A review of epidemiology, clinical characteristics, and management. *World J Clin Cases* 2015 May 16;3(5):430-441.
- (152) Liu XY, Bonnet SI. Hard tick factors implicated in pathogen transmission. *PLoS Negl Trop Dis* 2014 Jan 30;8(1):e2566.
- (153) Sim S, Ramirez JL, Dimopoulos G. Dengue virus infection of the *Aedes aegypti* salivary gland and chemosensory apparatus induces genes that modulate infection and blood-feeding behavior. *PLoS Pathog* 2012;8(3):e1002631.
- (154) Cardoso FL, Brites D, Brito MA. Looking at the blood-brain barrier: molecular anatomy and possible investigation approaches. *Brain Res Rev* 2010 Sep 24;64(2):328-363.
- (155) Sips GJ, Wilschut J, Smit JM. Neuroinvasive flavivirus infections. *Rev Med Virol* 2012 Mar;22(2):69-87.
- (156) Palus M, Vancova M, Sirmarova J, Elsterova J, Perner J, Ruzek D. Tick-borne encephalitis virus infects human brain microvascular endothelial cells without compromising blood-brain barrier integrity. *Virology* 2017 Jul;507:110-122.
- (157) Hirano M, Muto M, Sakai M, Kondo H, Kobayashi S, Kariwa H, et al. Dendritic transport of tick-borne flavivirus RNA by neuronal granules affects development of neurological disease. *Proc Natl Acad Sci U S A* 2017 Sep 12;114(37):9960-9965.
- (158) Araujo AQ, Silva MT, Araujo AP. Zika virus-associated neurological disorders: a review. *Brain* 2016 Aug;139(Pt 8):2122-2130.
- (159) Carteaux G, Maquart M, Bedet A, Contou D, Brugieres P, Fourati S, et al. Zika Virus Associated with Meningoencephalitis. *N Engl J Med* 2016 Apr 21;374(16):1595-1596.
- (160) Willison HJ, Jacobs BC, van Doorn PA. Guillain-Barre syndrome. *Lancet* 2016 Aug 13;388(10045):717-727.
- (161) Sejvar JJ, Baughman AL, Wise M, Morgan OW. Population incidence of Guillain-Barre syndrome: a systematic review and meta-analysis. *Neuroepidemiology* 2011;36(2):123-133.

- (162) Parra B, Lizarazo J, Jimenez-Arango JA, Zea-Vera AF, Gonzalez-Manrique G, Vargas J, et al. Guillain-Barre Syndrome Associated with Zika Virus Infection in Colombia. *N Engl J Med* 2016 Oct 20;375(16):1513-1523.
- (163) Driggers RW, Ho CY, Korhonen EM, Kuivanen S, Jääskeläinen AJ, Smura T, et al. Zika Virus Infection with Prolonged Maternal Viremia and Fetal Brain Abnormalities. *N Engl J Med* 2016 Jun 2;374(22):2142-2151.
- (164) Rasmussen SA, Jamieson DJ, Honein MA, Petersen LR. Zika Virus and Birth Defects--Reviewing the Evidence for Causality. *N Engl J Med* 2016 May 19;374(20):1981-1987.
- (165) Barkovich AJ, Guerrini R, Kuzniecky RI, Jackson GD, Dobyns WB. A developmental and genetic classification for malformations of cortical development: update 2012. *Brain* 2012 May;135(Pt 5):1348-1369.
- (166) Shapiro-Mendoza CK, Rice ME, Galang RR, Fulton AC, VanMaldeghem K, Prado MV, et al. Pregnancy Outcomes After Maternal Zika Virus Infection During Pregnancy - U.S. Territories, January 1, 2016-April 25, 2017. *MMWR Morb Mortal Wkly Rep* 2017 Jun 16;66(23):615-621.
- (167) Tang H, Hammack C, Ogden SC, Wen Z, Qian X, Li Y, et al. Zika Virus Infects Human Cortical Neural Progenitors and Attenuates Their Growth. *Cell Stem Cell* 2016 May 5;18(5):587-590.
- (168) Pagani I, Ghezzi S, Ulisse A, Rubio A, Turrini F, Garavaglia E, et al. Human Endometrial Stromal Cells Are Highly Permissive To Productive Infection by Zika Virus. *Sci Rep* 2017 Mar 10;7:44286.
- (169) El Costa H, Gouilly J, Mansuy JM, Chen Q, Levy C, Cartron G, et al. ZIKA virus reveals broad tissue and cell tropism during the first trimester of pregnancy. *Sci Rep* 2016 Oct 19;6:35296.
- (170) Quicke KM, Bowen JR, Johnson EL, McDonald CE, Ma H, O'Neal JT, et al. Zika Virus Infects Human Placental Macrophages. *Cell Host Microbe* 2016 Jul 13;20(1):83-90.
- (171) Mladinich MC, Schwedes J, Mackow ER. Zika Virus Persistently Infects and Is Basolaterally Released from Primary Human Brain Microvascular Endothelial Cells. *MBio* 2017 Jul 11;8(4):10.1128/mBio.00952-17.
- (172) Bardina SV, Bunduc P, Tripathi S, Duehr J, Frere JJ, Brown JA, et al. Enhancement of Zika virus pathogenesis by preexisting ant flavivirus immunity. *Science* 2017 Apr 14;356(6334):175-180.
- (173) Paul LM, Carlin ER, Jenkins MM, Tan AL, Barcellona CM, Nicholson CO, et al. Dengue virus antibodies enhance Zika virus infection. *Clin Transl Immunology* 2016 Dec 16;5(12):e117.
- (174) Castanha PMS, Nascimento EJM, Braga C, Cordeiro MT, de Carvalho OV, de Mendonca LR, et al. Dengue Virus-Specific Antibodies Enhance Brazilian Zika Virus Infection. *J Infect Dis* 2017 Mar 1;215(5):781-785.
- (175) Paz-Bailey G, Rosenberg ES, Doyle K, Munoz-Jordan J, Santiago GA, Klein L, et al. Persistence of Zika Virus in Body Fluids - Preliminary Report. *N Engl J Med* 2017 Feb 14.

- (176) Taba P, Schmutzhard E, Forsberg P, Lutsar I, Ljostad U, Mygland A, et al. EAN consensus review on prevention, diagnosis and management of tick-borne encephalitis. *Eur J Neurol* 2017 Aug 1.
- (177) National Institute of Allergy and Infectious Diseases/National Institutes of Health, NIAID/NIH, Zika Virus Vaccines. 2017; Available at: <https://www.niaid.nih.gov/diseases-conditions/zika-vaccines>.
- (178) Du L, Zhou Y, Jiang S. The latest advancements in Zika virus vaccine development. *Expert Rev Vaccines* 2017 Aug 07:1-4.
- (179) Centers for Disease Control and Prevention, CDC, Prevention. 2017; Available at: www.cdc.gov/zika/prevention, 2017.
- (180) Lebreton S, Jaunbergs J, Roth MG, Ferguson DA, De Brabander JK. Evaluating the potential of vacuolar ATPase inhibitors as anticancer agents and multigram synthesis of the potent salicylilhalamide analog saliphenylhalamide. *Bioorg Med Chem Lett* 2008 Nov 15;18(22):5879-5883.
- (181) Jääskeläinen J, Kalliomaki P, Paetau A, Timonen T. Effect of LAK cells against three-dimensional tumor tissue. In vitro study using multi-cellular human glioma spheroids as targets. *J Immunol* 1989 Feb 1;142(3):1036-1045.
- (182) Schwaiger M, Cassinotti P. Development of a quantitative real-time RT-PCR assay with internal control for the laboratory detection of tick borne encephalitis virus (TBEV) RNA. *J Clin Virol* 2003 Jul;27(2):136-145.
- (183) Verma S, Ziegler K, Ananthula P, Co JK, Frisque RJ, Yanagihara R, et al. JC virus induces altered patterns of cellular gene expression: interferon-inducible genes as major transcriptional targets. *Virology* 2006 Feb 20;345(2):457-467.
- (184) Radonic A, Thulke S, Mackay IM, Landt O, Siegert W, Nitsche A. Guideline to reference gene selection for quantitative real-time PCR. *Biochem Biophys Res Commun* 2004 Jan 23;313(4):856-862.
- (185) Reed LJ, Muench H. A simple method for estimating endpoints. *The American Journal of Hygiene* 1938;27:493-497.
- (186) Jääskeläinen A, Tonteri E, Pieninkeroinen I, Sironen T, Voutilainen L, Kuusi M, et al. Siberian subtype tick-borne encephalitis virus in *Ixodes ricinus* in a newly emerged focus, Finland. *Ticks Tick Borne Dis* 2016 Feb;7(1):216-223.
- (187) MIRA sequence assembler. 2017; Available at: <http://mira-assembler.sourceforge.net>.
- (188) Chevreux, B., Wetter, T. and Suhai, S. . Genome Sequence Assembly Using Trace Signals and Additional Sequence Information. *Computer Science and Biology: Proceedings of the German Conference on Bioinformatics (GCB)*; 1999. p. 45-46.
- (189) Langmead B, Salzberg SL. Fast gapped-read alignment with Bowtie 2. *Nat Methods* 2012 Mar 4;9(4):357-359.
- (190) Okonechnikov K, Golosova O, Fursov M, UGENE team. Unipro UGENE: a unified bioinformatics toolkit. *Bioinformatics* 2012 Apr 15;28(8):1166-1167.

- (191) Tamura K, Stecher G, Peterson D, Filipski A, Kumar S. MEGA6: Molecular Evolutionary Genetics Analysis version 6.0. *Mol Biol Evol* 2013 Dec;30(12):2725-2729.
- (192) Drummond AJ, Rambaut A, Shapiro B, Pybus OG. Bayesian coalescent inference of past population dynamics from molecular sequences. *Mol Biol Evol* 2005 May;22(5):1185-1192.
- (193) Rambaut A. Tracer v1.4. 2007; Available at: <http://beast.bio.ed.ac.uk/Tracer> 2007.
- (194) Drummond AJ, Suchard MA, Xie D, Rambaut A. Bayesian phylogenetics with BEAUti and the BEAST 1.7. *Mol Biol Evol* 2012 Aug;29(8):1969-1973.
- (195) Denisova OV, Söderholm S, Virtanen S, Von Schantz C, Bychkov D, Vashchinkina E, et al. Akt inhibitor MK2206 prevents influenza pH1N1 virus infection in vitro. *Antimicrob Agents Chemother* 2014 Jul;58(7):3689-3696.
- (196) R software. Available at: <https://www.r-project.org/>.
- (197) Gene Set Enrichment Analysis, GSEA. Available at: www.broadinstitute.org/gsea.
- (198) Pheatmap package. Available at: <https://cran.rproject.org/web/packages/pheatmap/index.html>.
- (199) Halstead SB, Chow JS, Marchette NJ. Immunological enhancement of dengue virus replication. *Nat New Biol* 1973 May 2;243(122):24-26.
- (200) Mickiene A, Pakalniene J, Nordgren J, Carlsson B, Hagbom M, Svensson L, et al. Polymorphisms in chemokine receptor 5 and Toll-like receptor 3 genes are risk factors for clinical tick-borne encephalitis in the Lithuanian population. *PLoS One* 2014 Sep 16;9(9):e106798.
- (201) Palus M, Vojtiskova J, Salat J, Kopecky J, Grubhoffer L, Lipoldova M, et al. Mice with different susceptibility to tick-borne encephalitis virus infection show selective neutralizing antibody response and inflammatory reaction in the central nervous system. *J Neuroinflammation* 2013 Jun 27;10:77-2094-10-77.
- (202) Yoshii K, Moritoh K, Nagata N, Yokozawa K, Sakai M, Sasaki N, et al. Susceptibility to flavivirus-specific antiviral response of Oas1b affects the neurovirulence of the Far-Eastern subtype of tick-borne encephalitis virus. *Arch Virol* 2013 May;158(5):1039-1046.
- (203) Barkhash AV, Voevoda MI, Romaschenko AG. Association of single nucleotide polymorphism rs3775291 in the coding region of the TLR3 gene with predisposition to tick-borne encephalitis in a Russian population. *Antiviral Res* 2013 Aug;99(2):136-138.
- (204) Kindberg E, Vene S, Mickiene A, Lundkvist A, Lindquist L, Svensson L. A functional Toll-like receptor 3 gene (TLR3) may be a risk factor for tick-borne encephalitis virus (TBEV) infection. *J Infect Dis* 2011 Feb 15;203(4):523-528.
- (205) Denisova OV, Kakkola L, Feng L, Stenman J, Nagaraj A, Lampe J, et al. Obatoclax, saliphenylhalamide, and gemcitabine inhibit influenza a virus infection. *J Biol Chem* 2012 Oct 12;287(42):35324-35332.

- (206) Söderholm S, Anastasina M, Islam MM, Tynell J, Poranen MM, Bamford DH, et al. Immuno-modulating properties of saliphenylhalamide, SNS-032, obatoclax, and gemcitabine. *Antiviral Res* 2016 Feb;126:69-80.
- (207) Galmarini CM, Mackey JR, Dumontet C. Nucleoside analogues: mechanisms of drug resistance and reversal strategies. *Leukemia* 2001 Jun;15(6):875-890.
- (208) Söderholm S, Kainov DE, Ohman T, Denisova OV, Schepens B, Kuleskiy E, et al. Phosphoproteomics to Characterize Host Response During Influenza A Virus Infection of Human Macrophages. *Mol Cell Proteomics* 2016 Oct;15(10):3203-3219.
- (209) Yadav B, Wennerberg K, Aittokallio T, Tang J. Searching for Drug Synergy in Complex Dose-Response Landscapes Using an Interaction Potency Model. *Comput Struct Biotechnol J* 2015 Sep 25;13:504-513.
- (210) De Clercq E, Li G. Approved Antiviral Drugs over the Past 50 Years. *Clin Microbiol Rev* 2016 Jul;29(3):695-747.
- (211) Delvecchio R, Higa LM, Pezzuto P, Valadao AL, Garcez PP, Monteiro FL, et al. Chloroquine, an Endocytosis Blocking Agent, Inhibits Zika Virus Infection in Different Cell Models. *Viruses* 2016 Nov 29;8(12):E322.
- (212) Barrows NJ, Campos RK, Powell ST, Prasanth KR, Schott-Lerner G, Soto-Acosta R, et al. A Screen of FDA-Approved Drugs for Inhibitors of Zika Virus Infection. *Cell Host Microbe* 2016 Aug 10;20(2):259-270.
- (213) Choy MM, Zhang SL, Costa VV, Tan HC, Horrevorts S, Ooi EE. Proteasome Inhibition Suppresses Dengue Virus Egress in Antibody Dependent Infection. *PLoS Negl Trop Dis* 2015 Nov 13;9(11):e0004058.
- (214) Mastrangelo E, Pezzullo M, De Burghgraeve T, Kaptein S, Pastorino B, Dallmeier K, et al. Ivermectin is a potent inhibitor of flavivirus replication specifically targeting NS3 helicase activity: new prospects for an old drug. *J Antimicrob Chemother* 2012 Aug;67(8):1884-1894.
- (215) Diamond MS, Zachariah M, Harris E. Mycophenolic acid inhibits dengue virus infection by preventing replication of viral RNA. *Virology* 2002 Dec 20;304(2):211-221.
- (216) Chiappori AA, Schreeder MT, Moezi MM, Stephenson JJ, Blakely J, Salgia R, et al. A phase I trial of pan-Bcl-2 antagonist obatoclax administered as a 3-h or a 24-h infusion in combination with carboplatin and etoposide in patients with extensive-stage small cell lung cancer. *Br J Cancer* 2012 Feb 28;106(5):839-845.
- (217) Frumence E, Roche M, Krejbich-Trotot P, El-Kalamouni C, Nativel B, Rondeau P, et al. The South Pacific epidemic strain of Zika virus replicates efficiently in human epithelial A549 cells leading to IFN-beta production and apoptosis induction. *Virology* 2016 Jun;493:217-226.
- (218) Souza BS, Sampaio GL, Pereira CS, Campos GS, Sardi SI, Freitas LA, et al. Zika virus infection induces mitosis abnormalities and apoptotic cell death of human neural progenitor cells. *Sci Rep* 2016 Dec 23;6:39775.
- (219) Chia YL, Ng CH, Lashmit P, Chu KL, Lew QJ, Ho JP, et al. Inhibition of human cytomegalovirus replication by overexpression of CREB1. *Antiviral Res* 2014 Feb;102:11-22.

- (220) Albrecht JH, Poon RY, Ahonen CL, Rieland BM, Deng C, Crary GS. Involvement of p21 and p27 in the regulation of CDK activity and cell cycle progression in the regenerating liver. *Oncogene* 1998 Apr 23;16(16):2141-2150.
- (221) Retallack H, Di Lullo E, Arias C, Knopp KA, Laurie MT, Sandoval-Espinosa C, et al. Zika virus cell tropism in the developing human brain and inhibition by azithromycin. *Proc Natl Acad Sci U S A* 2016 Dec 13;113(50):14408-14413.
- (222) Gabriel E, Ramani A, Karow U, Gottardo M, Natarajan K, Gooi LM, et al. Recent Zika Virus Isolates Induce Premature Differentiation of Neural Progenitors in Human Brain Organoids. *Cell Stem Cell* 2017 Mar 2;20(3):397-406.e5.
- (223) Chan JF, Yip CC, Tsang JO, Tee KM, Cai JP, Chik KK, et al. Differential cell line susceptibility to the emerging Zika virus: implications for disease pathogenesis, non-vector-borne human transmission and animal reservoirs. *Emerg Microbes Infect* 2016 Aug 24;5:e93.

ORIGINAL PUBLICATIONS